universität wien

MASTERARBEIT / MASTER'S THESIS

Titel der Masterarbeit / Title of the Master's Thesis

„Characterization of a novel Parkinson's disease mouse model based on the inoculation with human wild-type α-synuclein pre-formed fibrils"

verfasst von / submitted by

Jenny Marie Král, BSc

angestrebter akademischer Grad / in partial fulfilment of the requirements for the degree of

Master of Science (MSc)

Wien, 2023 / Vienna, 2023

Studienkennzahl lt. Studienblatt / degree programme code as it appears on the student record sheet:	UA 066 834
Studienrichtung lt. Studienblatt / degree programme as it appears on the student record sheet:	Masterstudium Molekulare Biologie
Betreut von / Supervisor:	ao. Univ.-Prof. Dr. Christian Pifl

Acknowledgements

First of all, I want to thank Prof. Rosario Moratalla for giving me the opportunity to join her laboratory at the Cajal Institute as a master's student. It was a great honour to work with so many amazing colleagues whom I would like to thank for their help and support – Mónica, Elena, Sarah, Adrián, Mario, Carlos, Noelia, Blanca, Aida, Laura. I want to express my particular thanks to Sarah and Mario for helping me with the automatic quantification analysis and Elena, for sharing her experience and being such a good friend in the lab. I'm extremely grateful to Mónica for being the best co-supervisor of my thesis. Without you it would not have been possible. Gracias por tu ayuda, tu esfuerzo, y por creer en mí. Eres una investigadora increíble y estoy agradecida de haber aprendido de ti.

I also wish to thank Prof. Daniela Pollak, Micaela Glat, and Anna Gundacker for their support and encouragement during my bachelor's thesis. I appreciate your excitement for science and thank you for awakening my interest in neuroscience. Further, I would like to thank Prof. Peter Swoboda and Andrea Coschiera who I worked with at the Karolinska Institute. It was an honour to be part of your laboratory where I learned a lot. Additionally, I thank Prof. Christian Pifl for the chance to conduct an internship in his lab, for sharing his knowledge with me and for being the internal supervisor of the University of Vienna for my master's thesis.

Most importantly, I want to thank my family – my mum, dad and brother – for their support and giving me so many opportunities in my life. Ohne euch wäre ich nicht die, die ich heute bin. I would also like to thank my support system, my friends Heli, Klara and Maritta, who always have my back no matter what. Ich bin sehr glücklich, euch in meinem Leben zu haben.

At the end I would love to say that I am beyond grateful for all the experiences I made and opportunities I got throughout my years at university. Not only have I learned a lot academically, but also have I got to know myself better, experienced living abroad, learned a new language, and met many people, some of which turned into great friends.

Table of Contents

Acknowledgements **3**

Abstract **7**

Zusammenfassung **8**

Resumen **9**

Introduction **10**

Parkinson's disease (PD) **10**
Neuropathological hallmarks of PD 10
Basal ganglia and related nuclei 11
Motor and non-motor symptoms 13
Lewy pathology 14
Aetiology: from genetic and environmental factors to aging 16
Diagnosis 19

α-Synuclein **20**
Structure and physiological function 20
Aggregation and toxicity 21
Propagation and spreading 24

Models of Parkinson's disease **26**
Toxin-based models 26
Genetic models 26
α-Syn propagation models 28

Hypothesis and objectives **31**

Experimental design **32**

Material and Methods **33**

Animals **33**

Injection material and administration **33**
Pre-formed fibrils (PFFs) 33
Stereotaxic injection 33

Behaviour experiment **34**
Challenging beam transversal test 34

Histological stainings **34**
Sample extraction 34
Immunohistochemistry (IHC) 35
Immunofluorescence 35

Image acquisition and analysis **36**
Scoring of pα-syn pathology 36
Quantification of pα-syn aggregates 36
Quantitative assessment of innervation density 37
Stereological quantification of TH-positive cells 37

Statistical analysis **38**

Results **39**

Effect of human wild-type α-syn PFF inoculation on α-syn pathology **39**

Effect of human wild-type α-syn PFF inoculation on the integrity of the nigrostriatal pathway **44**

Effect of human wild-type α-syn PFF inoculation on motor behaviour 47
Correlation studies 48
Analysis of sex differences 50
Discussion 53
Aggregation and spreading of α-syn 54
Impact of α-syn pathology on dopaminergic neurodegeneration 58
Effect of α-syn pathology on motor behaviour 60
Correlation studies 61
Sex-specific differences 62
Future outlook 63
Conclusions 66
References 67
List of Figures 91
List of Tables 91
List of Abbreviations 92
Supplementary Material 93

Abstract

Parkinson's disease (PD) is the most common neurodegenerative movement disorder of unknown aetiology. The neuropathological hallmarks of PD are Lewy bodies/neurites (LBs/LNs), deposits of abnormal aggregated proteins, mainly α-synuclein (α-syn), and the progressive loss of dopaminergic neurons in the substantia nigra pars compacta (SNpc), causing striatal dopaminergic deficiency responsible for the classic motor symptoms observed in PD patients.

To unravel the molecular mechanisms involved in the neurodegenerative process and the establishment of therapeutic interventions, robust animal models are needed. However, no model system has yet been developed that efficiently replicates all main pathological and clinical features of the disease. In this study we aimed to establish a novel model of PD based on the inoculation of human wild-type α-syn pre-formed fibrils (PFFs) into the striatum of *SNCA*-OVX transgenic mice. Our results show that pathological α-syn induces the neurodegenerative process in the *SNCA*-OVX model by facilitating the conversion of endogenous α-syn to pathological α-syn inclusion bodies that exhibit morphological and molecular properties of human LBs/LNs. We demonstrate α-syn propagation to distant brain areas, possibly along interneuronal pathways. Furthermore, we detect that PFF-seeded α-syn pathology has an impact on the integrity of the nigrostriatal pathway, resulting in the loss of SNpc dopaminergic neurons and dopaminergic denervation in the striatum. No robust motor deficits were observed, but additional assays need to be conducted to complement our results.

Therefore, our findings indicate that the PFF-injected *SNCA*-OVX mouse model is a suitable model to reproduce human α-syn pathology, to study its impact on disease progression and to investigate new therapeutic approaches aimed to prevent or halt pathological α-syn aggregation and propagation.

Zusammenfassung

Die Parkinson-Krankheit ist die häufigste neurodegenerative Motor-Erkrankung, deren Ätiologie bislang unbekannt ist. Neuropathologisch äußert sich die Krankheit durch das sukzessive Absterben dopaminerger Neuronen der Substantia nigra pars compacta (SNpc), sowie dem Auftreten von abnormalen Proteinablagerungen, die Lewy-Körperchen/Neuriten (LBs/LNs) genannt werden und hauptsächlich das Protein α-synuclein (α-syn) enthalten. Der Verlust dopaminerger Nervenzellen führt zu einem striatalen Mangel and Dopamin, der für die klassischen Motorsymptome verantwortlich ist, die bei Parkinson-Patienten zu beobachteten sind.

Zur Untersuchung der zugrundeliegenden molekularen Mechanismen und der Entwicklung von Therapiemöglichkeiten werden robuste Tiermodelle in der Forschung benötigt. Bisher wurde noch kein Modellsystem entwickelt, das alle pathologischen und klinischen Merkmale der Krankheit effizient reproduziert. Das Ziel dieser Studie war die Etablierung eines neuen Parkinson-Krankheit-Modells, das durch die Injektion humaner *wild type* präformierten α-syn Fibrillen in das Striatum transgener *SNCA*-OVX Mäuse generiert wird. Unsere Beobachtungen zeigen, dass die Inokulation mit pathologischem α-syn neurodegenerative Prozesse in dem Modell induziert, indem es die Umwandlung von endogenem α-syn in pathologische α-syn Aggregate begünstigt. Die beobachteten α-syn Aggregate zeigen morphologische und molekulare Eigenschaften von humanen LBs/LNs und breiten sich von der Injektionsstelle in entfernte Hirnregionen aus, möglicherweise entlang neuronaler Verbindungen. Darüber hinaus verursachen pathologische α-syn Aggregate den Verlust von Dopamin-produzierender Neuronen in der SNpc und die Denervierung dopaminerger Nervenendigungen im Striatum. Es wurde keine robuste Motorbeeinträchtigung festgestellt, was mit weiteren Tests untersucht werden muss.

Die Ergebnisse der Studie demonstrieren, dass dieses Modellsystem, basierend auf der Administration von humanen *wild type* präformierten α-syn Fibrillen in *SNCA*-OVX Mäuse, geeignet ist, die humane α-syn Pathologie und dessen Auswirkung auf den progressiven Krankheitsverlauf widerzuspiegeln. Zudem können neue therapeutische Ansätze erforscht werden, die darauf abzielen, die pathologische Aggregation sowie Ausbreitung von α-syn zu unterbinden oder verlangsamen.

Resumen

La enfermedad de Parkinson (EP) es un trastorno neurodegenerativo motor de etiología desconocida, que cursa con un amplio espectro de síntomas motores y no motores. Se caracteriza por la pérdida de neuronas dopaminérgicas de la substancia negra pars compacta (SNpc) y la presencia de cuerpos/neuritas de Lewy (LBs/LNs), que son agregados de proteínas, restos de membranas y orgánulos subcelulares, cuyo componente principal es la proteína presináptica (α-syn). La degeneración de estas neuronas resulta en una deficiencia de dopamina en el estriado, responsable de los síntomas motores observados en los pacientes con EP.

Para desentrañar los mecanismos moleculares implicados en el proceso neurodegenerativo de la EP y desarrollar nuevas estrategias terapéuticas, se necesitan modelos animales robustos. Sin embargo, aún no se ha desarrollado ningún modelo animal que reproduzca de forma eficiente todas las características patológicas y clínicas de la enfermedad. En este estudio se pretende establecer un nuevo modelo basado en la administración de fibrillas preformadas de α-syn humana *wild type* en el estriado de ratones transgénicos *SNCA*-OVX. Nuestros resultados muestran que la α-syn patológica induce el proceso patológico y neurodegenerativo que caracteriza a la EP en el modelo murino *SNCA*-OVX, facilitando la conversión de la α-syn endógena a agregados patológicos de α-syn. Demostramos que estos agregados comparten características morfológicas y moleculares con los LBs/LNs observados en la EP humana. Además, demostramos la propagación de la patología de la α-syn a regiones cerebrales alejadas del sitio de la inyección, mediante la implicación de conexiones intraneuronales directas, pero posiblemente también mediante conexiones interneuronales. También mostramos que la patología de la α-syn inducida tras la inyección de PFFs impacta en la integridad de la vía nigroestriatal, resultando en la pérdida de terminales axonales en el estriado y de cuerpos celulares de las neuronas dopaminérgicas en la SNpc. Sin embargo, no observamos un déficit motor grave en el punto temporal post-inyección evaluado.

Por lo tanto, estos resultados indican que el modelo *SNCA*-OVX inyectado con PFFs de α-Syn reproduce la patología humana de α-syn, y es un modelo adecuado para estudiar su impacto en la progresión de la enfermedad e investigar nuevos enfoques terapéuticos dirigidos a prevenir o detener la agregación y propagación de la patología.

Introduction

Parkinson's disease (PD)

Parkinson's disease (PD) is a neurodegenerative movement disorder that was first medically described in "An Essay on the Shaking Palsy" by James Parkinson in 1817. Even though the first formal description is ascribed to James Parkinson, the disease was already known in several civilizations long time before but was often misinterpreted as other diseases (Raudino., 2012). It was not until 1872 that the french neurologist Jean-Martin Charcot separated PD from multiple sclerosis and other disorders characterized by tremor. He and his students described the clinical spectrum of this illness, differentiating two types, the tremorous and rigid/akinetic form, and distinguished bradykinesia as a separate cardinal feature. Also, Charcot was the first one proposing the term "Parkinson's disease" instead of the earlier used descriptions "paralysis agitans" or "shaking palsy", acknowledging that PD patients do not necessarily display tremor and are not markedly weak (Goetz, 2011; Charcot, 1872).

Today, PD is the second most common neurodegenerative disease after Alzheimer's disease with a global prevalence of more than 6 million individuals. From 1990 to 2016, the number of individuals diagnosed with PD globally increased 145%, making it the fastest growing neurological disorder (Dorsey et al., 2018; GBD 2016 Neurology Collaborators). Typically, the onset is between 55 and 65 years, affecting 1-2% of people over 60 years and rising to 3.5% at the age 85-89 years (Rizek et al., 2016). The prevalence of PD is higher in men than women. A study found a higher incidence rate among men with the relative risk being 1.5 times greater in men than women. The increased risk of PD in men might be explained by exposure to toxic substances, head trauma, neuroprotection by oestrogen, mitochondrial dysfunction, or X linkage of genetic risk factors (Wooten et al., 2004).

The cause of PD remains elusive, and no cure or preventive therapy has yet been discovered. Also, diagnosis remains a challenge because classic clinical features of the disease are shared with other neurodegenerative conditions, and a definitive diagnosis from the earliest stages is not possible with current diagnostic tests or biomarkers (Tolosa et al., 2021).

Neuropathological hallmarks of PD

The neuropathological hallmarks of PD are (1) the degeneration of dopaminergic cells in the substantia nigra pars compacta (SNpc), accompanied by (2) the formation of proteinaceous inclusions in form of Lewy bodies (LBs) and Lewy neurites (LNs) (**Fig. 1**). The cell bodies of SNpc dopaminergic neurons contain the dark-brown pigment neuromelanin (Marsden, 1983), hence the loss of these cells leads to the classical finding of SNpc depigmentation in PD. LBs are intraneuronal aggregates of more than 90 molecules (Wakabayashi et al., 2013, Wakabayashi et al., 2007) that are mainly composed of α-synuclein (α-syn) (Spillantini et al., 1997), a neuronal protein that is highly enriched in presynaptic nerve terminals (Maroteaux et al., 1988).

The cells of the SNpc are most vulnerable to neurodegeneration occurring in PD (see "Introduction – Parkinson's disease – Aetiology") and it selectively affects the ventrolateral cell groups (A9) that project to the posterolateral putamen, constituting the nigrostriatal pathway of the basal ganglia. On the other hand, dorsal and medial cell groups (A10) are more resistant and are part of the mesolimbic DA pathway (Dickson

et al., 2009; Dickson, 2018). The distinct pattern of nigral neuronal loss is consistent with the uneven loss of dopamine (DA) in the striatum, where the putamen is more impacted than the caudate nucleus. The loss of nigrostriatal projections leading to substantial DA loss in the putamen contributes to motor symptoms in PD patients (Rinne et al., 1993).

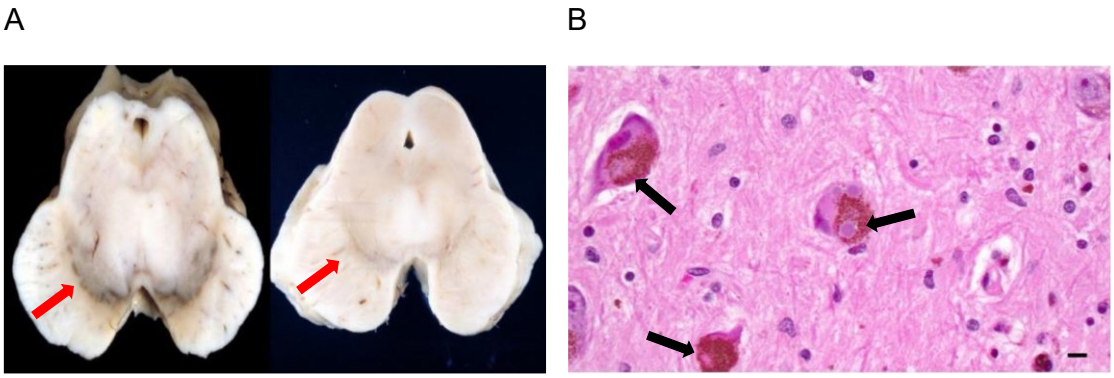

Fig. 1: Neuropathological hallmarks of Parkinson's disease (PD). (**A**) Macroscopic view of a transverse section of the mesencephalon. Dopaminergic cell loss of the SNpc is visible as depigmentation in the SN (red arrows) of a PD patient (right), compared to a healthy person (left). (**B**) Lewy bodies (black arrows) in pigmented neurons of the SN (Hematoxylin Eosin staining). Inclusions are also seen in neuronal processes, mostly axons, so-called Lewy neurites (not shown). Scale bar: 10 µm (Modified from Bloem et al., 2021, supplementary appendix)

Basal ganglia and related nuclei

The basal ganglia and related nuclei refer to various subcortical cell groups that primarily play a role in motor control, but also motor learning, executive functions and behaviour, and emotions. In the strictest sense, the *basal ganglia* consist of striatum (or caudate-putamen) and globus pallidus, while *related nuclei* include the subthalamic nucleus (STN) and substantia nigra (SN). To better understand the circuitry in the basal ganglia, its nuclei can be divided into (1) input nuclei, (2) output nuclei, and (3) intrinsic nuclei. Input nuclei consist of caudate nucleus, putamen and nucleus accumbens that receive information from different sources, mainly cortical, thalamic, nigral, but also striatal afferents. On the contrary, output nuclei are the internal segment of globus pallidus (GPi) and the substantia nigra pars reticulata (SNr) that send information from the basal ganglia to the thalamus. Intrinsic nuclei are located between input and output nuclei, namely the external segment of globus pallidus (GPe), STN, and SNpc (Lanciego et al., 2012).

The striatum contains medium-sized spiny neurons (MSNs) that are inhibitory neurons using GABA as neurotransmitter. MSNs from the dorsal striatum that project to the output nuclei GPi and SNr express dopamine receptor subtype 1 receptors (D_1R) (“direct” pathway), whereas MSNs that innervate the GPe nucleus (intrinsic nucleus) express the dopamine receptor subtype 2 (D_2R) (“indirect” pathway) (Lanciego et al., 2012). The differential expression of dopamine receptors is associated with distinct G-proteins that are coupled to different intracellular signalling pathways, resulting in distinct biochemical responses of MSNs upon DA receptor activation (Calabresi et al., 2014).

Striatal afferents include projections from multiple brain areas. The entire cortex, both ipsilateral and contralateral, innervate the striatum with glutamatergic projections. Also, thalamic innervations reach the striatum, being an additional source of glutamatergic

afferents. However, little is known about thalamic influence in basal ganglia function and dysfunction, consequently the thalamostriatal pathway is usually not mentioned in models of basal ganglia circuits. Moreover, the amygdaloid complex provides glutamatergic inputs to the striatum and serotonergic projections arise from the raphe nuclei, mainly the dorsal nucleus (Lanciego et al., 2012). The nigrostriatal system constitutes the major source of DA in the striatum and originates from the SNpc (A9 cell group). The second nucleus of the SN, the pars reticulata (SNr), projects inhibitory axons to the thalamus (Young et al., 2023) and receives dopaminergic projections from the ventral tier of the SNpc (Lanciego et al., 2012).

The classical model of functional organization of the basal ganglia is described by the direct and indirect striatopallidal pathway, working in opposition to one another (**Fig. 2**). Striatal neurons of the direct pathway (indicated in red), activated by DA, project to the GPi and SNr, exhibiting an inhibitory action on these nuclei. The inhibition of inhibitory GPi/SNr neurons leads to a disinhibition of the thalamus that sends excitatory connections to the motor cortex. As a result, the motor cortex is activated and facilitates locomotor activation and movement. The indirect pathway (indicated in blue), on the other hand, inhibits motor activity. MSNs expressing D2-family receptors are inhibited by DA and project indirectly to the GPi/SNr via the GPe and STN. The inhibition of GPe neurons results in disinhibition of the glutamatergic neurons of the STN which stimulates GPi/SNr inhibitory (GABA) projections to the thalamus. Ultimately, the motor cortex is inhibited, resulting in the reduction of locomotor activity and movement (Calabresi et al., 2014; Young et al., 2023).

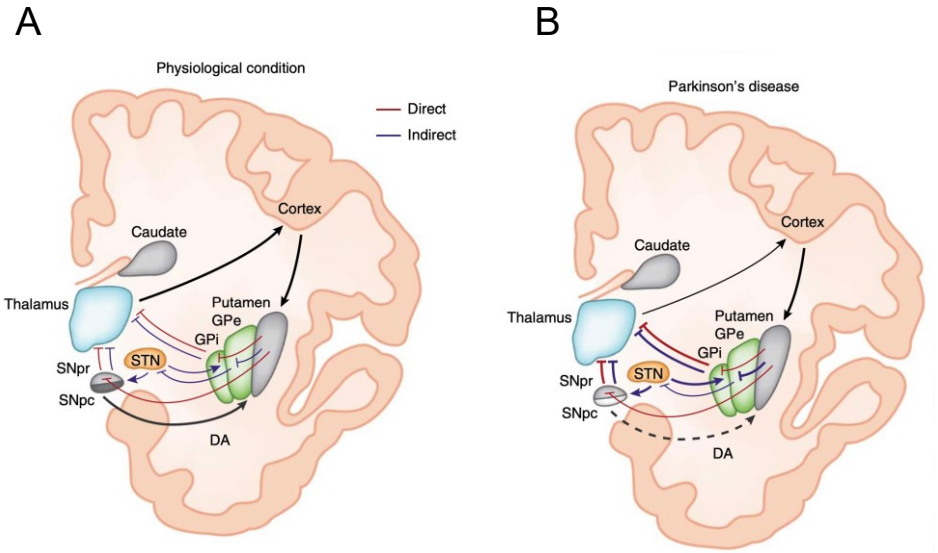

Fig. 2: Schematic overview of the classical direct/indirect motor pathway of the basal ganglia. (**A**) In physiological condition, DA input from the SNpc activates D1-expressing striatal MSNs of the direct pathway (red) and inhibits D2-expressing striatal neurons of the indirect pathway (blue). The output nuclei GPi/SNr project to the thalamus which sends efferents to the cortex. Appropriate execution of movement requires balance of both direct and indirect pathways. (**B**) In PD patients, the loss of dopaminergic SNpc neurons reduces striatal DA and thereby receptor stimulation in MSNs. The imbalance of direct and indirect pathway leads to canonical motor symptoms observed in PD. (Modified from Calabresi et al., 2014)

For the appropriate execution of normal movement an adequate balance of direct and indirect pathway is necessary. The loss of dopaminergic neurons in the SNpc underlying PD leads to striatal DA depletion and reduces DA receptor stimulation in striatal MSNs. This results in the imbalance of direct and indirect pathway stimulation

and over-inhibition of thalamic neurons projecting to the cortex. The abnormal activation of output nuclei manifests in the appearance of typical motor symptoms observed in PD patients (Calabresi et al., 2014; Dauer et al., 2003).

Motor and non-motor symptoms

The classic motor symptoms of PD are tremor, bradykinesia/hypokinesia/akinesia, rigidity and postural instability, amongst others (**Table 1**, left) (Balestrino et al., 2020). PD tremor appears at rest, decreasing with voluntary movement. Bradykinesia (slowness of movement), hypokinesia (reduction in movement amplitude), and akinesia (absence of normal unconscious movements) manifest as a variety of symptoms such as hypomimia (reduction of facial expressions), drooling (failure to swallow without thinking about it), and micrographia (decreased size of handwriting) (Dauer et al., 2003).

Motor symptoms	Non-motor symptoms
Tremor	Hyposmia, anosmia
Rigidity	Psychiatric symptoms Depression, anxiety, apathy, halluciantions, psychosis
Bradykinesia, akinesia, hypokinesia hypomimia, hypophonia, drooling, micrographia	Dementia, cognitive impairment
Postural instability	Sensory symptoms
Postural abnormality camptocormia, Pisa syndrome	Genitourinary symptoms urinary frequency, urgency, reduced libido, sexual dysfunction
Gait disturbances freezing, festination, start/target/obstacle hesitation	Gastrointestinal symptoms constipation, delayed/reduced stomach emptying
Alterations in blinking, eye movements	Dysphagia, sialorrhoea, dysarthria, hypophonia
	Disturbances of sleep and wakefulness
	Cardiovascular symptoms blood pression variations (postural, postprandial), dysrhythmias

Table 1: Motor and non-motor symptoms of PD. (Modified from Balestrino et al., 2020)

Even though PD is defined as a movement disorder, the disease comprises multiple non-motor features (**Table 1**, right). Symptoms range from olfactory impairment, dysphagia, sialorrhoea, gastrointestinal and cardiovascular symptoms, to sleep, sensorial, cognitive and neuropsychiatric disturbances (Balestrino et al., 2020). It has been shown that non-motor symptoms contribute to a great extent to the disability of affected individuals and have a negative impact on health-related quality of life in PD (Santos-García et al., 2013; Santos García et al., 2019).

Interestingly, several of these symptoms have been shown to arise up to 10 years before the manifestation of motor impairment, the prodromal phase of PD, and are concurringly termed “prodromal symptoms” (Postuma et al., 2012). 90% of PD patients manifest olfactory deficits, that are usually bilateral and can occur before the onset of DA loss-related motor symptoms (Bohnen et al., 2008). Also, rapid eye movement (REM) sleep behaviour disorder (RBD) can occur in the early course of the disease process, before the manifestation of motor signs (Postuma et al., 2015). Among prodromal symptoms, RBD stands out in that more than 90% of those with isolated RBD develop neurodegenerative parkinsonism, commonly PD or PD dementia (Iranzo et al., 2013; Dauvilliers et al., 2018). Further, depression is common in patients with PD and may as well precede motor signs (Shiba et al., 2000; Reijnders et al., 2008). Gastrointestinal disturbances such as constipation may be observed before the alteration in motor function, as well (Abbott et al., 2001). The cause of gastrointestinal

dysfunctions is not well understood and may be attributed to extrinsic and intrinsic pathological and biochemical changes. Also, multiple neurotransmitter and neuromodulators (such as acetylcholine, dopamine, noradrenaline, etc.) influence bowel function, explaining the complexity of symptomatology (Schapira et al., 2017).

Until relatively recently, PD has primarily been considered a motor disorder and research primarily focused on the investigation of motor deficits, which is why neuropathological mechanisms underlying non-motor features of PD are poorly understood. However, growing evidence propose the implication of dopaminergic as well as non-dopaminergic systems, along with the involvement of diverse structures outside the nigrostriatal pathway (Schapira et al., 2017). Besides DA, neurotransmitter systems involved in the non-motor symptoms of PD pathophysiology include the noradrenergic system of the locus coeruleus, the serotonergic system of the dorsal raphe nuclei, and the cholinergic system of the nucleus basalis of Meynert and the pedunculopontine nucleus (Qamar et al., 2017). It is important to unravel the molecular basis involved in the development of non-motor symptoms, and to develop tools that allow early diagnosis of the disease, as early detection provides a wide time window to prevent disease development and progression.

Lewy pathology

As mentioned before, Lewy pathology is one of the hallmarks of PD as well as other synucleinopathies such as dementia with Lewy bodies (DLB), and multiple systems atrophy (MSA). LBs are proteinaceous intracellular inclusion bodies of abnormal aggregated proteins, mainly consisting of α-syn (Spillantini et al., 1997) together with more than other 90 molecular components such as p62/sequestosome 1, proteasomes, ubiquitin-pathway-related proteins (Wakabayashi et al., 2007, Wakabayashi et al., 2013).

LBs have been found within α-syn-expressing neuronal populations in PD and DLB affected individuals (Spillantini et al., 1998b), and oligodendrocytes in MSA patients (Spillantini et al., 1998a). In PD and DLB, widespread α-syn aggregation has additionally been found in neighbouring astroglial cells (Song et al., 2009). Yet, phosphorylated α-syn inclusions are not only found in cell bodies but also in cellular processes, mostly axonal, so-called Lewy neurites (LNs) (Wakabayashi et al., 1992; Wakabayashi et al., 2013). Lewy pathology is also defined by crowded environment of membranes that include vesicular structures and fragmented organelles. Dysmorphic mitochondria, lipid membranes, and lysosomal structures are found, together with proteins of degradation pathways such as ubiquitin and p62/SQSTM1. This finding indicates the contribution of damaged organelles in the formation of LBs (Shahmoradian et al., 2019).

Although LB pathology has been reported in the SNpc and contributes to neurodegeneration of dopaminergic neurons, it has been shown that α-syn pathology is not exclusively restricted to this brain region. Braak and colleagues have discovered the presence of LBs in non-PD post-mortem brains and proposed the olfactory bulb (OB) and the enteric nervous system (ENS) of the gastrointestinal tract (GIT) as putative sites of origin for α-syn aggregation. From these starting points, the pathology spreads via the olfactory tract and vagus nerve, respectively, to other brain regions following neural connectivity, with α-syn pathology being present in the midbrain and cortex at later disease stages (**Fig. 3 A**). Hence, the progression of α-syn pathology is

thought to follow a distinct caudo-rostral pattern throughout the CNS (Braak et al., 2003; Braak et al., 2004). According to this theory, PD was divided in 6 stages, defined by the development of α-syn inclusions in specific brain areas, including dorsal motor nucleus of the vagus nerve (DMX), OB, dorsal raphe nuclei (DR), magnocellular portions of reticular formation, locus coeruleus, SN, and cortex. Each stage corresponds to specific symptomology of PD (**Fig. 3 B**) (Rizek et al., 2016).

A

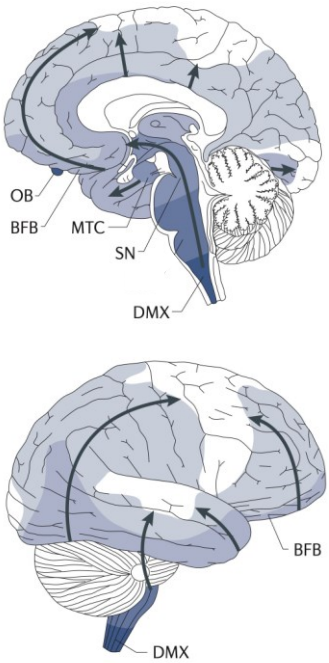

B

Lewy pathology (Braak et al., 2003)	Major sympotoms
Stage 1	
Olfactory bulb (OB) Dorsal motor nucleus of the vagus nerve (DMX) Peripheral autonomic neurons	Constipation Anosmia
Stage 2	
Locus coeruleus Dorsal raphe nuclei (DR)	Sleep and mood dysfunction
Stage 3	
Substantia nigra (SN) Basal forebrain (BFB) Central subnucleus of amygdala	Classical PD motor symptoms (see **Table 1**)
Stage 4	
Thalamus Medial temporal cortex (MTC) Hippocampus Cortical and basolateral nuclei of amygdala	Dementia Psychosis
Stage 5 and 6	
Cortical regions	

Fig. 3: Braak staging of Lewy body deposition. Braak et al. (2003) proposed that LB progression begins from the OB and DMX, respectively, and spreads via the olfactory tract and vagus nerve to other brain regions, ultimately reaching cortical areas. (**A**) Schematic representation of the progression of Lewy pathology throughout the brain, following a specific caudo-rostral pattern. (Modified from Schapira et al., 2017) (**B**) PD was divided in 6 stages depending on LB pathology, each corresponding to specific symptomology. (Modified from Rizek et al., 2016)

Neuropathological findings support the “gut-brain” axis in PD and early α-syn aggregation in the periphery, including gastric myenteric and submucosal plexuses and gastrointestinal tissues, during prodromal stages of PD (Braak et al., 2006; Stokholm et al., 2016). Environmental factors (e.g., changes in gut microbiome, toxins) are hypothesized to initiate disease progression by causing inflammation and oxidative stress which leads to abnormal α-syn aggregation. The spreading of ENS-formed α-syn seeds towards the CNS is enabled by increased permeability of the intestinal barrier (“leaky gut”) via the DMX (**Fig. 3 A**) (Del Tredici et al., 2016; Jan et al., 2021).

As discussed above, distinct non-motor features (**Table 1**) have been shown to appear years before the manifestation of motor deficits, the prodromal phase of PD (Ross et al., 2012; Postuma et al., 2012). This observation is interesting in the context of the Braak’s hypothesis (Braak et al., 2003; Braak et al., 2004) as the onset of prodromal symptoms corresponds to a stage where pathological changes involve extranigral sites, such as the lower brain stem, the olfactory bulb and tracts, and the peripheral autonomic nervous system (**Fig. 3 B**) (Schapira et al., 2017; Tolosa et al., 2021). For instance, the DMX is a key modulator of autonomic control of the bowel, where pathological changes occur early in the disease progress, explaining constipation as a possible prodromal feature of PD (Abbott et al., 2001). Consistently, the pre-motor development of hyposmia and RBD has been explained with the concept of early brain

stem involvement in α-syn pathology (Boeve et al., 2007; Ferrer et al., 2011; Schapira et al., 2017).

Although Lewy pathology is usually observed in PD, some findings challenge the concept of α-syn as a key feature of development and progression of the disease. First, not all cases of parkinsonism are characterized by α-syn inclusions. Studies revealed that familial PD mutations in *Parkin*, and the *LRRK2* G2019S mutation evoke neurodegeneration in the absence of LBs (Gaig et al., 2009; Johansen et al., 2018). Moreover, post-mortem analysis showed that LBs/LNs may be present in the brain without clinical PD symptoms (Parkkinen et al., 2005). Another observation was made in advanced PD patients, where only a minority of grafted neurons demonstrated Lewy body-like inclusions, while their appearance did not have functional consequences for neurons surviving for long time periods (Kordower et al., 2008; Gómez-Benito et al., 2020).

Aetiology: from genetic and environmental factors to aging

Until today, the aetiology of PD remains unresolved. However, studies have shown that a complex interplay between risk and protective factors, including genetic and environmental ones, contribute to disease pathogenesis. Hence, PD is considered a multifactorial disorder with age being the greatest risk factor. Changes in the nigrostriatal system during normal aging contribute to the pathogenesis of PD affecting the morphological and functional integrity of cells. The prevalence and incidence increase nearly exponentially with age and peak after 80 years (Driver et al., 2009; Pringsheim et al., 2014). Interestingly, 10 to 15% of patients have family history among first-degree relatives (Thacker et al., 2008), and in a minority of affected individuals a single gene mutation is found, usually associated with a younger age of onset (Verstraeten et al., 2015). As well, in sporadic forms of PD a genetic susceptibility has been proven in genome-wide association studies (GWAS) (Nalls et al., 2014; Nalls et al., 2019).

The common cellular and molecular converging pathways implicated in PD pathogenesis in all the different PD phenotypes are processes involved in the regulation of protein homeostasis, or proteostasis, including abnormalities in protein aggregation, intracellular protein and membrane trafficking, and protein disposal by ubiquitin-proteasome and lysosome-autophagy systems, along with processes involved in mitochondrial function and mitophagy, synaptic function and DA transmission (Kalia et al., 2015).

Many studies investigated the genetics underpinning PD. Several genes implicated in monogenic familial forms of PD have been identified, genetic mutations underlying Gaucher disease have been related to PD (García-Sanz et al., 2017) and GWAS revealed additional risk factors for developing PD (**Table 2**) (Delamarre et al., 2017).

Monogenic genes, or mendelian inherited genes, can be distinguished between autosomal dominant transmission and recessive transmission. Mutations in the genes *SNCA* (*PARK1*; encoding α-synuclein), *LRRK2* (*PARK8*; encoding dardarin), *VPS35* (encoding vacuolar protein sorting 35), *CHCHD2*, and *EIF4G1* have been shown to cause autosomal dominant forms of PD. On the contrary, mutations in *Parkin* (*PARK2*), *PINK1* (*PARK6*; PTEN-induced kinase 1), *DJ-1* (*PARK7*), *ATP13A2* (*PARK9*), *PLA2G6*, *FBXO7*, *DNAJC6*, and *RAB39B* have been shown to cause autosomal recessive PD and/or parkinsonism (Delamarre et al., 2017; Hernandez et al., 2016).

Combining all monogenic forms of PD, about 30% of familial and 3-5% of sporadic cases can be explained (Kumar et al., 2011; Hernandez et al., 2016).

Mendelian transmission	Autosomal dominant	*SNCA, LRRK2, VPS35, CHCHD2, EIF4G1*
	Autosomal recessive	*Parkin, PINK1, DJ1, ATP13A2, PLA2G6, FBXO7, DNAJC6, RAB39B*
PD-linked genetic disease	Gaucher disease	*GBA1*
Non-mendelian transmission	SNPs increasing PD risk (GWAS)	*SNCA, MAPT, LRRK2, HLA-DRB5, BST1, GAK, ACMSD, STK39, MCCC1/LAMP3, SYT11, CCDC62/HIP1R, etc.*

Table 2: Genetics of PD. Genes implicated in mendelian and non-mendelian transmission of PD. (Modified from Delamarre et al., 2017)

For a long time, PD was considered a sporadic disease without genetic influence. However, in 1997, the α-synuclein encoding gene *SNCA* was the first gene to be discovered, causing autosomal dominant PD (Polymeropoulos et al., 1997). Today a total of seven point mutations are associated with *SNCA* familial forms of synucleinopathies: A30P, E46K, H50Q, G51D, A53E, A53T, and A30G (Polymeropoulos et al., 1997; Krüger et al., 1998; Zarranz et al., 2004; Lesage et al., 2013; Proukakis et al., 2013; Pasanen et al., 2014; Liu et al., 2021). Moreover, duplications and triplications of the complete *SNCA* gene were linked to PD (Klein et al., 2012; Hernandez et al., 2016). It has been discovered that genomic duplications and triplications of the *SNCA* gene lead to early-onset of PD. The severity and age of disease onset correlate with copy number of *SNCA*, indicating a gene-dose effect (Hernandez et al., 2016).

Additionally, several mutations have been discovered in the *Leucine-rich repeat kinase 2* (*LRRK2*) gene which are the most frequent genetic cause of late-onset PD, being found in familial (autosomal dominant) as well as sporadic cases (Lesage et al., 2006; Lesage et al., 2009; Klein et al., 2012; Hernandez et al., 2016). Another autosomal dominant mutation was detected in the *vacuolar protein sorting 35* homolog gene (*VPS35*) (Zimprich et al., 2011), encoding a protein that is possibly involved in degradation of α-syn (Delamarre et al., 2017; Hernandez et al., 2016). In general, a mutation in the gene is rare (1% of familial, 0.2% of sporadic PD) (Delamarre et al., 2017; Zimprich et al., 2011; Hernandez et al., 2016), and symptoms as well as disease onset resembles typical idiopathic PD (Kumar et al., 2012).

Unlike autosomal dominant PD that usually has an onset similar to sporadic PD, recessively inherited parkinsonism is more frequently linked to early onset PD. Autosomal recessive genes include *Parkin*, *PINK1*, *FBXO7* and *DJ1* (**Table 2**). Interestingly, the neuropathology of *Parkin* mutations consists of strong loss of SNpc neurons, but lack of post-mortem LBs in most cases (Mori et al., 2003). A possible explanation for missing LB pathology might be the early onset of the disease (Doherty Hardy, 2013), considering that no cases of juvenile-onset PD have been reported that demonstrated post-mortem LBs (Mizutani et al. 1991; Hernandez et al., 2016). Mutations in *PINK1*, *FBXO7* and *DJ1* are similarly reported to cause early-onset autosomal recessive PD. *DJ1* acts as a chaperone protein that acts against the aggregation of α-syn and its mutation leads to altered mitochondrial shape and increased ROS levels (Delamarre et al., 2017; Hernandez et al., 2016).

The most important risk factor yet discovered for PD are the mutations in the glucocerebrosidase (*GBA1*) gene, encoding the lysosomal enzyme glucocerebrosidase

(GCase). Studies have indicated that 7-10% of PD patients carry a *GBA1* mutation and *GBA1*-linked PD is clinically indistinguishable from idiopathic PD (Migdalska-Richards et al., 2016). The presence of a *GBA1* gene mutation generates the reduction in GCase enzyme activity or stability, leading to impaired lysosomal function, ER stress, Golgi fragmentation, increased apoptosis, decline of α-syn degradation/increasing α-syn aggregation, mitochondria dysfunction and fragmentation (García-Sanz et al., 2017). Homozygous mutations lead to Gaucher disease (GD), the most frequent lysosomal storage disorder. Both homozygous and heterozygous mutations in *GBA1* gene can increase the PD risk 20-30-fold (Schapira, 2015; Migdalska-Richards et al., 2016; García-Sanz et al., 2017; García-Sanz et al., 2021).

More recently, GWAS discovered single nucleotide polymorphisms (SNPs) of genes associated with increased risk of developing PD. Studies reported several additional gene associations with PD including components of the immune system and confirmed the involvement of known genes such as *SNCA* and *tau*. In 2019, the largest meta-analysis of GWAS identified 90 independent, genome-wide, statistically significant risk factors that make up for 16-36% of the heritable risk of PD (Nalls et al., 2014, Nalls et al., 2019).

In addition to genetic factors, lifestyle and environmental factors are important when talking about the multifactorial aetiology of PD. Established risk factors include environmental toxins such as pesticides, consumption of dairy products, and traumatic brain injury. Several protective factors have also been reported in multiple studies such as smoking, caffeine intake (coffee- and tea-drinking), anti-inflammatory drug use, high plasma urate levels, or physical activity (Delamarre et al., 2017; Fan et al., 2020; Balestrino et al., 2020; Bloem et al., 2021). Interestingly, estrogen might be a protective factor against PD since PD is more frequent in men compared to women, yet controversial results have been reported (Miller et la., 2010). Most recently, is has been proposed that an infection with SARS-CoV-2 shares clinical manifestations and inflammatory/molecular pathways with PD and might stimulate neurodegenerative and neuroinflammatory cascades, possibly increasing the risk of developing parkinsonism and PD (Mysiris et al., 2022).

As mentioned above, age has been shown to be the greatest risk factor for idiopathic PD. Aging can be described as a progressive accumulation of molecular and cellular dysfunction causing the breakdown of tissues that is needed to sustain life. Biological processes that are affected in aging involve mitochondrial homeostasis, protein homeostasis and inflammation. Several molecular hallmarks seen in aging brains overlap with mechanisms that are involved in PD neurodegenerative processes (**Fig. 4**). These mechanisms include oxidative damage and mitochondrial dysfunction, loss of protein homeostasis, neuroinflammation, impaired stress response. Age-related dysfunction likely affects neurons vulnerable to PD-linked risk factors (genetic and/or environmental) impairing the same processes which results in additional dysfunction and potentially promotes α-syn pathology (Coleman et al., 2022).

It is well known that dopaminergic neurons of the SNpc are most affected by neurodegeneration in PD and have been shown to be more vulnerable to cell loss in aging compared to other brain areas. Elucidating why DAergic cell populations, especially that of the SNpc, are more susceptible to age-related processes might give insights into PD disease mechanisms. The cellular environment of the SN might be an important factor for the selective vulnerability of dopaminergic SN neurons in aging and

PD. The cells of the SN are in many ways special as they are believed to be in additional oxidative stress due to DA metabolism and as well exhibit pace making activity (therefore have special calcium dynamics, see “Introduction – Parkinson’s disease – α-Synuclein – propagation and spreading”), potentially important for the maintenance of DA levels within the striatum. These characteristics make cells of the SN more sensitive to changes in protein degradation pathways and mitochondrial impairment. Age-related processes such as the loss of neuromelanin (possibly neuroprotective) pigmentation, accumulation of reactive oxygen species (ROS) generated as a by-product during DA metabolism, decreasing ability of neurons and mitochondria to handle calcium and iron levels, and decline in protein degradation efficiency are exemplary stressors that lead to cell loss of vulnerable neurons as soon as additional insults occur. Additional insults can be mitochondrial dysfunction (e.g., complex I deficiency) or α-syn mutation/accumulation of toxic species. Yet, in some cases changes in protein degradation pathways and mutations in mitochondrial DNA alone have been sufficient to cause SN cell loss. Hence, it is believed that neurons get weakened with increasing age which eventually leads to the disability to respond to further insults seen in PD. It is the ensemble of all processes that eventually induce cell loss. Interestingly, it has been shown that in addition to SN cells other neuronal cell populations are affected by similar processes such as mitochondrial alterations and LB pathology. These observations suggest that the unique mixture of these features within the SN contributes to its vulnerability and thus, to the development of PD (Reeve et al., 2014).

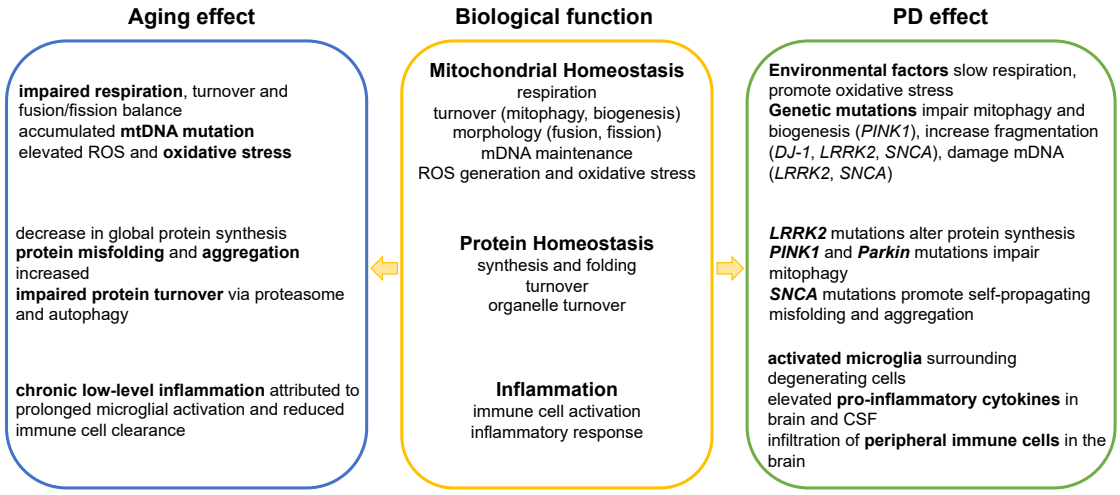

Fig. 4: Key biological processes that are affected in aging and PD. It has been shown that overlapping effects of aging and PD exist on biological processes involved in mitochondrial, protein homeostasis and inflammation. Environmental as well as genetic factors contribute to the dysfunction of processes. For additional detailed information see the review Coleman et al., 2022. (Modified from Coleman et al., 2022)

Diagnosis

When motor symptoms become evident in patients with PD, DA in the putamen is depleted around 80%, and approximately 60% of SNpc dopaminergic neurons have already degenerated. Clinically, any disease including the loss of DA in the striatum may lead to “parkinsonism”, a syndrome characterized by tremor at rest, rigidity, slowness or absence of voluntary movement, postural instability and freezing. Accounting for approximately 80% of cases, PD is the most common cause of parkinsonism (Dauer et al., 2003). In practice, PD is a clinical diagnosis including history taking and neurological examination. However, a definitive diagnosis can

usually only be made based on typical neuropathological changes in the brain (**Fig. 1**) (Bloem et al., 2021). Patients must exhibit the core clinical features as well as responsiveness of motor symptoms to levodopa administration is required to satisfy the criteria for diagnosis of PD (Berardelli et al., 2013).

Nevertheless, several non-motor symptoms, including hyposmia and RBD, arise in the prodromal phase of PD, several years before the onset and diagnosis of classic motor impairment (see “Introduction – Parkinson’s disease – Motor and non-motor symptoms”) (Ross et al., 2012; Postuma et al., 2012). It is evident that the prodromal phase is an important opportunity to identify individuals at high risk of developing PD, to gain insight in disease development and progression and constitutes a promising therapeutic window for neuroprotective treatments before the occurrence of massive neurodegeneration (Schapira et al., 2017; Balestrino et al., 2020). Prodromal symptoms have been proposed to be most effective as early biomarker in combination with other biomarkers like imaging, more-specific clinical, genetic, and/or biochemical parameters (Schapira et al., 2017). In this regard, α-syn has been suggested to be a promising biomarker in PD (Fayyad et al., 2019). Studies reported that the detection of α-syn in the cerebral spinal fluid (CSF) might present a promising tool to identify PD, reporting a decrease in the total level of α-syn levels in patients compared to control individuals (Parnetti et al., 2014; Eusebi et al., 2017; Mollenauer et al., 2019), while oligomeric α-syn species were significantly increased (Hansson et al., 2014; Fayyad et al., 2019).

α-Synuclein

The intracellular protein α-syn received initial attention when it was identified as the major component of LBs and LNs (Spillantini et al., 1997), one of the neuropathology hallmarks of PD. Since then, the protein has been linked to several neurodegenerative diseases that are commonly known as synucleinopathies, including PD, DLB, and MSA. The exact molecular mechanisms underlying pathogenesis are still unsolved, but the process of pathological aggregation of α-syn is a shared event in all diseases (Villar-Piqué et al., 2016).

Structure and physiological function

α-Syn is a small cytoplasmatic protein spanning a length of 140 amino acids. It is enriched in the presynaptic terminals, playing a role in the assembly of the SNARE complexes (Burré et al., 2010; Jan et al., 2021), and is highly expressed in the brain, but also in other organs of the adult human (Ltic et al., 2004). The protein is a product of the *SNCA* gene which is located at position 21 in the long arm of chromosome 4 (Shibasaki et al., 1995), which is the first gene identified to cause autosomal dominant PD (Polymeropoulos et al., 1997). In several studies genetic mutations (point mutations, duplications, triplications, SNPs) of *SNCA* have been linked to PD development (Polymeropoulos et al., 1997; Krüger et al., 1998; Zarranz et al., 2004; Klein et al., 2012; Lesage et al., 2013; Proukakis et al., 2013; Pasanen et al., 2014; Nalls et al., 2014; Nalls et al., 2019; Liu et al., 2021).

Structurally, α-syn can be divided in three core elements: (1) the amphipathic lysine-rich N-terminal, residues 1-60, that is known to be implicated in lipid-binding (Ulmer et al., 2005), (2) the central non-amyloid-component (NAC) domain, residues 61–95, that consists of a highly hydrophobic motif which is critical for α-syn aggregation (Giasson

et al., 2001), and (3) the acidic carboxyl-terminal region, residues 96–140, responsible for the protein's chaperone-like activity (Souza et al., 2000). Truncations or deletions of the C-terminus have been shown to enhance aggregation and cytotoxicity of α-syn *in vitro* (Hoyer et al., 2004; Tofaris et al., 2006; Ma et al., 2018).

The physiological function of α-syn remains a controversial subject. It has been suggested that α-syn acts at the presynaptic terminal regulating synaptic vesicle dynamics (Ghosh et al., 2017). This hypothesis is consistent with findings of α-syn within in the synapse (Maroteaux et al., 1988), its co-localization with reserve pool of synaptic vesicles (Lee et al., 2008), its interaction/binding with/to synaptobrevin-2 (VAMP2, a component of the SNARE complex required for synaptic vesicle fusion) and its implication in the assembly of the SNARE complex (Burré et al., 2010). Further, it has been reported that a α-syn might be implicated in DA neurotransmission (Abeliovich et al., 2000). Besides being highly abundant in the presynaptic terminals of neurons, its localization has been confirmed in most subcellular compartments such as nucleus, cytoplasm, Golgi complexes, endoplasmic reticulum (ER), mitochondria and axons (Zhang et al., 2008; Ghosh et al., 2017). Hence, it has been proposed that α-syn might have a function in the nucleus since it was initially found in the nuclear compartment, however, this finding remains controversial (Maroteaux et al., 1988; Huang et al., 2011). The protein might play a role in gene expression pathways, but it is not known if α-syn directly interacts with DNA or regulates important players in transcription (Villar-Piqué et al., 2016).

Aggregation and toxicity

The native conformation of α-syn under physiological conditions remains undetermined. It is proposed that α-syn exists in various conformations, primarily occurring as soluble intrinsically disordered monomer in the cytosol but adopting a highly ordered α-helix-rich form upon membrane binding (Jao et al., 2004; Burré et al., 2013). Also, the existence of an alternative, tetrameric, aggregation-resistant α-syn population has been reported, which remains controversial (Bartels et al., 2011). As an intrinsically disordered protein, α-syn is thought to change between various conformations, ranging from fully unfolded to a fully folded protein (**Fig. 5 A**).

On the other hand, α-syn as an amyloid protein can form aggregates. It has been shown that the natively unfolded protein contains the property to self-assemble into higher-order structures (amyloid fibrils) upon *in vitro* incubation for a long time (Conway et al., 2000; Ghosh et al., 2017; Polinski et al., 2018). Isoforms can perform drastic structural changes that produce β-sheet-like assemblies, precursors of more complex amyloid forms of the protein. After initial aggregation, small oligomeric species (intermediate species in the aggregation process) are formed that are stabilized by sheet interactions, giving rise to higher molecular weight, insoluble protofibrils that polymerize into amylogenic fibrils which are found in LBs (Estaun-Panzano et al., 2023). The self-assembly pathway of α-syn is presented in **Fig. 5 B**. While the primary nucleation process is critical for the formation of initial fibrils from monomers, later amyloid structures are similarly problematic since they act as a "black hole", attracting more and more monomers to form fibrils. This process is known as secondary nucleation and involves the fragmentation of pre-formed fibrils which increases the number of ends for the elongation process. Also, it catalyses the formation of more oligomers by interaction of monomers with the surface of fibrils (Ghosh et al., 2017; Estaun-Panzano et al., 2023). The process of α-syn self-assembly follows a sigmoidal

growth curve of three phases: (1) initial lag phase, where the aggregation prone nucleus is formed (primary nucleation), (2) growth phase of fibril elongation, and (3) plateau phase of fibril maturation (Jan et al., 2021; Ghosh et al., 2017; Estaun-Panzano et al., 2023).

In vitro several external factors have been shown to induce misfolding and aggregation of α-syn: acidic pH, increasing temperature, molecular crowding, organic solvents, pesticides, metal ions and α-syn binding proteins. Further, membranes and membrane binding might influence physiological function and aggregation of α-syn along with post-translational modifications such as phosphorylation, ubiquitination, nitration, N-terminal acetylation, lysine modification, truncation (Ghosh et al., 2017, Jan et al., 2021). In general, physiological processes such as mitochondrial impairment, defect of lysosomal autophagy and ubiquitin-proteasome systems, oxidative stress, and neuroinflammation are processes that not only contribute to the misfolding of α-syn, but also the spreading of pathology and progression of PD (Gómez-Benito et al., 2020).

Notably, the vast majority of α-syn accumulated in LBs are phosphorylated at the C-terminally located serine residue-129 which makes Ser129 hyperphosphorylation a widely regarded pathological hallmark of PD and other synucleinopathies (Fujiwara et al., 2002). But not only environmental aspects, also genetic features influence the state of α-syn regarding oligomer and fibril formation. Investigating familial PD-linked *SNCA* mutations *in vitro* revealed distinct effects on the aggregation properties (oligomerization and fibrillation) of α-syn. So far, studies discovered that E46K (Choi et al., 2004), A53T (Conway et al., 1998), H50Q (Ghosh et al., 2013) mutations, enhance α-syn fibril formation, while A30P (Conway et al., 2000), G51D (Fares et al., 2014), A53E (Ghosh et al., 2014) mutations decelerate α-syn fibrillation rate. Moreover, A30P (Conway et al., 2000) and G51P (Fares et al., 2014) mutations were proposed to accelerate non-fibrillar aggregation by α-syn.

Importantly, the final structure of amyloid fibrils is dependent on several factors: (1) the possible β-sheet conformations of monomers as the initial starting point and (2) external factors such as pH, specific cellular and/or extracellular environment. Different condition result in different species of α-syn aggregates (polymorphs) with variable toxicity and manifestations. These different species are also known as α-syn strains and target distinct brain regions and cell types, giving rise to different pathological responses dependent on their properties (Lau et al., 2020; Estaun-Panzano et al., 2023). Among synucleinopathies different types of cerebral α-syn inclusions can be observed which might be attributed to the heterogeneity of α-syn strains, each reflecting the spread and growth of different amyloid species (Estaun-Panzano et al., 2023). While the presence of LBs/LNs within neurons is the pathological hallmark of PD and DLB (Spillantini et al., 1998b), MSA is characterized by the cytoplasmatic aggregation of α-syn in oligodendrocytes (Spillantini et al., 1998a).

Regarding toxicity of α-syn species, it is not answered yet whether oligomers, rather than mature fibrils are the most potent neurotoxic species causing degeneration in PD. Many findings support the notion of oligomeric α-syn species being the most toxic form (Winner et al., 2011; Karpinar et al., 2009). Consistently, increased levels of soluble α-syn oligomers have been found in brain and CSF of patients containing LB pathology compared to healthy controls (Paleologou et al., 2009; Hansson et al., 2014). Studies revealed that non-fibrillar oligomers bind to the cell membrane, cause toxicity, and increase reactive ROS (Ghosh et al., 2017). However, several studies suggest toxicity

for fibrillar and mature α-syn species since α-syn fibrils display prion-like behaviour and can seed α-syn aggregation. Exogenous introduced α-syn fibrils have the capacity to get internalized in the cell to induce endogenous α-syn of the cell to form LB-like inclusions, cause toxicity and spread the disease pathology through cell-to-cell transmission mechanisms (Volpicelli-Daley et al., 2011; Luk et al., 2012a, Luk et al., 2012b, Recasens et al., 2014). These findings indicate that not only oligomers, but also fibrils exhibit pathological features. Another theory suggests mature α-syn aggregates to be a protection mechanism to trap toxic oligomers, as the formation of aggregates has been linked to decreased cytotoxicity, and α-syn inclusions might constitute protective cell aggresomes (Tanaka et al., 2004; Wakabayashi et al., 2007; Villar-Piqué et al., 2016).

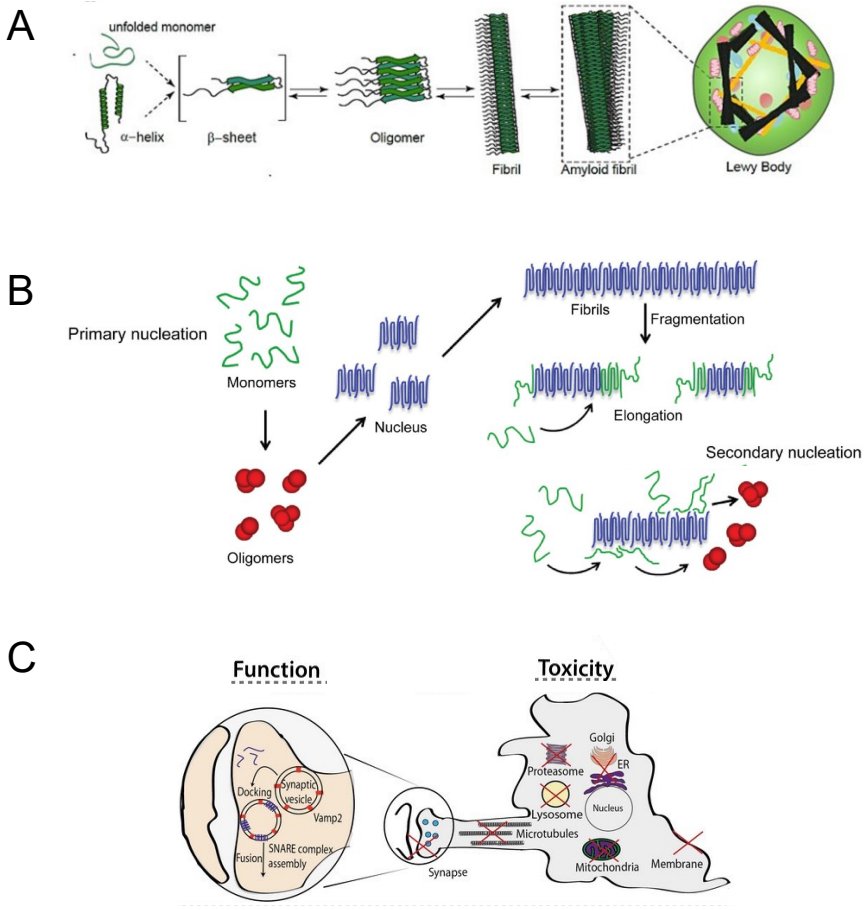

Fig. 5: Schematic representation of α-syn aggregation, nucleation processes and the physiological functions of α-syn that are impaired in pathological α-syn state. (**A**) Aggregation process of α-syn. Different monomeric conformations exist in an equilibrium, ranging from a fully unfolded to a fully folded state. Aggregation involves the formation of β-sheet assemblies that lead to the formation of complex fibrillated forms which are found in LBs. (Modified from Estaun-Panzano et al, 2023) (**B**) Self-assembly pathway of α-syn. Primary nucleation describes the initiation of the aggregation process, when monomers form oligomeric species, while secondary nucleation involves the formation of oligomeric species from monomers in a fibril-catalyzed manner. (Modified from Ghosh et al., 2017) (**C**) Function of α-syn and defects in pathological state. Among other tasks, α-syn functions at the presynaptic terminal, regulating synaptic vesicle dynamics and is implicated in the assembly of the SNARE complex. In its toxic state, α-syn becomes dysfunctional affecting intracellular organelles and pathways including proteasomes, ER-to-Golgi trafficking, lysosomes, microtubules, mitochondria, and membranes. (Modified from Villar-Piqué et al., 2016)

Several findings have shown that the pathological aggregation of α-syn affects synaptic function by inducing calcium dyshomeostasis, mitochondrial impairment, ER stress,

impairment of protein clearance pathways such as autophagy, disruption of biological membranes, neuroinflammation and oxidative stress. In general, pathological α-syn aggregates disturb several intracellular organelles and pathways including proteasomes, lysosomes, synapses, microtubules, ER-to-Golgi trafficking, mitochondria, and membranes (**Fig. 5 C**) (Villar-Piqué et al., 2016; Gómez-Benito et al., 2020; Jan et al., 2021). α-Syn degradation occurs via the autophagy-lysosomal and ubiquitin-proteasome system (UPS) pathway (Webb et al., 2003). Hence, disruption of clearance pathways further aggregation of abnormal α-syn and its self-propagation. Also, lipid membranes and crowded organelles have been found in LBs, suggesting that alteration of these structures contribute to LB formation (Shahmoradian et al., 2019). Moreover, α-syn aggregates in the presynaptic terminal disturbs SNARE complex-assembly and consequently decreases the efficiency of DA release from nerve terminals, causing impairment of synaptic function (Garcia-Reitböck et al., 2010).

Propagation and spreading

The findings of α-syn aggregations in form of LBs and LNs in grafted fetal mesencephalic progenitor neurons in the striatum of PD patients provided initial evidence supporting the hypothesis of “prion-like” propagation of α-syn (Kordower et al., 2008; Li et al., 2008). Since then, *in vitro* studies have revealed that (1) cultured neurons are able to secrete into and take up α-syn from the extracellular space and (2) the treatment of cultured cells with recombinant α-syn fibrils induces the assembly of endogenous α-syn into Lewy-like structures (Luk et al., 2009; Volpicelli-Daley et al., 2011; Reyes et al., 2015). These findings suggest the potential of α-syn to seed pathological conversion of endogenous α-syn and to propagate throughout the brain.

Based on these *in vitro* studies, observations have been confirmed in *in vivo* models of PD. It has been reported that α-syn seeds from recombinant proteins (pre-formed fibrils) (Kim et al., 2019; Luk et al., 2012a; Patterson et al., 2019; Paumier et al., 2015; Rey et al., 2016; Shimozawa et al., 2017) or aggregates containing-lysates from diseased brains (Recasens et al., 2014; Herman et al., 2023) can induce propagation of α-syn in rodents and non-human primates, supporting the hypothesis of its prion-like nature. Additionally, studies of neural stem cell transplantation into transgenic mice expressing human α-syn (Deplats et al., 2009) further support the ability of long-distance α-syn propagation.

Despite the evidence of α-syn containing the ability of cell-to-cell transfer, the underlying molecular pathways remain largely elusive. It is thought that α-syn undergoes exocytosis, being released from the cell into the interstitial compartment as naked protein or in vesicles, so-called exosomes (Shi et al., 2014; Stuendl et al., 2016; Peng et al., 2020; Jan et al., 2021). Interestingly, not only neurons, but also microglial exosomes might significantly contribute to the progression of α-syn pathology (Guo et al., 2020). However, the conformational properties regarding conformational state are unknown. Once released, α-syn might interact with extracellular components, and has been shown to be taken up by neighbouring cells via various routes which include (1) direct penetration of the membrane, (2) fluid-phase or (3) receptor-mediated endocytosis, (4) fusion of plasma-exosomal membranes, and (5) tunnelling nanotubes that directly connect two adjacent cells (Abounit et al., 2016; Peng et al., 2020; Jan et al., 2021). Within the recipient cell, α-syn seeds undergo post translational modifications, including truncation, phosphorylation, ubiquination, which promote the

interaction with α-syn monomers and other cytosolic proteins, enhancing α-syn aggregation and propagation (Peng et al., 2020; Jan et al., 2021).

However, not all PD patients exhibit LB pathology, and the presence of LB pathology does not necessarily lead to functional deficits in surviving neurons. These observations have challenged the theory of "prion-like" nature of α-syn (Parkkinen et al., 2005; Kordower et al., 2008; Gómez-Benito et al., 2020). It has led to the postulation of the "selective neuronal vulnerability" hypothesis, stating that certain neuronal population are more at risk to adverse stimuli from the local microenvironment (e.g., neuroinflammation, metabolic defects) due to their inherent cellular and functional properties, which in turn contributes to the propagation of α-syn (see "Introduction – Parkinson's disease – Aetiology"). It has been reported that, in a cytoarchitectural aspect, cells typically affected by α-syn pathology are CNS projection neurons with thin, long unmyelinated, or poorly myelinated axons, and high number of axonal terminals (e.g., hyperbranching axons) (Cheng et al., 2010; Jan et al., 2021). Interestingly, in the rat brain a dopaminergic neuron makes up to a quarter million striatal synapses, whereas the human brain contains 10-times higher number of vesicle release sites (Matsuda et al., 2009). Also, functional properties of cell populations have been postulated as factor predisposing neurons to α-syn related toxicity, which does not necessarily correlate with LB burden. For instance, SNpc dopaminergic neurons exhibit autonomous pace making activity that includes large intracellular Ca^{2+} oscillations and low Ca^{2+} buffering. This activity enables the sustained release of DA which is necessary for the proper functioning of target structures, including the striatum (Guzman et al., 2009; Jan et al., 2021). Impaired calcium handling is part of age-related dysfunctions that occur in dopaminergic SNpc neurons. These observations give a hint on why specific neuron populations, here DAergic SNpc cells, might be more susceptible to adverse stressors such as aggregation and propagation of α-syn. Several age-related processes involved in dopaminergic cell death in SNpc neurons are discussed above (see "Introduction – Parkinson's disease – Aetiology"), further supporting selective neuronal vulnerability hypothesis of the dopaminergic SNpc population.

Moreover, it has been shown that glial cells and neuroinflammation play an unneglectable role in α-syn pathology. The intramuscular injection of α-syn fibrils in human A53T transgenic mice did not only produce α-syn pathology and neurodegeneration, but also astrogliosis at a later timepoints (Sorrentino et al., 2018). Similarly, hind limb intramuscular injection of α-syn in wild-type (WT) and transgenic mice induced widespread CNS α-syn pathology, accompanied by astrogliosis, microgliosis, and motor impairments (Sacino et al., 2014). Misfolded α-syn might trigger the activation of microglia, while activated microglia can promote the abnormal aggregation of α-syn via toxic cytokine release, creating a positive feedback loop between inflammation and aggregation. Hence, it remains unclear if inflammation is the cause or consequence of protein aggregation in this context (Olanow et al., 2019; Gómez-Benito et al., 2020). These findings support the concept that glial cells influence the formation and propagation of α-syn aggregates, possibly having an effect on the local environment of neuronal populations.

Models of Parkinson's disease

In general, the use of animal models is highly needed in research to understand biological mechanisms in health and disease, and the development of diagnostic methods and therapeutical strategies. PD is considered a heterogenous disease with multiple factors causing disease onset, various symptoms, and distinct rate of progression. The heterogeneity of the disease has led to the establishment of numerous models to study the different aspects of PD, while no model can perfectly mimic all pathological and clinical features of human PD. PD model systems can be distinguished between (1) toxin-based models, (2) genetic models, and (3) α-syn propagation models based on the introduction of exogenous α-syn species.

Toxin-based models

The most classical models of PD remain neurotoxin models. These models are based on the degeneration of dopaminergic neurons which is induced by the local or systemic administration of neurotoxins. Neurotoxins used include 6-hydroxydopamine (6-OHDA) and 1-methyl-4-phenyl-1,2,3,6-tetrahydropyridine (MPTP), and other pesticides such as rotenone, paraquat, maneb, and trichloroethylene, while 6-OHDA and MPTP are the most commonly used toxins. These models are valuable since they are relatively easy to establish, and their results can be compared with a large amount of previously conducted studies. Nevertheless, a huge drawback of neurotoxin models is that they only elicit motor symptoms, reflecting the late, chronic, dopamine-depleted state, without reliably presenting neuropathological features, including α-syn pathology (Kin et al., 2019). Further, the analysis non-motor features can be impeded by robust motor phenotypes (Taguchi et al., 2020).

Genetic models

Genetics plays an important part in the development of PD as several disease-modifying mutations have been found in familial PD and several genetic risk factors have been identified in GWAS (see chapter "Parkinson's disease – Aetiology"). The α-syn encoding gene *SNCA* was the first gene to be associated with PD, together with the finding of α-syn aggregates being the major component of LBs (Spillantini et al., 1997; Polymeropoulos et al., 1997). Since then, research has focused on α-syn based models, but also additional monogenic PD mutations have been used to generate PD models and study the effects of mutated proteins in PD (**Table 3**) (Konnova et al., 2018).

Genetic manipulation is achieved by (1) generating transgenic organisms or (2) administrating viral vectors that mediate the overexpression of α-syn (Kirik et al., 2002; Kirik et al., 2003; Decressac et al., 2012; Oliveras-Salvá et al., 2013). Mutated genes in transgenic animals include *SNCA* (Giasson et al., 2002; Rockenstein et al., 2002; Tofaris et al., 2006; Cannon et al., 2013; Janezic et al., 2013) and other PD-related genes such as *DJ-1* (Goldberg et al., 2005; Kim et al., 2005), *Parkin* (Goldberg et al., 2003), *Pitx3* (Hwang et al, 2003), *LRRK2* (Lin et al., 2009; Hinkle et al., 2012), and *PINK1* (Akundi et al., 2011).

Transgenic models modifying α-syn are useful to investigate the role of α-syn and its relation to PD and similarities to other synucleinopathies. Though, it has to be considered that, in general, transgenic modulation affects early development stages, which interferes with the modelling of late onset neurodegeneration. Also, there is an

inherent risk of transgenic models which is the development of compensatory mechanisms and additional deficits during development (Konnova et al., 2018). Some studies of genetic models revealed changes in motor function and behaviour (Hinkle et al., 2012), yet many studies assessing the integrity of the nigrostriatal DA system did not observe loss of dopaminergic neurons (Goldberg et al., 2003; Hinkle et al., 2012; Blesa et al., 2014). Until now, various α-syn overexpression transgenic models have been developed, though results remain very variable. It has been observed that the extent of dopaminergic neurodegeneration primarily depends on the promotor used to drive transgene expression and protein expression level. In general, the findings suggest that genetic alternation in transgenic mice are insufficient to reproduce all the neuropathological hallmarks of PD (Blesa et al., 2014).

Locus	Gene	Mutation	Protein	Inheritance
PARK1	*SNCA*	A30P, A53T, E46K	α-syn	Dominant
PARK2	*PRKN*	Various mutations, exonic deletions, duplication and triplication	Parkin	Recessive
PARK4	*SNCA*	Duplication and triplication	α-syn	Dominant
PARK5	*UCH-L1*	I93M and S18Y	UCH-L1	Dominant
PARK6	*PINK1*	G309D, exonic deletions	PINK1	Recessive
PARK7	*DJ-1*	Homozygous exon deletion, L166P	DJ-1	Recessive
PARK8	*LRRK2*	G2019S, R1441C/G, and others	Dardarin	Dominant

Table 3: Familial mutations that have been used in genetic animal models of PD. Mutation used are in genes encoding for proteins implicated in biological processes linked to PD progression. (Modified from Konnova et al., 2018)

In 2013, Janezic and colleagues created a transgenic mouse line overexpressing α-syn which was generated by injecting a bacterial artificial chromosome (BAC) construct carrying the complete 111-kb human wild-type *SNCA* locus and endogenous promotor sequences into C57/Bl6 pronuclei. The BAC technology allows the expression of a transgene under the control of native promoters and regulatory elements, enabling a physiological spatio-temporal expression profile of the transgene product. The *SNCA*-OVX mouse line expresses WT human α-syn onto an α-syn-null ($Snca^{-/-}$) pure C57/Bl6 background to prevent interactions with endogenous mouse α-syn. The level of α-syn overexpression in *SNCA*-OVX mice mirrors the alteration in human α-syn levels resulting from a triplication of *SNCA* locus in familial PD (Miller et al., 2004). Additionally, elevated levels of α-syn have been reported in sporadic PD in which a 6-fold increase in α-syn mRNA levels was observed in remaining DA midbrain neurons from patients (Gründemann et al., 2008). Therefore, this model was proposed to be useful for modelling both familial and sporadic PD. The mice display early deficits in DA release from terminals in the dorsal striatum, which is followed by neurodegeneration of SNpc DA cells and reduced spontaneous firing rate of these neurons. In sum, the greatly reduced DA output, results in motor impairments in aged animals. However, DA dysfunction and neurodegeneration occurred although no pathological protein aggregation was present in the striatum and SNpc (Janezic et al., 2013).

Regarding viral vector-mediated models, advantages are targeting of the nigrostriatal system, the induction of pathology in adulthood, and the possibility to adjust dosage. To induce overexpression of α-syn in rodents, recombinant adeno-associated virus

(rAAV) and lentivirus (LV)-based vectors have been used in previous studies. It has been shown that not only the genetic variant of the gene, but also the viral vectors, the dose administered, and the transfection efficiency influence the PD phenotype (Konnova et al., 2018; Van der Perren et al., 2015; Kirik et al., 2002).

The overexpression of α-syn mediated by rAAV is an important model to study α-syn aggregation and its contribution to neurodegeneration, and consequently motor and cognitive impairment, along with evaluation of potential therapeutics (Gómez-Benito et al., 2020). By overexpressing WT α-syn or expressing PD-associated mutations (A53T, A30P) of α-syn utilizing rAAV, dopaminergic SNpc neurons are progressively lost (Koprich et al., 2011; Oliveras-Salvá et al., 2013; Ip et al., 2017) and striatal DA is decreased (Koprich et al., 2011; Ip et al., 2017). However, the degree of neurodegeneration is variable among studies, depending on serotypes, promotors, α-syn species, doses, injection site. Also, species, strain and age of animals used influence the phenotype observed (Gómez-Benito et al., 2020). In addition to dopaminergic loss, some studies show motor alterations following rAAV-mediated α-syn overexpression, appearing several weeks after viral injection (Kirik et al., 2002; Decressac et al., 2012; Oliveras-Salvá et al., 2013; Ip et al., 2017). Moreover, rAAV-mediated overexpression models induce α-syn pathology with a dramatic increase in the levels of the protein (Kirik et al., 2002; Oliveras-Salvá et al., 2013; Van der Perren et al., 2015; Ip et al., 2017; Gómez-Benito et al., 2020). These levels were higher than those found in idiopathic PD or even in patients with *SNCA* multiplications suggesting that this model might not be suitable to reproduce human PD and study mechanisms related to idiopathic PD (Duffy et al., 2018a). Injections of rAAV overexpressing α-syn generate hyperphosphorylated syn (pα-syn) immunoreactive inclusions that are proteinase-K resistant (Ip et al., 2017), but do not reproduce morphological features of human LBs. Immunoreactive pα-syn inclusions are frequently localized to the nucleus (Duffy et al., 2018a) and are present as small and punctuate structures (Ip et al., 2017; Gómez-Benito et al., 2020), in contrast to large, cytoplasmic aggregates found in human Lewy pathology. Further, it has been observed that α-syn expression is maintained within striatal MSNs, travelling from the cell body to the terminals in an anterograde manner. No transmission of α-syn aggregates to other non-transduced cells was observed, despite expression of endogenous α-syn. Hence, α-syn pathology is restricted to neurons transduced by rAAV which makes this model not useful to study the prion-like behaviour of pathological α-syn aggregates (Gómez-Benito et al., 2020).

α-Syn propagation models

A suitable model for studying the prion-like behaviour of α-syn and its propagation through the brain is the inoculation with exogenous α-syn. As described in chapter “α-Synuclein – propagation and spreading” several *in vitro* and *in vivo* studies have previously shown the potential of α-syn to seed pathological conversion of endogenous α-syn and its ability to propagate throughout the brain. Most of these models based on the inoculation with pre-formed fibrils (PFFs) or PD brain lysates have demonstrated progressive protein aggregation, neuronal loss, neuroinflammation, and development of motor deficits (Recasens et al, 2014; Paumier et al., 2015; Shimozawa et al., 2017; Patterson et al., 2019; Chung et al., 2019). These studies report that endogenous α-syn is required for developing the pathology, and PFFs α-syn might act as a template for endogenous α-syn to convert into pathological inclusions (Luk et al., 2012b; Kim et al., 2019; Recasens et al., 2014; Gómez-Benito et al., 2020).

The intracerebral introduction of PFFs induce the accumulation of phosphorylated α-syn, localized in the soma as well as cellular processes. Some studies reported co-localization of pα-syn inclusions with markers found in human Lewy pathology, indicating that they share common properties (Gómez-Benito et al., 2020). Moreover, aggregates are hyperphosphorylated at Ser129, thioflavin S-positive, proteinase-K-resistant, and co-localize with p62 and ubiquitin (Rey et al., 2016; Paumier et al., 2015; Luk et al., 2012a; Luk et al., 2012b; Duffy et al., 2018b; Chung et al., 2019). However, pα-syn immunoreactive aggregates present different morphological features than human LBs: from granules with cytoplasmic staining, wrapped around the nucleus, to compact, rounded structures with dark staining in the entire cell (Luk et al., 2012a; Paumier et al., 2015; Rey et al., 2016; Gómez-Benito et al., 2020).

All studies have shown the spreading of pathological α-syn from the injection site to anatomically interconnected brain regions. It is proposed that fibrils are taken up by nerve terminals, and then travel to the cell body following a fibrillary retrograde transport (Gómez-Benito et al., 2020). When PFFs are injected into the striatum, α-syn inclusion are picked up by terminals close to the injection site, and can be detected in other brain areas over time, such as locus coeruleus, SNpc, thalamus, hypothalamus, amygdala, neocortex, indicating that there is a time-dependent propagation of α-syn pathology (Luk et al., 2012a; Luk et al., 2012b; Paumier et al., 2015; Patterson et al., 2019). Depending on injection site and rodent model, unilateral inoculation can generate bilateral pathology. Still, contralateral pathology has been shown to develop at lower levels and later time points compared to the ipsilateral hemisphere. The fibers are mainly found in the striatum, but also motor cortex, amygdala, and SN (Luk et al., 2012a; Luk et al., 2012b; Paumier et al., 2015; Gómez-Benito et al., 2020; Polinski et al., 2021).

Even though the striatum is the most commonly used intracerebral injection site, also OB, hippocampus, SN has been used for inoculation with PFFs, along with peripheral sites such as intramuscular, intraglossal, intraperitoneal, intestinal and intravitreal injections (Chung et al., 2019; Polinski et al., 2021; Pérez-Acuña et al., 2023). It is evident that the propagation pattern is variable depending on injection site since α-syn spreading follows neural connection trajectories. But not only the injection site, also the amount and type of PFFs contribute to high variability between PFF-injected models (Polinski et al., 2021; Chung et al., 2019) and the animal/strain used (Luk et al., 2012a). Another important aspect is the high precision is needed during surgical procedures to enable adequate inoculation at the site of interest (Gómez-Benito et al., 2020). Also, it has been shown in previous studies that species from which α-syn PFFs are derived seems to be critical for the efficient formation and propagation of aggregates, indicating more efficient aggregate formation when PFFs are derived of the same origin as endogenous α-syn (Fares et al., 2016, Luk et al., 2016; Rey et al, 2016; Kim et al., 2019).

According to the Braak's hypothesis (Braak et al, 2003; Braak et al., 2004), α-syn PFFs have also been administered through peripheral routes such as OB and GIT. Supporting the viewpoint of the "gut-brain" axis, several models have been established where α-syn was injected into the GIT. Exogenous inoculation with PFFs or PD brain lysates into the GIT of WT rats have shown emergence of α-syn aggregation in the ENS, subsequently inclusions in the DMX two days post injection (Holmqvist et al., 2014). Initial models of α-syn fibril injections into the stomach of mice did not show

further propagation from the DMX to the CNS (Uemura et al., 2018), mice injected with α-syn fibrils into the stomach and duodenum displayed α-syn propagation from the brainstem to the midbrain, amygdala, hippocampus, and eventually olfactory bulb (Kim et al., 2019). 1 month post inoculation stool number per passage and water content were reduced, motor symptoms, anxiety/depression, memory impairment was observed after 7 months, and finally 9 months post injection the olfactory system was affected. This α-syn propagation model was able to reproduce motor as well as non-motor symptoms of PD from prodromal disease stages (Taguchi et al., 2020). In a study where PFFs were injected into the OB of mice, pathological pα-syn aggregation was found in areas distant to the injection site which indicates the spatial progression of α-syn pathology over time. Further, DA cell loss and olfactory dysfunction was observed 1 month post injection (Rey et al., 2016; Rey et al., 2018). These models are valuable to study α-syn propagation in early disease stages and investigate prodromal PD symptoms.

It can be concluded that models of α-syn propagation are a valuable tool to reproduce the LB-like pathology, investigate the spatio-temporal propagation of pathological aggregates, determine their anatomical, molecular and behavioural impact, as well as to develop and test therapies aiming to impede formation of inclusions and their spreading. Yet, there is great variability among results of generated PFF-based models, especially between research groups. Therefore, standard protocols for the preparation of PFFs are needed, along with studies to improve optimal conditions for generating the models (e.g., concentration/origin of PFFs, site of injection, strain) to obtain efficient and robust phenotypes (Chung et al., 2019; Gómez-Benito et al., 2020). Here, we have established a new murine model of PD by injecting human wild-type α-syn PFFs into the dorsal striatum of the *SNCA*-OVX transgenic mouse model (Janezic et al., 2013).

Hypothesis and objectives

Parkinson's disease (PD) is a heterogenous disease with many different phenotypes, patterns of progression, pathological findings, genetic predispositions, whose complex aetiology is not completely understood. To unravel the molecular bases that lead to the onset and progression of the disease, as well as the development of therapeutic strategies that can prevent or slow down disease progression, animal models that accurately recapitulate the PD pathology are needed. However, so far, models developed only reproduce certain aspects of the disease, leaving room for improvement of PD models.

Recently, a transgenic mouse line that overexpresses human α-syn (*SNCA*-OVX) was generated, displaying early DA release deficits from terminals in the dorsal striatum, followed by the loss of dopaminergic SNpc neurons and motor impairment in aged animals in the absence of pathological protein aggregation. The model reflects the spatio-temporal expression pattern of human α-syn, is absent of murine endogenous α-syn, and shows α-syn expression levels similar to those in familial and sporadic human PD (Janezic et al., 2013). Furthermore, previous studies have shown that intracerebral or systemic administration of synthetic α-syn PFFs (Kim et al., 2019; Luk et al., 2012a; Patterson et al., 2019; Paumier et al., 2015; Rey et al., 2016; Shimozawa et al., 2017), PD-patient derived LB extracts (Recasens et al., 2014) and CSF-extracellular vesicles from patients (Herman et al., 2023) induces PD-like pathology in rodents and non-human primates. It is well established that these models are a valuable tool for studying the spreading of α-syn, dopaminergic neurodegeneration and neuroinflammation.

Based on these previous findings the following hypothesis and objectives are proposed for this master thesis.

Hypothesis

The intrastriatal inoculation with human wild-type α-syn pre-formed fibrils (PFFs) of the *SNCA*-OVX transgenic mouse model boosts α-synuclein neuropathology, further disrupting nigrostriatal pathway and worsening motor symptomology.

General objective

The overall objective of this thesis was to establish and characterize a novel Parkinson's disease (PD) mouse model. Therefore, the *SNCA*-OVX transgenic mouse line was inoculated with human wild-type α-syn PFFs. Resulting PD-like pathology was characterized including induction of α-synuclein aggregation and spreading, dopaminergic neurodegeneration, and motor behaviour.

Specific objectives

1. To characterize α-syn pathology in the *SNCA*-OVX mouse model following human wild-type α-syn PFF inoculation into the dorsal striatum.
2. To determine the integrity of the nigrostriatal pathway upon human wild-type α-syn PFF injection into the *SNCA*-OVX mouse model.
3. To evaluate the motor impairment after α-syn PFF injection into the *SNCA*-OVX mouse model.

Experimental design

The experimental design of this study is illustrated in **Fig. 6**. To establish a novel PD mouse model, transgenic *SNCA*-OVX mice were unilaterally injected with human wild-type α-syn pre-formed fibrils (PFFs) into the right dorsal striatum. 150 days post injection (dpi), PFF-inoculated mice performed the challenging beam transversal test to assess motor performance and fine motor control. Then, animals were sacrificed 150 dpi and histological analysis was performed to investigate PD-related pathology on a histological level. As control, intact *SNCA*-OVX and *Snca*$^{-/-}$ (Ctrl) mice were used.

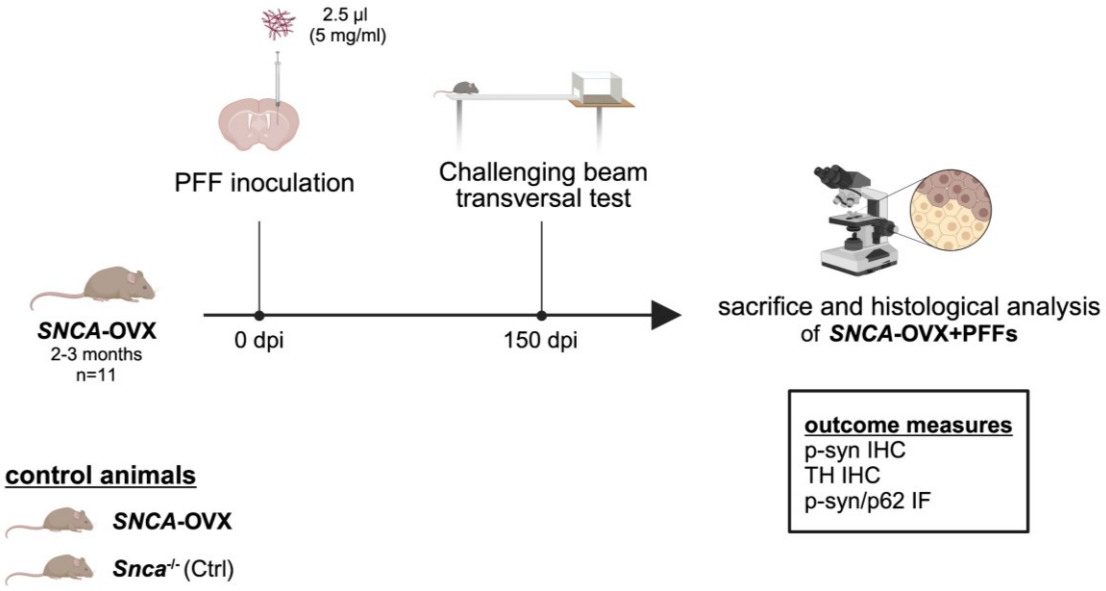

Fig. 6: Experimental design of the study. *SNCA*-OVX mice were injected with human wild-type α-syn PFFs. 150 dpi animals performed the challenging beam transversal test and were sacrificed for histological analysis. Control animals were intact *SNCA*-OVX and *Snca*$^{-/-}$ (Ctrl) mice. (Created using BioRender.com)

Material and Methods

Animals

In this study the *SNCA*-OVX transgenic mouse model (C57BL/6OlaHsd) was used as previously described in Janezic et al. (2013). A total of 11 female and male *SNCA*-OVX mice between 2 and 3 months of age were used for the inoculation with human wild-type α-syn PFFs. As control, *SNCA*-OVX and *Snca*$^{-/-}$ (Ctrl) of both sexes were included in this study. 6-months-old *SNCA*-OVX mice, along with *Snca*$^{-/-}$ (C57BL/6OlaHsd) (Specht et al., 2001) of 6 and 12 months, respectively, were used. For the behavioural test, control animals were different from those used for histochemical analysis. Animals were 6 months old (both sexes). The number of subjects for each experiment is indicated in figures and graphs.

Animals were housed under standard laboratory conditions at 22°C room temperature, a humidity of 20% in a 12-h light/dark cycle with water and food ad libitum. Mice were reared in social groups of 3-6 mice per cage. Animal care, husbandry and experiments complied with current European (2010/63/EU) and Spanish (RD53/2013) legislation. All procedures have been approved by the Animal Experimentation Ethics Committee of the Cajal Institute, the CSIC (Consejo Superior de Investigaciones Cientificas) and the Community of Madrid.

Injection material and administration

Pre-formed fibrils (PFFs)

The human wild-type α-syn PFFs were obtained from the laboratory of Kelvin C. Luk (University of Pennsylvania, Department of Pathology and Laboratory Medicine, USA) and prepared as previously described (Giasson et al., 2001, Luk et al., 2009, Volpicelli-Daley et al., 2011, Luk et al., 2012b). In short, full-length wild-type human α-syn was expressed in *Escherichia coli* followed by purification and an *in vitro* fibril assembly of purified α-syn monomers (5 mg/ml). Human PFFs were collected after 5 days of incubation at 37°C with constant agitation and stored in aliquotes at -80°C until use. Shortly before intracerebral injection, PFFs were diluted in sterile PBS (2 mg/ml) and sonicated. Injected volume of PFFs was 2.5 µl per animal.

Stereotaxic injection

Stereotaxic surgical procedures were performed as previously described (Zhang et al., 2019, Luk et al., 2012b, Chatterjee et el., 2018). Mice were placed under deep surgical anaesthesia (1% isoflurane) during all surgical procedures and set into a stereotaxic frame with a mouse adaptor. For inoculation with α-syn PFFs animals received unilateral injections of prepared human α-syn PFFs (2.5 µl, 5 µg) into the right dorsal striatum using the following coordinates: AP +0.2 mm, ML +2.0 mm, DV -3.56 mm from the cranium (**Fig. 7**). Injections were performed with a Hamilton syringe at a flow rate of 0.4 µl/min with the needle kept in place for ≥ 5 minutes. Control animals did not receive an injection.

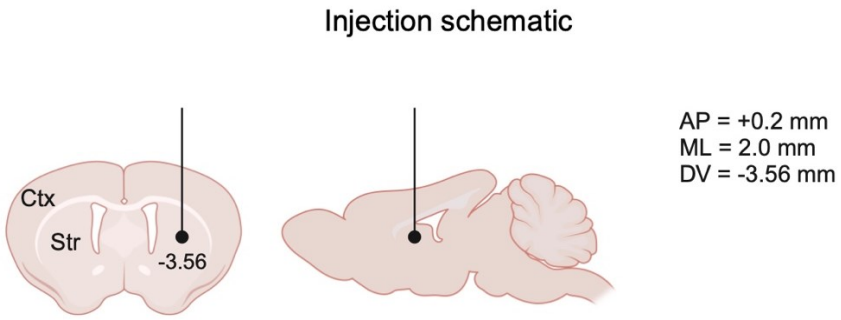

Fig. 7: Schematic diagram of stereotaxic PFF injection into the right dorsal striatum. Coordinates of intrastriatal injection of human wild-type α-syn PFFs are illustrated. Coronal view (left), sagittal view (right). (Idea from Luk et al., 2012a) (Created using BioRender.com)

Behaviour experiment

Challenging beam transversal test

Motor performance was measured using a beam test previously described in detail by Fleming et al. (2004). The test was carried out on a Plexiglas beam of 1 m length and 17 cm height that progressively gets narrow from 3.5 cm to 0.5 cm. The end of the beam lead directly into the animal's home cage. Animals were transferred to the testing room 30 minutes prior to the first trial for acclimation. On two consecutive days animals were trained to cross the beam from the widest to the narrowest section. On the first training day, animals received one assisted and one unassisted trial. Guidance included positioning the home cage in close proximity the animal to encourage forward movement along the beam. On the consecutive training day, animals traversed the beam without guidance of the experimenter. On the third day, a metal grid with 0.8 cm-diameter holes was placed 1 cm above the beam and animals were recorded while traversing the beam for a total of 2 trials.

Videotapes were viewed in slow motion and each animal was rated manually for latency and number of steps needed to traverse the beam along with the number of errors conducted. Parameters were only measured when animals performed a forward movement. A timer was set when animals started walking towards their home cage after being placed on the beam and stopped when the head crossed the edge of the beam into the home cage. Steps were counted for each forward-directed movement of the left hindlimb. An error was counted when a limb (forelimb or hindlimb) slipped through or missed the grid and was visible between the grid and the beam surface. Trials of animals that did not cross the beam within 120 seconds were excluded. Time, number of steps, and errors per step scores were calculated for both trails and averaged.

Histological stainings

Sample extraction

For morphological and stereological studies, the animals were anaesthetised with sodium phentobarbital (100 mg/kg) and perfused transcardially with cold saline followed by 4% paraformaldehyde (PFA) in phosphate buffer (PB) at 4°C (pH 7.4). Brains were removed, immersed overnight in the same fixative solution and maintained in PB until further use. Samples were included in 3% agarose and serial coronal

sections (30 µm) were obtained on a slicing vibratome (Leica Microsystems, Madrid, Spain). Sections were stored in PB/0.02% sodium azide at 4°C until immunohistochemical processing.

Immunohistochemistry (IHC)

Immunohistochemical procedures were carried out on free-floating 30 µm sections using standard avidin-biotin protocols (Ortiz et al., 2010; Ares-Santos et al., 2012). Washing steps were performed using PBS-0.2% Tx (Triton X-1009) (Sigma, ref. T8787) and endogenous peroxidase activity was blocked with 3% H_2O_2 in PBS-0.2% Tx for 10 minutes. Sections were pre-blocked with 10% Normal Goat Serum (NGS) (Merck-Millipore, ref. S26-100mL) in PBS-0.2% Tx for 2 hours to prevent non-specific binding. Sections were incubated in specific primary (Ab1) and secondary (Ab2) antibodies, respectively (**Table 4**). All antibodies were prepared in PBS-0.2% Tx containing 1% NGS. Samples were incubated in Streptavidin conjugated with Horseradish peroxidase (HRP) (Invitrogen, ref. 434323) for 1 hour (1:5000, RT) and developed by providing samples with the HRP substrate 3,3'-Diaminobenzidina (DAB) (Sigma, ref. D5637). The chromogenic reaction was monitored every 5 minutes using an optical microscope (Leica Microsystems, Spain). After washing, sections were mounted on gelatine-coated glass slides air-dried, dehydrated in a graded series of ethanol, cleared with xylene (VWR, ref. 141769.2711) and cover-slipped using the mounting medium DPX (Merck, ref. 1.00579.0500). Representative images were taken on an optical microscope (Leica Microsystems, Madrid, Spain) equipped with a Leica DFC 290 HD video camera using a 4x, 5x 10x and 20x objective, respectively (specific magnification is indicated in figure legend).

Antibody	Manufacturer	Dilution	Host	Incubation
Anti-p-syn (biotinylated) (Ab1)	Wako, pSyn #64	1:1000 (IHC), 1:500 (IF)	Mouse	2 nights, 4°C, rotation
Anti-p62/SQSTM1 (C-Terminal) (Ab1)	Progen, GP62-C	1:400 (IF)	Guinea pig	1 night, RT, rotation
Anti-TH (Ab1)	Merck-Millipore, AB152	1:1000 (IHC+IF)	Rabbit	1 night, 4°C, rotation
Anti-guinea pig conjugated Alexa Fluor 488 (Ab2)	Invitrogen, A11073	1:500	Goat	5 hours, RT, rotation
Anti-rabbit conjugated Alexa Fluor 594 (Ab2)	ThermoFisher, #A-21207	1:500	Donkey	5 hours, RT, rotation
IgG anti-rabbit (biotinylated) (Ab2)	Vector, BA-1000	1:500	Goat	1 hour
Streptavidin conjugated Alexa Fluor 568	Life, S11226	1:500		5 hours, RT, rotation

Table 4: Primary and secondary antibodies used in this study.

Immunofluorescence

Free-floating 30 µm sections were used for immunofluorescence double-staining. Sections were pre-blocked in 10% Normal Goat Serum (NGS) for 2-3 hours, followed by primary and secondary antibody incubation (**Table 4**). Antibodies were prepared in 1% NGS. Then, samples were mounted on gelatine-coated glass slides and covered with a cover slip using mounting medium ProLongGoldTM (ThermoFisher, ref.

P36930). Representative images were taken with a confocal microscope (Leica SP-5 inverted, Leica Microsystems) using a 63x objective.

Image acquisition and analysis

Scoring of pα-syn pathology

To semi-quantify α-syn pathology throughout the brain, scoring of pα-syn positivity was performed as described in Rey et al. (2016). Briefly, whole-brain images of pα-syn immunostained tissue (1:12 series) were taken using a Thunder microscope (Leica microsystems) with a 20x objective. Merged whole-brain images of 9 PFF-inoculated animals were used to assess pα-syn positivity in selected brain regions of sections corresponding to +1.70, +0.98, +0.26, -0.46, -1.22, -1.94, -2.70, -3.16, -4.16 and -4.84 from Bregma (from striatum to DR). Immunopositivity for pα-syn (phosphorylated at Ser129) was scored from 0 to 4 (0, no pathology; 1, mild [few neurites and/or 1 soma]; 2, moderate [more neurites and 1-2 somas]; 3, dense [many neurites and cell bodies]; 4, severe [very strong pathology]). The score was assigned to each region of each brain section per animal by comparing with template images. Studied brain regions and the template scoring scale are presented in **Fig. S1**. Score values per region are shown in a representative brain map using a colour code and correspond to mean score values of all animals.

Quantification of pα-syn aggregates

For pα-syn quantification in the striatum, whole-brain images of pα-syn immune-stained tissue (1:12 series) were captured by a Thunder microscope (Leica Microsystems) with a 20x objective. To specifically quantify the number of pα-syn aggregates in the striatum, the individual images containing the contralateral and ipsilateral striatum, respectively, were selected and used for automatic analysis in ImageJ (Rasband, W.S., ImageJ, U. S. National Institutes of Health, Bethesda, Maryland, USA, https://imagej.nih.gov/ij/, 1997-2018). Image segmentation was performed in pα-syn JPEG images from the striatum using the plugin Labkit (Arzt et al., 2022). This ImageJ plugin is designed for manual and automated image segmentation via pixel classification and works efficiently on big image data sets. The classifier was manually trained to recognize the total number of pα-syn aggregates/fibers based on representative images. As an output, the classifier creates a binary image distinguishing background from pixels of interest or objects (**Fig. S2 B**). Then, skeletonization was performed using Skeletonize 2D/3D plugin (Lee et al., 1994) to find the centrelines of the segmented objects in the input image by symmetrically eroding their surface until the skeleton remains, creating high-resolution morphologically accurate objects of segmented fibers (**Fig. S2 C**). After this, the Analyze Skeleton plugin (Arganda-Carreras et al., 2010) was used to obtain descriptive parameters of the objects, such as fiber branch length, and total number of branches, in order to comprise the features of interest of each segmented and skeletonized fiber in a file. To exclude artifacts and unspecific segmented objects, a size-dependent filter was applied excluding objects with a total size under 10 pixels (**Fig. S2 D**). The parameter of interest was the total number of pα-syn aggregates in each section, and the total number of pα-syn aggregates per animal. Approximately, 10-20 images per hemisphere (ipsilateral/contralateral) for each section and 6 sections per animal were analysed. Data are represented as the mean value of sections per animal and was calculated via Python.

To assess the number of phosphorylated α-syn aggregates in the SNpc tissue immunostained for pα-syn (1:12 series) was captured on an optical microscope using a 5x objective. The total number of pα-syn aggregates were counted manually using a cell counting aid of ImageJ. Both hemispheres of 2-3 sections per animals were analysed (**Fig. S3**). Data are represented as mean number of pα-syn aggregates per animal.

Quantitative assessment of innervation density

To assess the dopaminergic innervation density in the striatum and SNr TH expression was quantified as described previously (Ares-Santos et al., 2014, Fernández-Pérez et al., 2022). Images were captured using an optical microscope (Leica Microsystems). With the aid of Analytical Imaging Station software (Imaging Research, Linton, UK) colour intensities were converted into a gray scale to quantify the area of staining in the striatum as a proportion of stained pixels (stained area) in relation to total pixels in the scanned area. The threshold for stained pixels was obtained from the previous measurement of the signal in a control animal and applied to all animals. Both hemispheres were quantified in PFF-inoculated animals, while only 1 hemisphere was measured in control animals.

To investigate the density of dopaminergic terminals in the striatum TH-immunostained sections (1:12 series) were captured using a 4x objective. 6-8 sections per animal were used and averaged per animal (n number indicated in figure legends). Data are presented as the percentage of TH-stained area, normalized to the mean of control animals (100%).

To assess the fiber density in the SNr TH-immunostained sections (1:4 series) were imaged using a 40x objective. Per animal sections of 3 caudo-rostral levels were quantified using images in the same region of the SNr (**Fig. S4**). Values for each animal correspond to the mean of sections. Data are normalized to control.

Stereological quantification of TH-positive cells

The total number of TH-positive neurons in the SNpc was estimated by (unbiased) stereological counting method using the optical fractionator probe StereoInvestigator (Microbrightfield Bioscience, Colchester, VT) coupled to a Nikon Eclipse 80i microscope. This unbiased method of cell counting is neither affected by the volume of reference (SNpc) nor the size of the counted element (neurons). The region of interest (SNpc) was detected and traced at low magnification (2x objective) and data recording was performed at high magnification (100x objective). To avoid double counting of neurons with unusual shapes, only TH-stained cells in optimal focus were counted. Every fourth of section of biological replicates were recorded throughout the entire extent of the SNpc of 30 µm coronal slices, yielding 7-9 sections per animal. Cell counting was performed in the ipsilateral and contralateral hemisphere for PFF-inoculated animals, while only one hemisphere was counted for control mice (Granado et al., 2008, Ares-Santos et al., 2014). Representative pictures were captured with an optical microscope (Leica Microsystems, Madrid, Spain) equipped with a Leica DFC 290 HD video camera (5x objective).

Statistical analysis

All data are presented as mean ± standard error of the mean (SEM). Statistical analysis was performed, and graphs were generated using the GraphPad Prism version 8.0.2. Before analysis, data were tested for normal distribution using the D'Agostino-Pearson Test. Comparisons between two groups were performed with a t-test or Mann Whitney test, while 3 groups were compared using one-way ANOVA. Correlation was calculated using the Pearson correlation coefficient with 95% confidence interval. To statistically evaluate the differences between sexes a 2-way ANOVA was applied. Statistical significance was set at * $p<0.05$, ** $p<0.01$, *** $p<0.001$, **** $p<0.0001$. All information including sample size and specific statistical test are indicated in figure legends.

Results

Effect of human wild-type α-syn PFF inoculation on α-syn pathology

1. Human wild-type α-syn PFF injection into the dorsal striatum of *SNCA*-OVX mice leads to widespread α-syn accumulation throughout the brain.

In several studies it has been shown that the unilateral administration of human α-syn PFFs into the striatum of mice induces the accumulation of pathological α-syn in the brain (Earls et al., 2020, Fares et al., 2016, Luk et al., 2012b, Luk et al., 2016, Milanese et al., 2018). It has been reported in numerous studies that more than 90% of α-syn within LBs are phosphorylated at the residue Ser129, this post-translational modification being considered a pathological marker for human LBs/LNs (Fujiwara et al., 2002; Oueslati, 2016, Gómez-Benito et al., 2020; Ghanem et al., 2022). Therefore, to determine whether human α-syn PFF injection results in widespread pathological α-syn accumulation, we performed an immunohistochemical staining against phosphorylated α-syn (pα-syn).

As seen in **Fig. 8**, pα-syn accumulations are found in the brain of PFF-injected *SNCA*-OVX mice. Aggregates are clearly visible in the striatum (Str), especially at the site of injection, along with several other brain areas (**Fig. 8 A**). More specifically, the pathology is found in the ipsilateral hemisphere (from left to right) in the internal capsule (CI), motor cortex (M Ctx), ectorhinal cortex (Ect Ctx), piriform cortex (Pir Ctx), thalamus (Thal), hypothalamus (Hyp), hippocampus (Hipp), anterior basolateral amygdala nucleus (BLA), postmedial cortex amygdala nucleus (PMCo), substantia nigra pars compacta (SNpc), dorsal raphe nucleus (DR), olfactory bulb (OB), cingulate cortex (Cg Ctx) and corpus callosum (cc) (**Fig. 8 B**). No accumulation of pα-syn is observed in the striatum or any other brain regions of control (Ctrl) and non-injected OVX animals (**Fig. 8 B**, below).

Additionally, pα-syn-positive aggregates can be found in brain regions of the contralateral hemisphere such as striatum, cortical areas, hippocampus and nuclei of the amygdala (**Fig. 8 C**). Interestingly, pα-syn accumulations are present in white matter structures that connect the right and left cerebral hemispheres, namely the corpus callosum (cc) and anterior commissure (ac) (**Fig. 8 C**). The presence of pα-syn inclusions in commissural fibers that extend bilaterally might explain interhemispheric transmission of α-syn pathology.

We observe that 150 dpi different brain regions are affected by varying degrees. In the ipsilateral hemisphere, the striatum, especially the injection site, amygdala nuclei and internal capsule contain a relatively high number of pα-syn, while other brain areas like thalamus, hypothalamus, DR and SN display few pα-syn aggregates. Also, corpus callosum and anterior commissure contain a high number of pα-syn aggregates. On the contralateral side, a smaller number of pα-syn immunopositive inclusions are detected (**Fig. 8 B**, **C**).

For a better visualization and semi-quantification of the extent of α-syn pathology, we created a diagram illustrating the anatomical pattern of pα-syn propagation in the brain on coronal sections (**Fig. 8 A**). For this purpose, the degree of pα-syn aggregations was scored per brain region at multiple caudo-rostral levels. The represented value for each brain regions corresponds to the mean score value of all animals and is displayed in a colour code that represents the extent of pα-syn aggregation. The propagation

map semi-quantitatively represents the observations discussed before. The pathology spreads rostrally to the frontal lobe, and caudally to the DR.

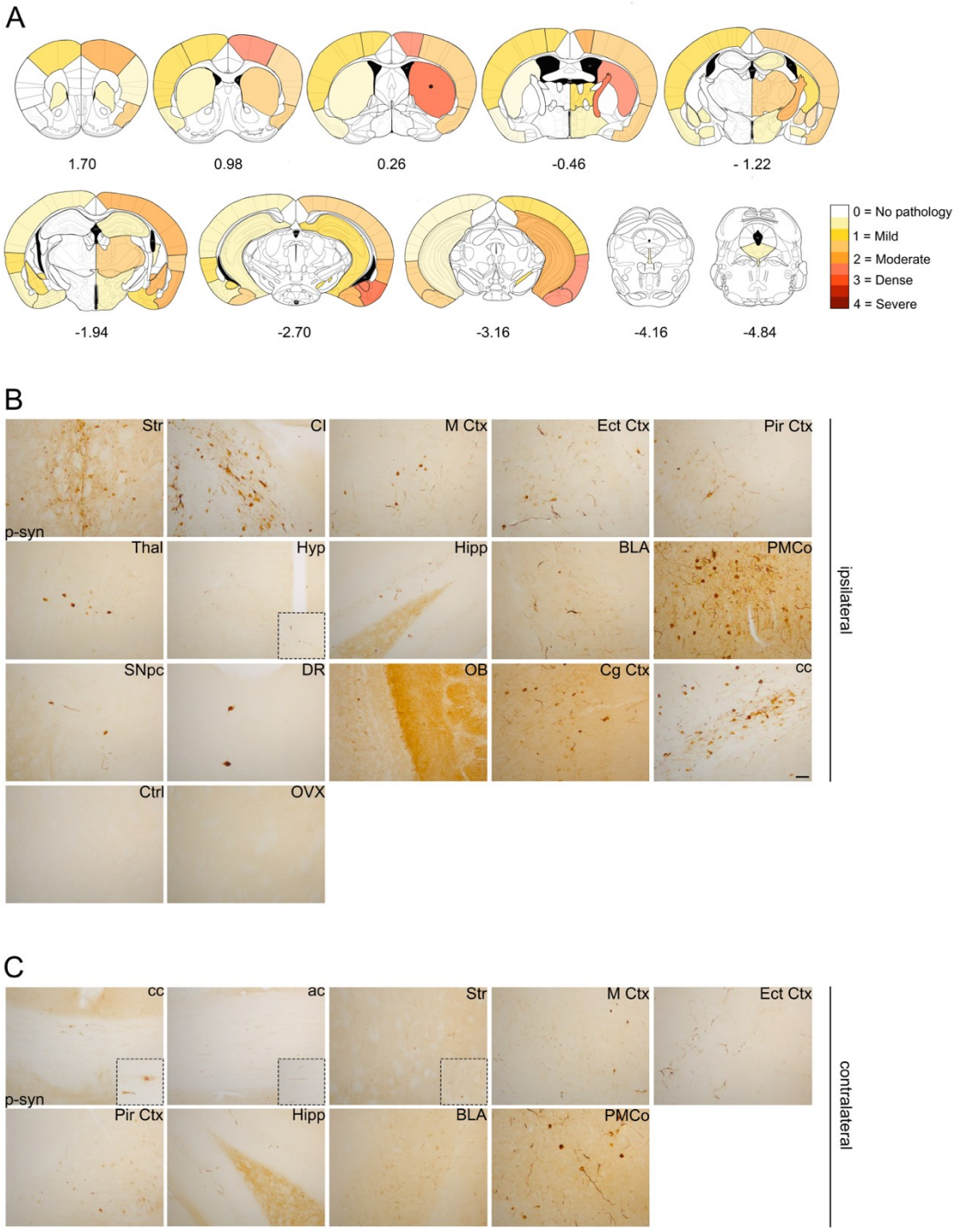

Fig. 8: Induction and transmission of pα-syn pathology after intrastriatal inoculation with human α-syn PFFs. (**A**) A propagation map of pathological α-syn throughout the brain is illustrated. Caudo-rostral levels of brain sections are indicated from Bregma. The severity of pathology is indicated using a color code (from white, no pathology, to red, severe pathology). The mean score value per brain section and region/area at each level is illustrated (n=9). The injection site is indicated with a black dot. (**B**) Representative images of pα-syn immunohistochemistry of selected brain areas ipsilateral to the injection site (Bregma: 0.26). No pα-syn pathology was observed in the striatum of control animals (B, below). (**C**) Representative images of pα-syn staining of selected brain areas contralateral to the injection site. Staining in the OB and Cg Ctx (rostral) was performed in only one animal. Scale bar: 50 µm (20x). Complete terminology of brain regions can be found in the List of abbreviations.

Overall, these results indicate that the unilateral α-syn PFF inoculation into the dorsal striatum of *SNCA*-OVX mice induces the aggregation of pathological α-syn. Further, we demonstrate that pathological α-syn spreads from the injection site to interconnected brain areas throughout the brain.

2. α-Syn aggregates induced upon human wild-type α-syn PFF injection mimic the pathological properties of human Lewy bodies.

To further characterize pathological α-syn aggregates found in the brain of PFF-injected animals, immunofluorescence staining was performed against pα-syn, p62/SQSTM1 and TH in the striatum and SN, respectively. The protein p62/sequestome 1 (p62/SQSTM1) is a molecular component of LBs required for α-syn autophagy and is commonly used as a key marker of human LBs (Watanabe et al., 2012, Wakabayashi et al., 2013, Kuusisto et al., 2001). TH is the rate-limiting enzyme in the biosynthesis of dopamine, commonly used as a marker for identifying dopaminergic neurons.

In **Fig. 9 A** immunofluorescence staining against pα-syn (red) and p62/SQSTM1 (green) in the striatum is shown. Merged images reveal co-localization of these proteins, demonstrating that pα-syn aggregates found after human α-syn PFF injection share common features with human LBs/LNs. In the SN co-localization of pα-syn/p62/SQSTM1 can be observed in TH-positive cells (blue) (**Fig. 9 B**), indicating that α-syn PFFs induce LB-like pα-syn inclusions in dopaminergic neurons of the SN. These results demonstrate that PFFs seed intraneuronal inclusions that share common features with human LBs/LNs.

Additionally, we observe that the pα-syn-positive aggregates display different morphologies (**Fig. 8 B**, **C**, higher augmentation: **Fig. S5**). They are present as dense, round inclusions or fine fibers. In this work I will use the terms pα-syn or pathological α-syn aggregates/inclusions/accumulations/deposits, referring to pα-syn-immunopositive accumulations distributed both in perikaryal/cell body and neurites, regardless of their morphology.

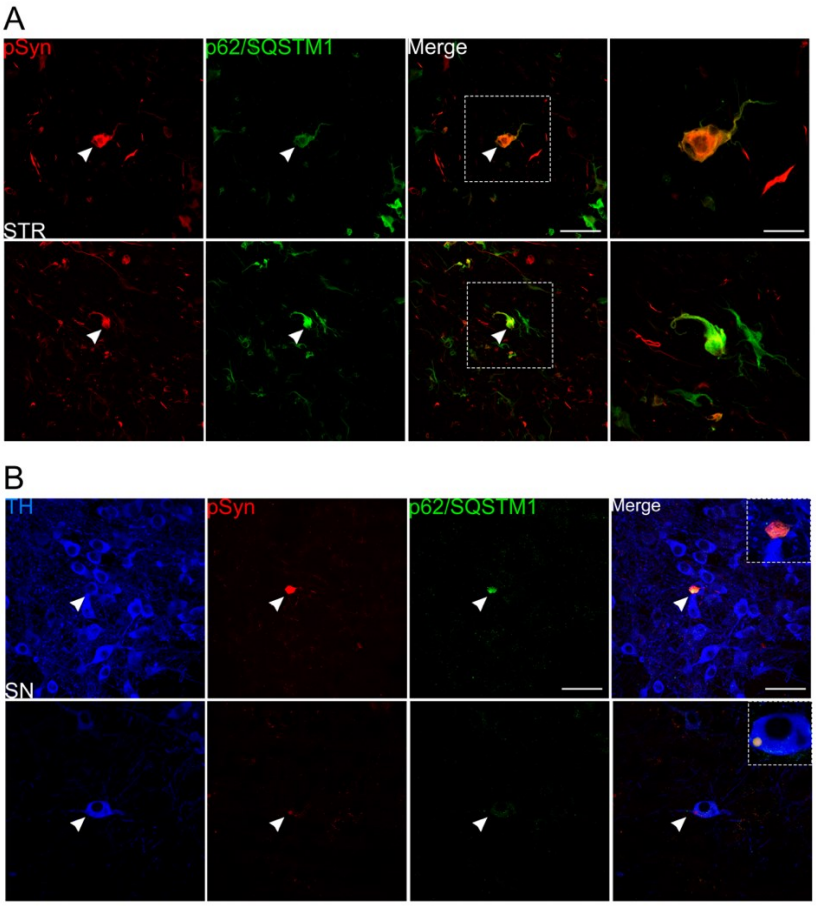

Fig. 9: Pathological characterization of α-syn aggregates. (**A**) Immunofluorescence staining against pα-syn and p62/SQSSTM1 reveals co-localization in the striatum of PFF-injected animals. (**B**) Immunofluorescence staining against TH, pα-syn and p62/SQSTM1 shows co-localization in the SN of injected animals. Scale bar: 50 µm (63x, left), 20 µm (zoom 2.5, right)

3. Unilateral human wild-type α-syn PFF injection results in the bilateral accumulation of pα-syn inclusions in the striatum.

As described before, PFF inoculation of *SNCA*-OVX mice results in pα-syn aggregation throughout the brain (**Fig. 8**). We wanted to take a closer look at the pathology in the striatum, a brain region affected in PD. Striatal DA depletion caused by the loss of dopaminergic neurons in the SNpc is responsible for the typical motor symptoms observed in PD patients (Dauer et al., 2003). As α-syn PFFs were injected in the dorsal striatum, pα-syn pathology is severe in this region and aggregates are highly abundant close to the injection site (**Fig. 10 A**). Aggregates are observed in both hemispheres but are more pronounced in the ipsilateral, where pα-syn aggregates are detected as dense inclusions along with fibers. In contrast, only fine fibers are visible in the contralateral hemisphere (**Fig. 10 A**, left).

In Ctrl and non-injected OVX mice there is a lack of pα-syn accumulation (**Fig. 10 B**), suggesting that α-syn PFF inoculation is needed to induce the accumulation of pathological α-syn. Hence the lack of α-syn or exclusive overexpression of human α-syn is not sufficient to induce pathological α-syn inclusions.

Moreover, we quantified the number of pα-syn immunopositive accumulations in the ipsilateral and contralateral striatum. The automatic quantification of pα-syn aggregates revealed statistically significant higher number of pα-syn aggregates in the ipsilateral

hemisphere (302.40 ± 50.23 pα-syn aggregates) compared to the contralateral side (86.48 ± 13.23 pα-syn aggregates) (p=0.0007) (**Fig. 10 C**).

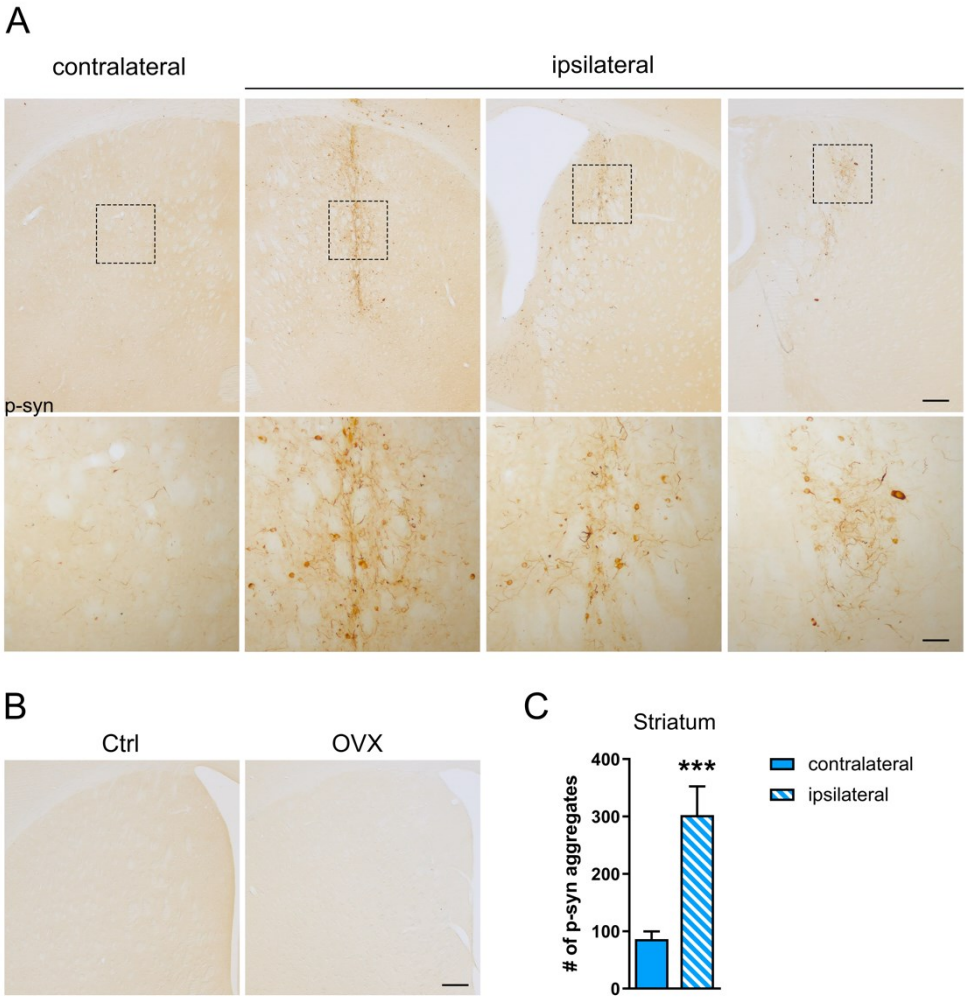

Fig. 10: PFF seeded pα-syn pathology in the striatum. (**A**) Staining against pα-syn in the striatum of PFF-inoculated OVX-mice. Images of ipsilateral striatum are presented from 3 different animals at similar caudo-rostral levels. Scale bar: 200 µm (5x, above), 50 µm (20x, below). (**B**) Staining against pα-syn in the striatum of non-injected control animals. Scale bar: 200 µm (5x) (**C**) Quantification of pα-syn aggregates in the striatum of contralateral and ipsilateral hemispheres of PFF-inoculated OVX-mice (n=9). Values expressed as mean ± SEM. *** p<0.001 compared with contralateral hemisphere, t-test.

4. Unilateral human wild-type α-syn PFF injection results in the ipsilateral accumulation of pα-syn inclusions in the SNpc.

After confirming the occurrence of pα-syn aggregates in the striatum, we wanted to investigate the pα-syn pathology in the SNpc 150 dpi with α-syn PFF. Immunohistochemistry against pα-syn in the SNpc revealed pathological α-syn aggregates in the ipsilateral hemisphere (**Fig. 11 A**), whereas no pathology is found in the contralateral hemisphere as well as in animals that were not injected with PFFs (**Fig. 11 B**). To quantitatively assess the number of pα-syn accumulations in the SNpc, aggregates were manually counted. Statistical analysis of data confirmed that pα-syn pathology found in the ipsilateral SNpc (11.15 ± 2.779 pα-syn aggregates) (p<0.0001), is significantly higher compared to the contralateral SNpc, where no pathology is found (**Fig. 11 C**).

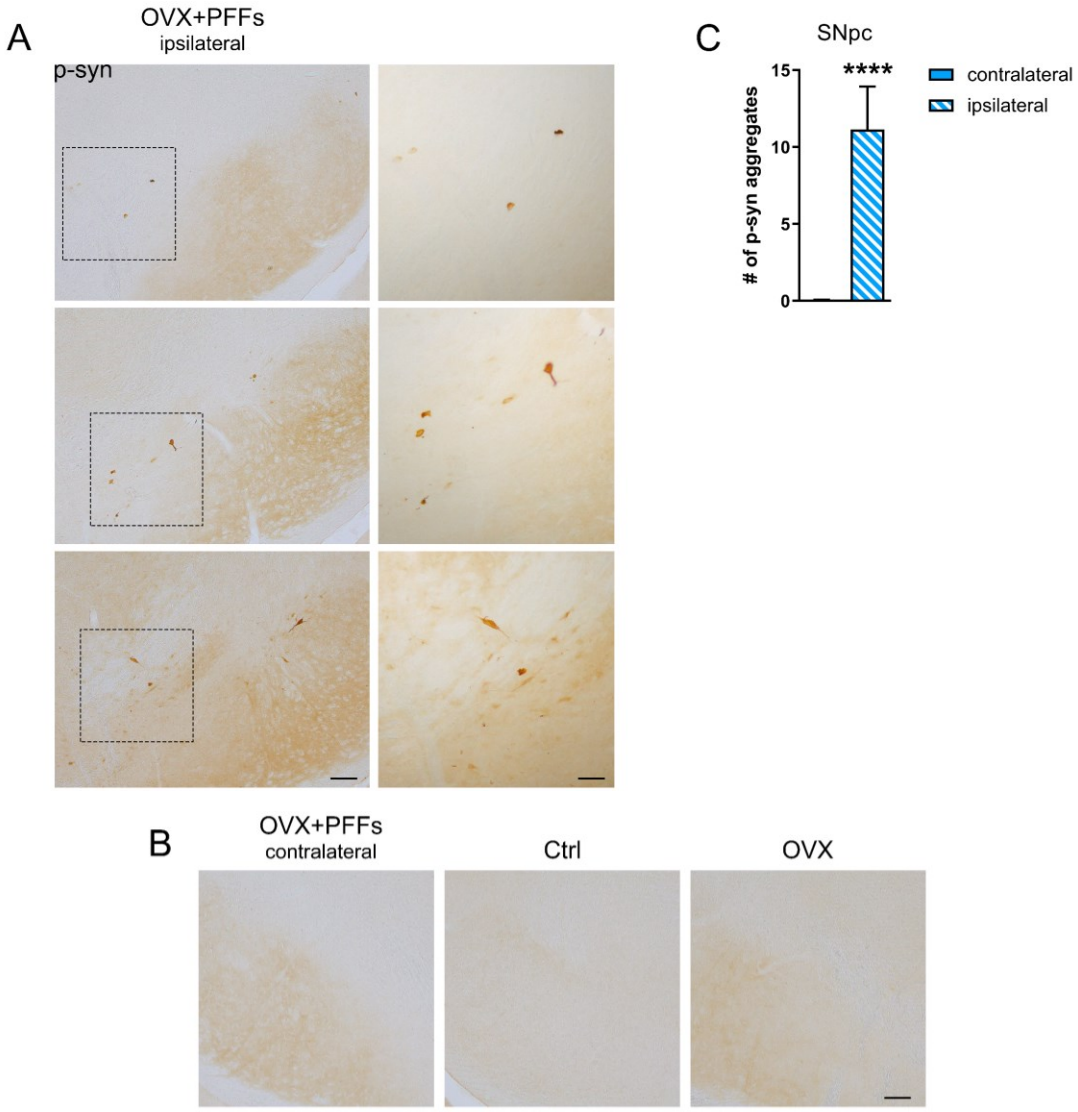

Fig. 11: Pathological pα-syn aggregates in the SNpc induced by α-syn PFFs. (**A**) Staining against pα-syn of PFF-inoculated animals. Representative images of pα-syn aggregates in the ipsilateral SN of 3 different animals. Note variability of number of aggregates. Scale bar: 100 µm (10x, left), 50 µm (20x, right) (**B**) Staining against pα-syn of PFF-injected (contralateral), Ctrl and non-injected OVX animals. No pα-syn aggregates are found. Scale bar: 100 µm (10x) (**C**) Quantification of pα-syn aggregates in the contralateral and ipsilateral SNpc (n=9). Values expressed as mean ± SEM. **** $p<0.0001$ compared to contralateral hemisphere, Mann-Whitney test.

Effect of human wild-type α-syn PFF inoculation on the integrity of the nigrostriatal pathway

1. Human wild-type α-syn PFF inoculation results in unilateral DA striatal denervation.

After confirming pathological α-syn aggregates in multiple brain areas including the striatum and SN, the nigrostriatal pathway was investigated. It has been shown that dopaminergic neurons of the SNpc that project to the striatum selectively degenerate in PD. The loss of these striatal innervations from the midbrain leads to DA deficiency in the striatum, especially the putamen, and causes motor symptoms that are observed in PD patients (Rinne et al., 1993; Dickson et al., 2009; Dickson, 2018). We aimed to explore whether the accumulation of pathological α-syn in mice injected with PFFs has

any impact on dopaminergic neurons and terminals of the nigrostriatal system. Therefore, immunohistochemistry against TH was conducted in the striatum and SN.

To analyse the loss of dopaminergic terminals in the striatum, we evaluated the TH-positive fiber density in the striatum of PFF-injected OVX mice and control animals. Representative images of the striatum reveal a reduction of TH-stained area in the ipsilateral hemisphere of PFF-inoculated *SNCA*-OVX mice (**Fig. 12 A**, right). This reduction is most prominent close to the injection site (dorsal striatum). The contralateral hemisphere does not show a significant decrease in TH-staining like control animals that were not injected with PFFs (**Fig. 12 A**, left). Also, no difference could be observed between hemispheres of control animals (not shown). The quantification of TH-stained area confirmed significant loss of TH-staining in the ipsilateral hemisphere compared to Ctrl (mean reduction of 29.69%, $p<0.01$), whereas the contralateral does not show significant difference compared to control animals (**Fig. 12 B**). Though, we observed that non-injected OVX animals and the contralateral hemisphere of PFF-injected mice show a lower percentage of TH-stained area compared to Ctrl, even if non-significant (contralateral: mean reduction of 13.63%, OVX: mean reduction of 13.31%). These results suggest that α-syn pathology induced upon PFF inoculation leads to striatal denervation in the ipsilateral hemisphere but not in the contralateral.

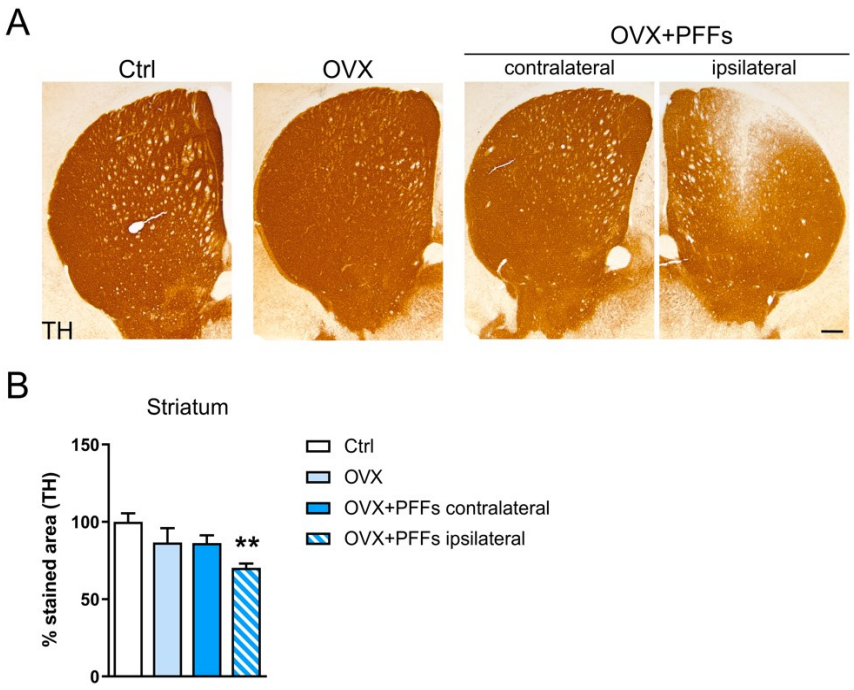

Fig. 12: Loss of dopaminergic innervation after inoculation with α-syn PFFs. (**A**) Representative pictures of staining against TH in the striatum of control and PFF-injected mice. Reduction of TH-stained area in the ipsilateral hemisphere of PFF-injected animals can be seen. Scale bar: 200 µm (4x) (**B**) Percentage of stained area for TH in the striatum are shown for Ctrl (n=7), OVX (n=5), and PFF-inoculated mice (n=9) (6-8 sections per striatum). For Ctrl and non-injected OVX mice only 1 hemisphere was measured. Data are normalized against Ctrl. Values expressed as mean ± SEM. ** $p<0.01$ compared to Ctrl hemisphere, Kruskal-Wallis test with Dunn's multiple comparisons test.

2. Human wild-type α-syn PFF inoculation produces a decrease in dopaminergic neurons in the ipsilateral SNpc accompanied by a loss of fiber density.

Next, we examined the loss of dopaminergic neurons in the SNpc upon human wild-type α-syn PFF inoculation. As seen in **Fig. 13 A**, OVX mice injected with PFFs have

fewer dopaminergic neurons in the ipsilateral SNpc compared to Ctrl and non-injected OVX animals. Stereological quantification reflects a marked neuronal loss in the ipsilateral SNpc (6079 ± 473.4 TH-positive cells) of OVX mice injected with PFFs compared to non-injected OVX (8705 ± 632.5 TH-positive cells) and contralateral SNpc (8628 ± 196.4 TH-positive cells) of OVX animals injected with PFFs (**Fig. 13 B**). These findings are statistically significant ($p<0.05$).

The cell number of the contralateral SNpc is comparable to that of control animals (**Fig. 13 A**). Stereological evaluation revealed that there is no difference in the number of dopaminergic cells of non-injected OVX (8705 ± 632.5 TH-positive cells) and contralateral OVX-injected mice (8628 ± 196.4 TH-positive cells) compared to Ctrl (8363 ± 514.5 TH-positive cells) (**Fig. 13 B**). Furthermore, no difference in the number of TH-positive cells can be observed between hemispheres of control animals (not shown). It can be concluded that human α-syn PFF inoculation leads to the loss of TH-positive neurons in the ipsilateral SNpc.

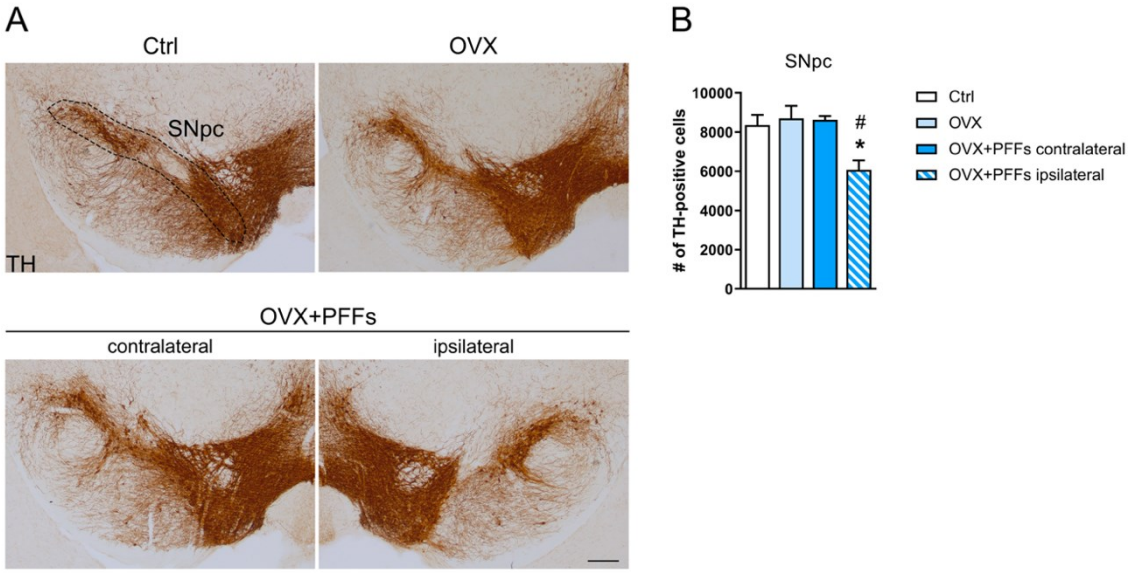

Fig. 13: Integrity of dopaminergic neurons in the SNpc after inoculation with α-syn PFFs. (**A**) TH-staining in the SN of control animals and PFF-injected mice in the contralateral as well as ipsilateral hemisphere. Loss of neuronal cells can be observed in the ipsilateral hemisphere of PFF-injected mice. Scale bar: 200 um (5x) (**B**) Quantification of TH-immunopositive neurons in the SNpc of Ctrl (n=7), non-injected OVX (n=5), and PFF-inoculated mice (n=8) (7-9 slices per animal analyzed). Data represented as number of cells ± SEM. * $p<0.05$ compared to OVX, # $p<0.05$ compared to contralateral hemisphere, Kruskal-Wallis test with Dunn's multiple comparisons test.

To further study the integrity of the nigral DA system, we examined the loss of dopaminergic projections from the SNpc to the SNr. Representative images in **Fig. 14 A** show an evident decrease of innervation density in the ipsilateral SNr of PFF-injected animals compared to non-injected Ctrl and OVX mice. The quantification of percentage of TH-stained area in the SNr confirms that the SNr of the ipsilateral hemisphere is significantly less innervated compared to the Ctrl hemisphere (mean reduction of 36.82%) ($p=0.0094$) (**Fig. 14 B**).

The contralateral SNr is slightly less densely innervated compared to Ctrl (mean reduction of 11.28%), as can be seen in representative pictures (**A**) and quantification (**B**). Still, projections to the contralateral SNr are of higher density than to the ipsilateral, even if statistically not significant. Interestingly, also OVX mice show marginally less projections to the SNr (mean reduction of 7%) which is not statistically

significant. Moreover, no difference in the number of TH-positive fibers is observed between hemispheres of control animals (not shown). Concludingly, PFF inoculation leads to decreased innervation of the ipsilateral SNr.

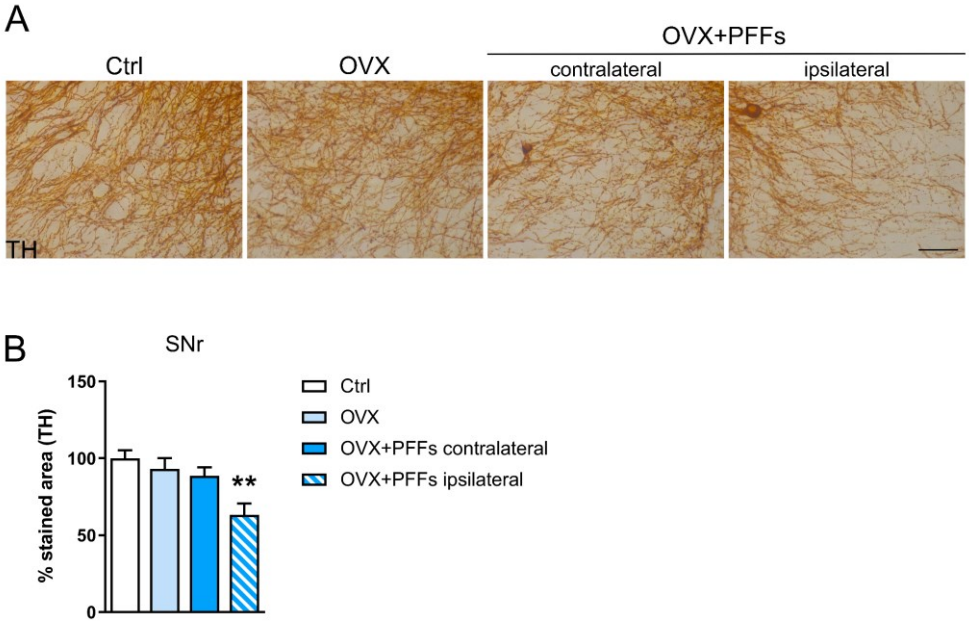

Fig. 14: Loss of dopaminergic innervation density of the SNr after inoculation with human wild-type α-syn PFFs. (**A**) TH staining in the SNr of Ctrl, OVX and PFF-inoculated animals is presented. Loss of innervation density is noted in the ipsilateral SNr. Scale bar: 50 um (40x) (**B**) Quantification of the percentage of TH-stained area in the SNr of Ctrl (n=8), OVX (n=5), and PFF-inoculated mice (n=9) is presented. Data are normalized against Ctrl. 3-6 sections per animal are analyzed. Data expressed as mean ± SEM. ** p<0.01 compared to Ctrl, Kruskal-Wallis test with Dunn's multiple comparisons test.

Effect of human wild-type α-syn PFF inoculation on motor behaviour

1. *SNCA*-OVX mice do not demonstrate clear motor deficits upon human wild-type α-syn PFF inoculation.

With the objective of determining whether striatal denervation and the lower number of dopaminergic neurons found in the ipsilateral SNpc of PFF-inoculated *SNCA*-OVX mice has any effect on the motor behaviour of these mice, we assessed motor performance and fine motor control using the challenging beam transversal test (**Fig. 15**). This behavioural assay was used in previous studies to evaluate the motor behaviour of parkinsonian mice (Fleming et al., 2004, Hwang et al., 2005). Parameters studied were errors per steps (**A**), steps (**B**), and time to traverse the beam (**C**).

Overall, no significant differences are seen between groups in any of the parameters after statistical analysis. Still, clear trends can be observed in the data. Ctrl animals cross the beam the fastest, while OVX mice, injected as well as non-injected, display a longer latency to cross the beam compared to Ctrl (**Fig. 15 C**). Animals of all three experimental groups take a similar number of steps to traverse (mean around 18 steps) (**Fig. 15 B**). Regarding errors per step, PFF-injected mice display a similar ratio as Ctrl animals (PFF: 0.16, Ctrl: 0.15), while OVX mice show a lower ratio (0.09) (**Fig. 15 A**).

I want to mention that values vary considerably within the group, especially for values of Ctrl animals for Errors per Steps (**Fig. 15 A**) as well as values of injected or non-injected OVX mice for the parameter time to traverse the beam (**Fig. 15 C**).

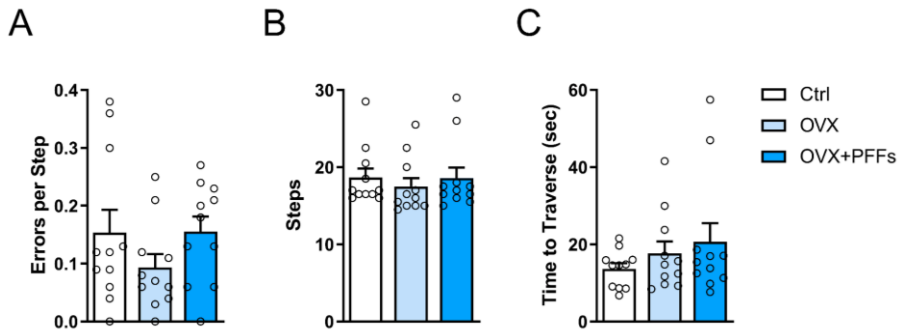

Fig. 15: Motor performance and fine motor control of control and PFF-inoculated mice. Motor behaviour was measured in Ctrl, non-injected OVX and PFF-inoculated OVX mice using the challenging beam transversal test. Parameters investigated were errors per step (**A**), total steps (**B**) and time (**C**) to traverse the beam. PFF-injected animals were 7-8 months of age, while Ctrl and OVX subjects were 6 months old (n=11 per group). Data expressed as mean ± SEM. Kruskal-Wallis test.

Correlation studies

Do observed pathologies have a correlational relationship?

During this work we have studied the neuropathology induced by PFF inoculation of *SNCA*-OVX mice, the impact of α-pathology on the nigrostriatal pathway and the motor behaviour. Then, we sought to put the information together to investigate putative correlation between pα-syn pathology and degeneration of the nigrostriatal pathway, as well as motor impairment and reduced striatal TH innervation (**Fig. 16**). To compute a measure for the interplay between parameters, the Pearson correlation was calculated between the number of pα-syn aggregates and percentage of stained area (TH) in the striatum (**A**), number of pα-syn aggregates and number of TH-positive cells in the SN (**B**), and the percentage of stained area (TH) in the ipsilateral striatum and errors per step (**C**).

In **Fig. 16 A** the correlation between the number of pα-syn aggregates and percentage of TH-stained area in the ipsilateral and contralateral striatum, respectively, are presented. A slight positive correlation can be observed in the contralateral hemisphere (r=0.1915), whereas a slight negative correlation is visible in the ipsilateral hemisphere (r=-0.09783). However, the results are considered non-significant as a consequence of high p-values (ipsilateral p=0,6496, contralateral p=0.8177). **Fig. 16 B** displays the correlation of number of pα-syn aggregates and number of TH-positive cells in the SNpc. Since no pathological α-syn accumulated in the contralateral SNpc, no correlation between parameters can be calculated. On the other hand, the ipsilateral hemisphere shows a moderate negative correlation between parameters (r=-0.5781), although considered not significant since the p-value is greater than 0.5 (p=0.1740). Lastly, TH-stained area of the ipsilateral striatum is correlated with errors per steps conducted during the challenging beam transversal test (**Fig. 16 C**). We observed a slight positive correlation (r=0.1005) that was statistically not significant (p=0.7970).

Overall, correlation studies confirm that the number of pα-syn aggregates is higher in the ipsilateral hemisphere compared to the contralateral of striatum and SNpc. Additionally, the percentage of striatal TH-stained area and the number of TH-positive neurons in the SNpc is higher in the contralateral than in the ipsilateral hemisphere (**Fig. 16 A**, **B**).

Furthermore, it is important to highlight that, in general, for the parameters evaluated, the values do not follow a linear trend, with the number of pα-syn aggregates being especially variable. This makes it difficult to establish robust correlations and reflects the great variability of the model, which is a surgery-dependent model.

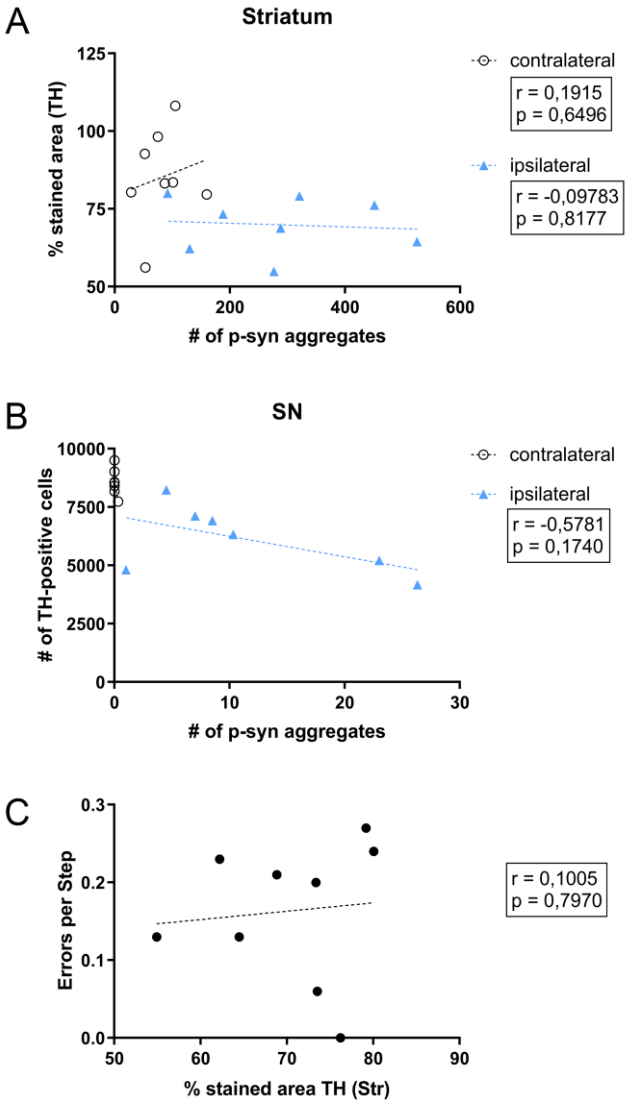

Fig. 16: Correlation studies of obtained results. Pearson correlation with 95% confidence interval was calculated. (**A**) Correlation of numbers of pα-syn aggregates and percentage of TH-stained area in the striatum. The correlation coefficient for contralateral was 0.1915 (P<0.6496, 95% CI -0.5932 to 0.7896). The correlation coefficient for ipsilateral was -0.098 (P<0.8177, 95% CI -0.7507 to 0.6518). (**B**) Correlation of number of pα-syn aggregates and number of TH-positive cells in the SN. The correlation coefficient for ipsilateral was -0.5781 (P<0.1740, 95% CI -0.9274 to 0.3098). (**C**) Correlation of the percentage of TH-stained area in the ipsilateral striatum and Errors per Steps. The correlation coefficient was 0.1005 (P<0.7970, 95% CI -0.6039 to 0.7168). A linear regression trend line was inserted in the scatter diagram. Sample size is indicated as dots.

Analysis of sex differences

Do obtained data display sex-specific differences?

To investigate if our results have differences between female and male animals, we divided our data of our experimental groups Ctrl, non-injected *SNCA*-OVX and PFF-injected *SNCA*-OVX animals, respectively, per sex for each parameter.

In **Fig. 17** the number of pα-syn aggregates in the striatum (**A**) and SNpc (**B**) are illustrated. In general, no significant differences are found (statistical tests indicated in the figure legend). However, in the ipsilateral striatum the mean number of pα-syn aggregates is higher for male than female mice (**Fig. 17 A**). In the contralateral striatum similar number of pα-syn aggregates are found between sexes. In the ipsilateral SNpc, a tendency for more pα-syn inclusions in male animals compared to females can be perceived (not significant) (**Fig. 17 B**) but note the high variability of male animals.

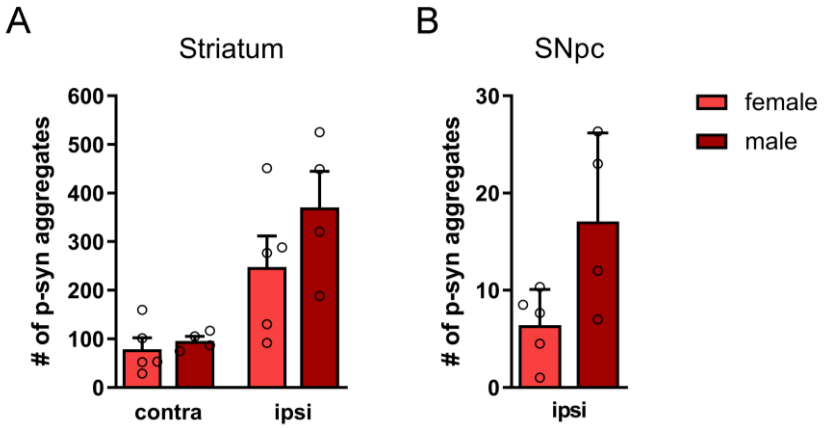

Fig. 17: Pathological α-syn inclusions in the Striatum and SNpc comparing sexes. Number of pα-syn aggregates in the striatum of both hemispheres (**A**) and ipsilateral SNpc (**B**) in female and male mice, respectively. No significant differences are observed between sexes. 2-way ANOVA (A), Mann-Whitney test (B). N numbers are indicated as dots.

In **Fig. 18** the striatal innervation density (**A**), the number of TH-positive cells in the SNpc (**B**), and the innervation density of the SNr (**C**) comparing sexes is demonstrated. In the striatum a significant difference is observed in TH-stained area between female and male of non-injected OVX animals, being smaller in male (mean difference of 33.98%) ($p<0.05$) (**Fig. 18 A**). Also, in the ipsilateral SNr the percentage of TH-stained area was significantly smaller in male PFF-injected OVX mice compared to female (mean difference of 38.22%) ($p<0.01$) (**Fig. 18 C**).

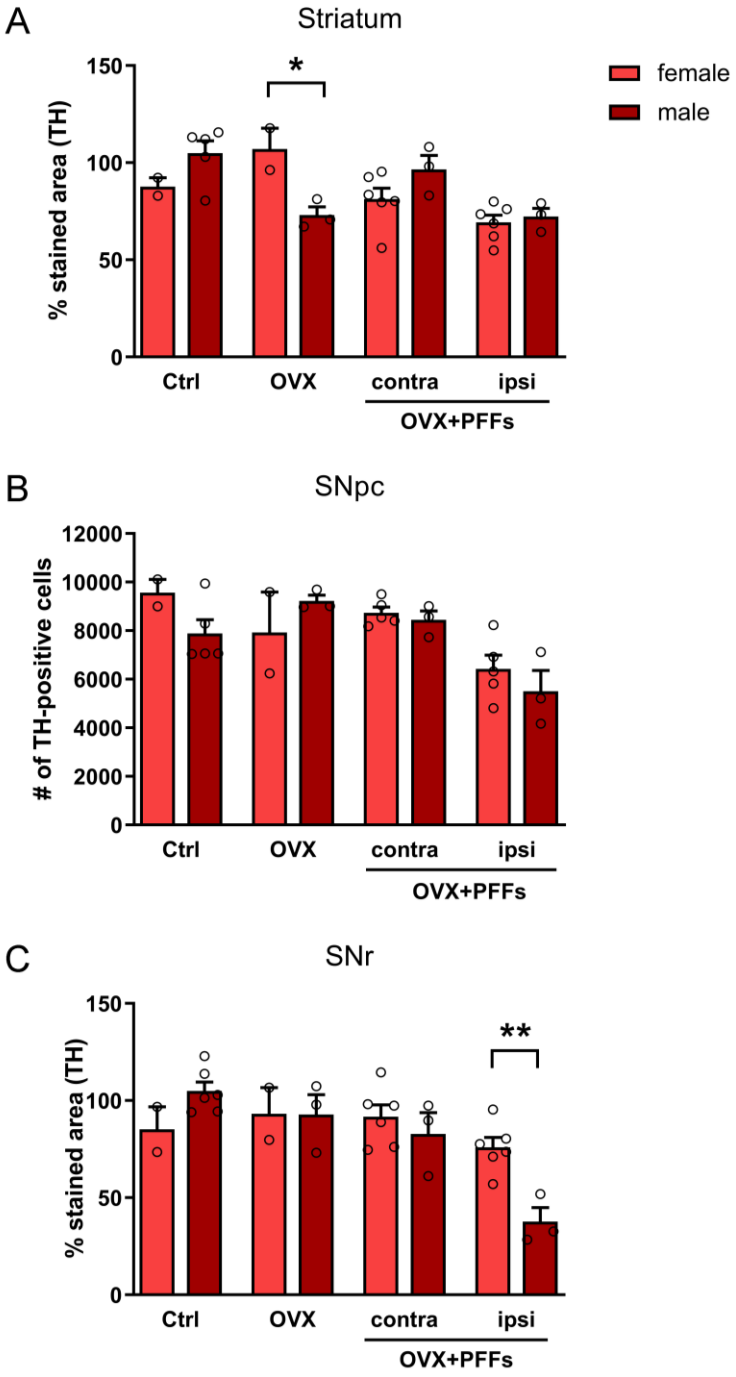

Fig. 18: Nigrostriatal pathway comparing sexes. (**A**) TH-stained area in the striatum of control animals and PFF-injected mice reflecting density of dopaminergic innervation. (**B**) Number of TH-positive cells in the SNpc of control and PFF-injected animals. No significant differences seen. (**C**) TH-stained area in the SNr of control and PFF-injected animals reflecting density of dopaminergic terminals in this region. Normalized data are represented (for A, C). 2-way ANOVA with Sidak's multiple comparisons test. * $p<0.05$ comparing male and female of OVX mice. ** $p<0.01$ comparing ipsilateral hemisphere of female and male of PFF-injected animals. N numbers are indicated as dots.

In **Fig. 19** the motor performance and fine motor control of Ctrl, non-injected OVX and PFF-injected animals is presented, separating data of female and male subjects. After statistical analysis no significant differences is observable between sexes. Yet, there is a trend towards higher errors per step of male Ctrl animals compared to female, but the high variability within the group must be acknowledged (**Fig. 19 A**).

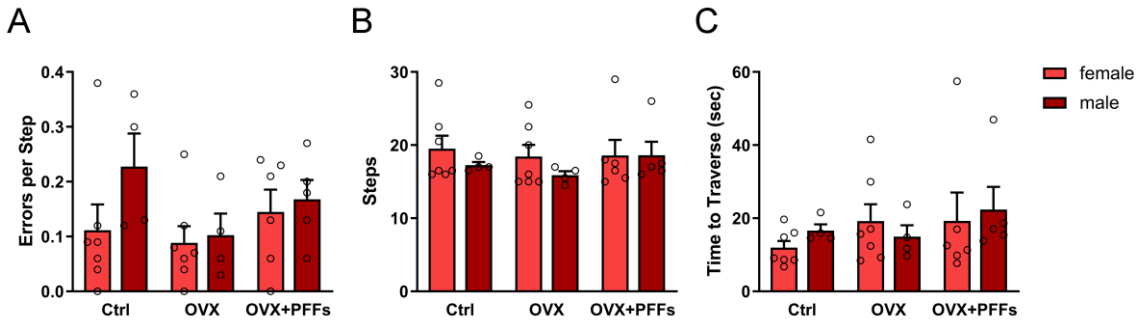

Fig. 19: Motor performance and fine motor control comparing sexes. A challenging beam transversal test was performed. Measured parameters were errors per step (**A**), steps (**B**), and time to traverse (**C**) the beam. No significant differences are observed between sexes. 2-way ANOVA with Sidak's multiple comparisons test. N numbers are indicated as dots.

Overall, no clear pattern is observed with values of female or male animals being (significantly) smaller/higher. Some trends are present, as described above. However, the high variability within groups must be recognized, along with a low number of animals per parameter.

Discussion

Parkinson's disease (PD) is the most common neurodegenerative movement disorder with a global prevalence of more than 6 million individuals and the fastest growing neurological disorder worldwide (Dorsey et al., 2018; GBD 2016 Neurology Collaborators). The typical onset of clinical symptoms is between 55 and 65 years (Rizek et al., 2016; Balestrino et al., 2020), when DA in the putamen is depleted around 80% and approximately 60% of SNpc dopaminergic neurons have already degenerated (Dauer et al., 2003). PD is a heterogenous disease of unknown aetiology in which environmental influence, aging, and causative and susceptibility genetic factor are involved in pathogenesis (Hernandez et al., 2016; Delamarre et al., 2017; Coleman et al., 2022). However, despite numerous efforts, the exact mechanisms contributing to PD development remain unknown which makes the early and precise diagnosis and adequate treatment of PD impossible. To date, no therapeutics have been discovered that efficiently demonstrate a disease-modifying effect, hence the development of interventions that slow or halt the progression of PD continues to be important in PD research (Vijiaratnam et al., 2021).

To overcome current challenges in the diagnosis and treatment of PD, it is crucial to better understand the mechanisms of disease development and progression. Therefore, animal models that efficiently replicate the core features of human PD are urgently needed in research. So far, no animal model has been discovered that mimics all aspects of the disease. This led to the objective of this study in which we aimed to establish a novel murine PD model based on the inoculation with exogenous α-syn. Previous studies have revealed that the intracerebral or systemic inoculation with synthetic α-syn PFFs into rodents or non-human primates elicits spreading of α-syn, dopaminergic neurodegeneration and neuroinflammation (Kim et al., 2019; Luk et al., 2012a; Patterson et al., 2019; Paumier et al., 2015; Rey et al., 2016; Shimozawa et al., 2017). Further, a recently established human α-syn overexpressing transgenic mouse line (*SNCA*-OVX) showed dopaminergic neurodegeneration in the absence of pathological protein aggregation (Janezic et al., 2013).

To establish a PD mouse model that develops PD-like pathology, we unilaterally injected *SNCA*-OVX transgenic mice with human wild-type α-syn pre-formed fibrils (PFFs) into the right dorsal striatum (**Fig. 6**). It is the first time that PFFs were injected into *SNCA*-OVX transgenic mice. In this transgenic model, the physiological spatio-temporal expression pattern of human α-syn is facilitated in mouse using BAC technology, and human α-syn is expressed onto a *Snca*$^{-/-}$ C57/Bl6 background to prevent the interaction with endogenous mouse α-syn (Janezic et al., 2013). In previous studies where human α-syn PFFs were injected into the striatum of α-syn overexpressing transgenic mice, the protein was expressed under the control of a prion protein (PrP) gene promotor (Luk et al., 2012b; Sorrentino et al., 2017; Earls et al., 2020) which does not reflect the native expression pattern of human α-syn. Further, in these studies mice lines were created onto a C57Bl/C3H background (Giasson et al., 2002), hence expressing endogenous murine α-syn. Therefore, the injection with PFFs in *SNCA*-OVX mice allows the investigation of exclusively human α-syn, that is expressed in the same temporal and spatial pattern as in humans. Moreover, overexpression of α-syn is a mechanism underlying sporadic and familial PD since elevated α-syn levels have been demonstrated in both forms (Miller et al., 2004; Gründemann et al., 2008). In *SNCA*-OVX mice the level of α-syn overexpression

resembles the alteration of α-syn expression levels resulting from *SNCA* gene triplication in familial PD (Miller et al., 2004; Janezic et al., 2013), making it a useful model to study human disease conditions compared to conventional transgenic overexpression models such as rAAv-mediated models that display a dramatic increase in the levels of the protein, unlike observed in human PD (Kirik et al., 2002; Oliveras-Salvá et al., 2013; Duffy et al., 2018a; Gómez-Benito et al., 2020). Taken together, the PFF-injected *SNCA*-OVX mouse model might constitute a novel model system that more precisely replicates human PD pathology and its underlying molecular mechanisms.

Aggregation and spreading of α-syn

To investigate whether inoculation with synthetic α-syn PFFs induces α-syn pathology in *SNCA*-OVX mice, we performed IHC staining against pα-syn, a marker of pathological α-syn in human LBs/LNs (Fujiwara et al., 2002). Consistent with previous findings, deposits of pα-syn were visible in the injection site, the dorsal striatum (**Fig. 8 B**). The great variability of this model system has been attributed to the PFF injection site, among other factors (Gómez-Benito et al., 2020; Polinski et al., 2021). Consistent with previous studies where PFFs were injected in to the striatum, we observe pα-syn accumulations in motor, cingulate, piriform, somatosensory, and entorhinal cortices, olfactory bulb, nuclei of the amygdala, striatum, thalamus and SNpc (**Fig. 8 A**, **B**) (Luk et al., 2012a; Luk et al., 2016; Paumier et al., 2015; Duffy et al., 2018b). These areas are directly interconnected with the injection site, providing abundant innervation to the striatum (Wall et al., 2013; Lanciego et al., 2012). The propagation map of α-syn pathology (**Fig. 8 A**) shows that pα-syn is most abundant in the injection site, and from there it spreads to other brain regions, mentioned above. The colour code illustrates extent of the pathology which is most severe at the injection site (dorsal striatum) and decreases in more distant areas. These observations demonstrate that PFF-seeded α-syn aggregates spread from the striatum to linked brain structures and suggest that pathological α-syn might propagate in a prion-like manner through interneuronal transmission mechanisms, as previously proposed (Kordower et al., 2008; Luk et al., 2012a; Masuda-Suzukake et al., 2013).

Previous publications have indicated that PFFs are taken up by nerve terminals, where they serve as a template and convert endogenous α-syn to pathological hyperphosphorylated form. Over time, abnormal α-syn aggregates accumulate into LNs/LBs inclusions and are transported to interconnected brain regions following a fibrillary retrograde manner (Duffy et al., 2018b; Gómez-Benito et al., 2020). Our findings of pα-syn deposits in regions that provide striatal afferents are consistent with the hypothesis of retrograde α-syn propagation.

In this study, we observe accumulations of pα-syn as dense inclusion bodies or fine fibers (**Fig. S5**), which suggests that these aggregates are localized in the cytoplasm of cell bodies or neuritic processes, as described previously (Luk et al., 2012a; Gómez-Benito et al., 2020). We confirm that pα-syn deposits are present within dopaminergic neurons of the SN (**Fig. 9 B**), again supporting the proposed propagation hypothesis via interneuronal connectivity. Human α-syn PFFs are picked up by the nerve terminals of dopaminergic neurons in the striatum, travelling from there to the cell bodies located in the SNpc. However, we did not investigate α-syn pathology in glial cells which is why we cannot exclude that observed pα-syn inclusions are present in other cell types than

neurons. Interestingly, neuroinflammation has been suggested to be one of the main mechanisms contributing to PD pathogenesis. However, the role of neuroinflammation in the progress of α-syn pathology has not been determined exactly; inflammation may be a response or to or cause of α-syn pathology. Future studies will be aimed at analysing the α-syn-like pathology in the inflammatory response cells, including microglia and astrocytes, and how these cells contribute to disease progression, as done in previous studies (Lai et al., 2021; Luk et al., 2012b).

Furthermore, pα-syn aggregates co-localize with p62/SQSTM1 in the striatum (**Fig. 9 A**) and dopaminergic neurons of the SN (**Fig. 9 B**), indicating that PFF-seeded inclusion share features with human LBs/LNs which is consistent with previous studies (Luk et al., 2012a; Luk et al., 2012b; Paumier et al., 2015; Rey et al., 2016; Chung et al., 2019). For further characterization of induced pα-syn deposits and detection of LBs/LNs-like properties, staining against ubiquitin (Kuzuhara et al., 1988) and heat-shock protein 90 can be conducted in the future. To evaluate amyloid behaviour of α-syn inclusions, digestion with the proteinase K enzyme can be performed since it has been shown that insoluble aggregates such as prions and amyloids prove increased resistance to proteinase K (Takeda et al., 1998; Recasens et al., 2014). Furthermore, thioflavin-S staining is useful to evaluate the solubility of found α-syn aggregates by evidencing the presence of amyloid plaques (Luk et al., 2012b).

Importantly, anti-pα-syn IHC demonstrates pα-syn pathology only in PFF-injected animals, whereas Ctrl mice, deficient of endogenous murine α-syn, and non-injected *SNCA*-OVX mice, overexpressing human wild-type α-syn, do not reveal immunoreactive pα-syn inclusions in any region of the brain (**Fig. 8 B**, **Fig. 10 B**, **Fig. 11 B**). Furthermore, several studies have shown that the injection of α-syn PFFs into murine *Snca*$^{-/-}$ transgenic mice does not lead to the formation of pathological α-syn inclusions (Luk et al., 2012b; Kim et al., 2019). Taken together, our and previous findings indicate that for the occurrence of α-syn pathology (1) endogenous α-syn is needed as a template, (2) human wild-type PFFs act as seeds to convert endogenous α-syn into aggregates of pα-syn and ultimately (3) PFF inoculation is sufficient to induce the spreading of abnormal pα-syn aggregation to distant brain areas.

Striatal inoculation with α-syn PFFs induces pα-syn immunopositive inclusions in the ipsilateral SNpc (**Fig. 8 B**, **Fig. 11 A**) and are detectable in TH-positive dopaminergic neurons within this brain region (**Fig. 9 B**). However, we do not detect pα-syn inclusions in the SNpc contralateral to the injection site (**Fig. 11 B**). Since the nigrostriatal pathway is exclusively unilateral, pathological pα-syn inclusions are restricted to the injected hemisphere, which is consistent with previous studies (Luk et al., 2012a; Paumier et al., 2015). It is well established that DA neurons in the ventral tier of the SNpc, which project mostly to sensory-motor territories of the dorsal striatum, are most vulnerable for neurodegeneration in PD (Dickson et al., 2009; Surmeier et al., 2017; Dickson, 2018; Wong et al., 2019; Young et al., 2023). As seen in **Fig. 11 A** the majority of pα-syn deposits are found in the ventral part of the SNpc, where in turn we can observe the greatest loss of TH-positive neurons (**Fig. 13 A**). These findings again support the interneuronal spread of α-syn aggregates from striatal terminals to cell bodies in the SNpc.

Moreover, pα-syn aggregates are present not only in the ipsilateral hemisphere, but also in some areas of the contralateral hemisphere to the injection site, especially in the striatum (**Fig. 10 A**), cortices, and nuclei of the amygdala (**Fig. 8 C**).

Immunohistochemical staining revealed that pα-syn aggregates in the contralateral site are less abundant compared to the ipsilateral hemisphere which is graphically illustrated in the propagation map (**Fig. 8 A**). To confirm our observation, the number of Ser129-phosphorylated α-syn aggregates was automatically quantified in the striatum (**Fig. 10 C**), confirming that significantly more pα-syn aggregates are detected in the ipsilateral hemisphere, in agreement with previous studies (Lai et al., 2021). Similarly, as mentioned before, no aggregates are found in the contralateral SNpc and manual quantification confirmed significant differences between hemispheres (**Fig. 11 B**, **C**). Future analysis will be aimed at determining the number of pα-syn inclusions in other brain areas of interest, such as the motor cortex or amygdala, using the quantification method developed (see “Material and methods – Image acquisition and analysis – Quantification of pα-syn aggregates”).

Immunoreactive accumulations of pα-syn are detected in fibers of the anterior commissure and corpus callosum (**Fig. 8 C**), suggesting a spread of α-syn along major white matter fibers and that they might serve as path for disease transmission. These tracts are commissural fibers that extend bilaterally and connect both hemispheres, which could explain the interhemispheric transmission of α-syn pathology, overserved in this and previous studies (Luk et al., 2012; Luk et al., 2012b; Paumier et al., 2015; Creed et al., 2022). Moreover, pα-syn positive deposits are visible in the internal capsule (**Fig. 8 B**), a white matter structure consisting of projection fibers to and from the cerebral cortex, passing through/fusing into the corpus striatum (Ni et al., 2018). Since this region is adjacent to the injection site, the internal capsule might take up pathological pα-syn seeds and provide a travel route to other brain areas, further indicating α-syn propagation following interneuronal connectivity.

Notably, pα-syn accumulations are particularly abundant in the cortices and nuclei of the amygdala, especially the PMCo, not only in the ipsilateral, but also in the contralateral hemisphere (**Fig. 8 C**). It is known that the entire cortex, both ipsilateral and contralateral hemisphere, innervate the striatum. As well, the striatum is bilaterally connected to the amygdala, receiving glutamatergic inputs (Pan et al., 2010; Lanciego et al., 2012). The high number of pα-syn aggregates in contralateral cortices and nuclei of the amygdala might be explained by the high degree of innervation from these brain regions, being in accordance with previous publications and proposed α-syn propagation along neuronal pathways (Luk et al., 2012a; Paumier et al., 2015; Patterson et al., 2019; Creed et al., 2022).

Further, we observe pα-syn inclusions in the DR (**Fig. 8 B**), although in a lower number compared to other brain regions (**Fig. 8 A**). This observation is in contrast with other studies where no α-syn aggregates were found in the DR until 180 days after intrastriatal inoculation with mouse α-syn PFFs in mouse (C57BL6/CH3, Luk et al., 2012a) and rat (Sprague Dawley, Paumier et al., 2015). In these studies, no α-syn pathology was found in distant monoaminergic cell groups, neither in the serotonergic DR, nor in the norepinephrine locus coeruleus. Hence, they proposed that monoaminergic populations are differentially vulnerable/susceptible to α-syn pathology. However, the DR (and locus coeruleus) constitute a brain area from where projections to the striatum arise, even though having a relatively sparse input (Lanciego et al., 2012; Pasquier et al., 1977), providing a route of transmission. The low number of aggregations in the DR observed in this study might be related to the low degree of innervation. Nevertheless, it is important to highlight the differences between our study

and previous ones, such as the animal species/strain, the dose, and the type of α-syn PFFs injected. Since all these factors are described to influence α-syn pathology (Gómez-Benito et al., 2020), they could explain the differences observed in the propagation pattern.

Interestingly, we detect pathological pα-syn deposits in the hippocampus of both the ipsilateral and contralateral hemispheres (**Fig. 8 B**, **C**). The α-syn pathology in this area is relatively low and slightly more pronounced in the ipsilateral hemisphere (**Fig. 8 A**), with fine α-syn deposits, possibly located in cellular processes. This observation is interesting as hippocampal projections to the dorsal striatum (injection site, **Fig. 7**) are not known, whereas direct projections from the hippocampus to the ventral striatum have been described (Thierry et al., 2000; Creed et al., 2022). We hypothesize that (1) it is possible that α-syn aggregates reach the ventral striatum despite having been injected dorsally or (2) due to the technical difficulty of stereotaxic injections, in some animals α-syn PFFs have been injected more closely to the ventral striatum, explaining the finding of pα-syn inclusions in the hippocampus. In past studies hippocampal pathology is typically not reported: immunopositive pα-syn accumulations were not found until 180 days after intrastriatal mouse α-syn inoculation in mouse (Luk et al., 2012a) and rat (Paumier et al., 2015). However, other publications reported hippocampal pα-syn aggregates upon unilateral inoculation into the striatum. Lai et al. (2021) found a low number of small immunopositive pα-syn inclusions at 30, 90, and 120 days after mouse α-syn PFF injection. Similarly, Luk et al. (2012b) found few pα-syn inclusions in the hippocampus 30 and 90 days after injection of C-terminally truncated human α-syn1-120 Myc PFFs in the right striatum and cortex. Also, Creed et al. (2022) detected bilateral pα-syn positive aggregates in the hippocampus at 3- and 6-months post injection of wild-type mice, intrastriatally injected with small length mouse PFFs. Creed and colleagues hypothesized that the preparation of shorter PFFs might facilitate the diffusion from the dorsal striatum to ventral striatum, from where α-syn aggregates could spread to the hippocampus. Further, hippocampal pathology was reported in transgenic mice upon direct hippocampal injection of recombinant α-syn in transgenic mice (Sacino et al., 2014), internal capsule/caudate putamen inoculation with full-length wild-type human/mouse α-syn fibrils in α-syn transgenic/non-transgenic mice (Sorrentino et al., 2017), and bilateral intrastriatal injection with α-syn PFFs generated using a distinct sonication protocol (Stoyka et al., 2021), similar to Creed et al. (2022). These findings show that injection site, origin and preparation of PFFs, and host species is crucial for the induction of α-syn pathology, which has been reported previously (Gómez-Benito et al., 2020). Interestingly, we find α-syn pathology in the internal capsule (**Fig. 8 B**), whose neuronal processes might be implicated in the propagation of α-syn to the hippocampus as hippocampal pα-syn pathology was detected upon mouse/human WT α-syn PFF inoculation into the internal capsule of transgenic mice (Sorrentino et al., 2017).

Lastly, I want to highlight that this α-syn based PD model constitutes a good model system to study both familial and sporadic PD. Janezic et al. (2013) reported that the transgenic mouse line *SNCA*-OVX overexpressing human wild-type α-syn mimics increased α-syn levels caused by *SNCA* triplication, and also mentioned that sporadic PD displays elevated α-syn mRNA levels. Here, we show that the inoculation with human α-syn PFFs induces α-syn pathology, that was absent transgenic *SNCA*-OVX animals (Janezic et al., 2013). Thereby, we managed to model pα-syn aggregation and propagation in a context with disease-relevant α-syn expression levels. Furthermore, in

this model we study the pathology of human α-syn by injecting human α-syn PFFs into human α-syn overexpressing mice, that lack endogenous murine α-syn (Janezic et al., 2013). Previous studies used wild-type mice for intrastriatal inoculation with mouse (Luk et al., 2012a; Lai et al., 2021; Creed et al., 2022) or human α-syn PFFs (Luk et al., 2016; Fares et al., 2016) for studying PD pathology. However, studying the human and not murine form of α-syn is important since it is similar but not identical to that found in the mouse. Furthermore, we excluded potential interactions of human α-syn with endogenous one to exclusively observe human α-syn pathology. Moreover, in our model the α-syn encoding *SNCA* gene expression is driven by endogenous promoters and regulatory elements to enable correct spatio-temporal regulation of expression (Janezic et al., 2013). That makes this model especially useful to determine which brain areas are most vulnerable to α-syn pathology in human disease since the pattern of expression in *SNCA*-OVX mice reflects the human α-syn expression profile. In contrast, in previous studies where PFFs were injected in α-syn overexpressing transgenic mice, α-syn was expressed under PrP gene promoters (Luk et al., 2012b; Sorrentino et al., 2017; Earls et al., 2020). Altogether, our model allows us to investigate disease mechanisms that resemble the human pathology of PD more closely compared to previous model systems.

Impact of α-syn pathology on dopaminergic neurodegeneration

To assess if PFF-seeded α-syn pathology in *SNCA*-OVX mice has an impact on the integrity of the nigrostriatal pathway, we performed IHC experiments against TH in the striatum, SNpc, and SNr.

We observed that α-syn pathology in PFF-injected *SNCA*-OVX mice is accompanied by a decrease in dopaminergic nerve terminal density in the striatum using TH immunoreactivity (**Fig. 12**), as observed in previous studies (Lai et al., 2021; Paumier et al., 2015). More specifically, the significant reduction in the ipsilateral hemisphere of PFF-injected animals and the minor (non-significant) decrease in the contralateral hemisphere is conclusive with observed PFF-seeded α-syn pathology in the striatum, where more pα-syn deposits are detected in the ipsilateral than in the contralateral hemisphere (**Fig. 10**). This finding suggests that α-syn pathology leads to a reduction in TH immunoreactivity, indicating a decrease of innervation density in the striatum. However, it must be considered that the reduction of cell markers like TH solely shows a downregulation of such but does not confirm that terminals are lost/degenerated. More specifically, it has been described that α-syn regulates/controls DA synthesis and its content in the different vesicular pools in dopaminergic neurons (Venda et al., 2010) and α-syn inhibits TH activity due to TH dephosphorylation through α-syn interaction with protein phosphatase 2A (Peng et al., 2005).

Moreover, the minor loss of TH immunoreactivity in non-injected *SNCA*-OVX mice compared to Ctrl (**Fig. 12**) might be consistent with the early deficits in DA transmission in the dorsal striatum of *SNCA*-OVX observed previously (Janezic et al., 2013). TH regulates DA neurotransmission at the DA biosynthesis step by being the rate-limiting enzyme that catalyses the conversion of L-tyrosine to (L-DOPA). Although, reduced DA release were not due to lower levels of DA content in the striatum as HPLC revealed similar net DA content compared to Ctrl (Janezic et al., 2013).

One limitation of this study is the control group as we did not inject pure vehicle into control animals. Typically, in previous studies control animals were injected with pure

PBS and/or α-syn monomers (Luk et al., 2012a; Rey et al., 2016; Duffy et al., 2018b; Creed et al., 2022) to demonstrate that (1) the injection and vehicle material itself does not affect the observed phenotype, and (2) specifically α-syn fibrils, not monomers, are needed to induce PD-like pathology. Many studies reported that monomers do not induce robust pα-synuclein immunoreactive inclusions (Volpicelli-Daley et al., 2011; Luk et al., 2012a; Rey et al., 2016; Creed et al., 2022), whereas others found inclusion-containing neurons at later time points, without nigrostriatal degeneration (Paumier et al., 2015; Patterson et al., 2019). Hence, it would be important to include a control group to confirm that α-syn pathology is induced by α-syn PFFs, but not α-syn monomers. Moreover, the dopaminergic system is particularly vulnerable to stress (see "Introduction – Parkinson's disease – aetiology"). Therefore, it is important to demonstrate that striatal loss of TH immunoreactivity is induced specifically by the formation of pα-syn aggregates and not due to stress associated with injection and/or vehicle material.

To further study PFF related effects on the nigrostriatal pathway, stereological quantification of TH-positive neurons was performed in the SNpc. We observed that α-syn pathology induced unilateral loss of TH immunoreactivity in the SNpc (**Fig. 13**) as observed in previous studies (Luk et al., 2012a; Luk et al., 2016; Lai et al., 2021; Creed et al., 2022). This is in line with our finding of ipsilateral pα-syn aggregates in the SNpc (**Fig. 11**), indicating that inclusions trigger the reduction of TH-positive cells. Yet, there are studies that report bilateral degeneration of nigral neurons in presence of ipsilateral SNpc pα-syn inclusions after unilateral α-syn PFF inoculation (Paumier et al., 2015; Duffy et al., 2018b), with later onset of contralateral degeneration at 6 months post injection (Patterson et al., 2019). This indicates a possible "inclusion-independent" mechanism affecting nigral degeneration in the contralateral hemisphere (Patterson et al., 2019). To study possible bilateral degeneration, IHC at later time points could be conducted.

Importantly, it would be interesting to confirm an actual degeneration of neurons and/or nerve terminals. Until now, we observed a reduction of TH-stained area which could also be related to a downregulation of TH expression but does not necessarily confirm the death of DA neurons/terminals. To investigate whether an actual reduction in cell number is present, tissue can be processed with hematoxylin and eosin staining (making cell nuclei visible) or NeuN staining (used to visualize neuronal nuclei), to assess the number of cells (Janezic et al., 2013). Another more selective method to study neuronal degeneration is silver staining (Ares-Santos et al., 2014).

Janezic et al. (2013) demonstrated the loss of dopaminergic SNpc neurons in 18 months-old *SNCA*-OVX mice in the absence of α-syn pathology. Hence, they proposed that pathological α-syn is not required for neuronal death in the SN but is a consequence of human α-syn overexpression. In this study, we observe a reduction of TH-positive cells in the ipsilateral SNpc in 7-8 months-old *SNCA*-OVX mice upon inoculation with α-syn PFFs (**Fig. 13**). This finding indicates that PFF-seeded α-syn aggregation is able to accelerate cell death in the SN to earlier timepoints, even though pathological α-syn aggregation might not be necessary for DA neurodegeneration and might occur anyways in aged *SNCA*-OVX animals, according to Janezic et al. (2013). Further, we did not observe a reduction in TH-immunoreactive cells in non-injected *SNCA*-OVX animals (7-8 months) compared to Ctrl *SNCA*-deficient mice (**Fig. 13**)

which is consistent with previously obtained results, where dopaminergic cell loss was only observed in aged *SNCA*-OVX mice of 18 months (Janezic et al., 2013).

Consistently, we observe a decrease of TH immunoreactivity in the ipsilateral SNr (**Fig. 14**), indicating that dopaminergic innervation density from the SNpc is decreased in this area. This finding additionally indicates that pα-syn aggregates found in the ipsilateral SNpc (**Fig. 11**) not only lead to unilateral SNpc neuron loss, but also to a reduction of dopaminergic SNpc projections. Future studies will aim to analyse morphological abnormalities in dopaminergic neurons of SNpc induced by α-syn aggregates, such as neuronal shrinkage (Chiu et al., 2021) or pathological changes including pyknotic perykaria, vacuolation of the cytoplasm, or swollen processes as described in previous studies (Tofaris et al., 2006).

Effect of α-syn pathology on motor behaviour

To investigate whether dopaminergic denervation in the striatum (**Fig. 12**) leads to motor deficits, we performed a challenging beam transversal test 150 days after human α-syn PFF inoculation (**Fig. 15**). Errors per step made is the parameter that might most reliably reflect fine motor deficits. We observe that PFF-injected animals display a higher errors per step ratio compared to non-injected *SNCA*-OVX animals, but practically the same ratio as Ctrl animals (**Fig. 15 A**). However, it is important to highlight the wide variability observed, especially in the Ctrl group, which could be attributed to the age of tested animals. Studies from our laboratory (unpublished data) show that the weight of mice changes considerably depending on the age and genotype of the animal (**Fig. S6**). We observe a prominent age-dependent weight gain in Ctrl mice that is not observed in *SNCA*-OVX mice. In particular, we find that the body weight of Ctrl mice is significantly higher at 6- and 12-months of age compared to *SNCA*-OVX mice. For behavioural testing, we used Ctrl and non-injected *SNCA*-OVX mice of 6 months. At this age, differences in weight are already observed between Ctrl and *SNCA*-OVX mice, which can complicate the interpretation of our results. Since we observed difficulties to traverse the beam for some Ctrl animals possibly due to higher body mass, we hypothesize that the weight of the animals is important for carrying out the test. In previous studies it has been taken into account that body weight might have an impact on motor behaviour in the rotarod test, a test to evaluate grip strength, motor coordination and balance (Brown et al., 2007; Wagner et al., 2019). Though, a previous study reported that the challenging beam transversal test might be less influenced by body weight in comparison to other tests assessing motor performance such as rotarod and pole test (Fleming et al., 2013). Still, for future studies it is important to weight animals before behavioural assessment to exclude body mass-related variabilities.

However, no differences are observed in the number of steps between groups (**Fig. 15 B**). Interestingly, non-injected *SNCA*-OVX and PFF-inoculated *SNCA*-OVX mice take slightly more time to traverse the beam compared to Ctrl (**Fig. 15 C**), with no apparent statistically significant differences between these two groups. Though, it has to be noted that some animals in all the measured parameter deviate from the values of the majority in the group, increasing the mean of the group. It is interesting that although PFF-injected mice do not take more steps to cross the beam or spend more time than non-injected *SNCA*-OVX mice, the ratio of errors per step is higher in PFF-injected animals.

Furthermore, it has to be considered that the latency to traverse the beam is not exclusively dependent on the worsening of motor behaviour but can be influenced by other factors like distraction or lack of motivation (Luong et al., 2011). We observed that many animals took more time to cross the beam because they were sniffing, not moving, or turning around and walking back to the start. We can exclude that animals did not understand how to fulfil the task because they already performed the test several times before recording the trials. Interestingly, we observed while conducting the behavioural experiments that *SNCA*-OVX mice display a more anxious behaviour compared to Ctrl animals. Supporting our observation, a recent publication reported an age-dependent increase in anxiety-like behaviour in *SNCA*-OVX mice (Lamontagne-Proulx et al., 2023). To confirm this observation, it would be interesting to perform additional tests to evaluate anxiety such as open field test or elevated plus maze (Walf et al., 2007; Luk et al., 2012a; Rey et al., 2016; Lamontagne-Proulx et al., 2023).

In this study, we did not find clear motor deficits, but the observations discussed above must be acknowledged. A limitation of the present study is the use of only one single behavioural test. To complement our results, we should perform further behaviour assays to determine whether striatal denervation produces motor impairment. Experiments to assess the deterioration of motor symptoms conducted in previous studies include rotarod test (Luk et al., 2012a; Kim et al., 2019; Lai et al., 2021), wire-hang test (Luk et al., 2012a; Lai et al., 2021), clasping test (Lai et al., 2021), pole test (Mao et al., 2016; Kim et al., 2019), grip strength test to assess neuromuscular strength (Mao et al., 2016; Kim et al., 2019), open-field activity to assess motor and anxiety-related deficits (Luk et al., 2012a; Rey et al., 2016; Patterson et al., 2019; Lamontagne-Proulx et al., 2023), cylinder task test to evaluate forelimb use asymmetry since extent of striatal denervation correlates with forelimb use (Paumier et al., 2015; Gombash et al., 2013; Patterson et al., 2019).

Correlation studies

In the end, we wanted to measure the interplay between obtained results using the Pearson correlation (**Fig. 16**). Correlations calculated were between the number of pα-syn aggregates and striatal TH-immunopositive area (**A**), number of pα-syn aggregates and number of TH-positive SNpc neurons (**B**), and the TH-immunopositive area in the ipsilateral striatum and errors per step (**C**).

Based on our hypothesis and previous studies we expected a negative correlation between parameters. In other words, we presumed that a higher number of pα-syn aggregates coincide with (1) a more pronounced striatal denervation and (2) increased loss of dopaminergic SNpc neurons. Further, we hypothesized that low striatal innervation coincides with high errors per step. In our study we observe that a higher number of pathological pα-syn deposits might correlate with lower dopaminergic cells in the SNpc (**Fig. 16 B**), however not significant. The other parameters did not display expected tendency. However, it is important to note that a loss of DA striatal terminals and neurons in the SNpc at a specific time point may involve a reduction in the number of pα-syn aggregates as a direct consequence of degeneration. This would establish a positive correlation between the number of pα-syn aggregates and the DA denervation/degeneration of the nigrostriatal pathway, as previously observed (Luk et al, 2012a; Lai et al., 2021).

We aimed to investigate the interplay between parameters, especially between individual animals. The presentation of data using the mean value of a group can mask observation of individual animals. To demonstrate findings for each animal, we performed the correlation analysis. It is well described that the model based on the inoculation with exogenous α-syn comes with high variability between animals (and research groups) due to the preparation of fibrils, the selected injection site and high precision that is required during stereotaxic procedures (Gómez-Benito et al., 2020). In that context I want to highlight that values are scattered and not all uniformly placed around the linear trend line, especially noticeable in **Fig. 16 C**. This finding reflects a variability between animals and the need to have a high number of injected mice to obtain homogenous results that provide robustness to the generated model.

Sex-specific differences

As a last part, I wanted to explore whether our obtained results display differences between female and male animals. It is well known, and many times reviewed that sex bias exist in basic research among all disciplines. It has been reported that many publications do not provide information about studied sex, even though sex might influence outcomes. Moreover, if sex was reported, the analysed sex was mainly male (Kong et al., 2016; Bryant et al., 2018; Coiro et al., 2019; Miličić Stanić et al., 2021). One review stated that, in animal research, 22% of papers would not specify the sex of animals. While of those publications that specified the sex, 80% included males only. Moreover, regarding the number of animals studied; 84% were male, and 16% female (Yoon et al., 2014).

Furthermore, it is known that differences between sexes are present in PD. Reportedly, the incidence rate of developing PD is higher in men with the relative risk being 1.5 times greater in men than women (Wooten et al., 2004). Reviews explored the sex-specific differences in PD regarding disease risk factors, manifestation of motor and non-motor symptoms, and response to treatment (Cerri et al., 2019; Vaidya et al., 2021). Interestingly, a recent publication investigated sex and age differences in the *SNCA*-OVX transgenic mouse model (Lamontagne-Proulx et al., 2023). This study reported a more abrupt nigrostriatal DA decrease, together with increased microgliosis in male *SNCA*-OVX animals compared to female. The difference in DA content was lost at 18 months of age, which authors attributed to the reduction of neuroprotection promoted by female sex steroids. Conjointly, these observations encouraged me to look into sex-specific differences in our obtained results and include this part into my thesis.

Overall, analysis of sex-specific variation in α-syn pathology (**Fig. 17**), nigrostriatal pathway integrity (**Fig. 18**), and motor performance and fine motor control (**Fig. 19**) did not reveal significant differences between female and male animals. However, it must be recognized that the number of animals per parameter, group and sex is low, and values are highly variable within the same group. In future experiments, it is desirable to increase the number of animals per group and equal the number between sexes.

Additionally, I want to mention that errors per step ratio is (not significantly) higher in males of the Ctrl group compared to Ctrl females (**Fig. 19 A**). This observation is consistent with our finding that weight increase is, overall, higher in males compared to females (**Fig. S6 B**, **C**). Male Ctrl mice display higher body mass at 6 months compared to females of the same group and time point. This observation again

supports that body weight could influence the errors made when crossing the beam, as discussed in the previous section (motor behaviour).

Future outlook

In the next section, future research ideas are presented, and additional experiments are proposed to fully characterize our novel PD model based on the inoculation with human wild-type α-syn PFFs into the dorsal striatum of *SNCA*-OVX mice.

In the future, it would be interesting to study inflammatory response upon PFF inoculation and determine how it contributes to the development and/or progression of the pathology. Previously, it has been shown in cell culture studies that both soluble and aggregated α-syn activate neuroinflammation (Zhang et al., 2005; Lee et al., 2009; Kim et al., 2013). Other studies reported activation of an inflammatory response at the same time or even prior to pathological α-syn accumulation, *in vivo* and *in vitro* upon administration of exogenous α-syn (Duffy et al., 2018b; Olanow et al., 2019; Kim et al., 2020; Lai et al., 2021). Duffy et al. (2018) demonstrated that intraneuronal pα-syn inclusions induced MHC-II expression and reactive microgliosis prior to neurodegeneration in the SNpc, providing evidence for microglial contribution to nigral cell loss. Olanow et al. (2019) observed activated microglia even before α-syn accumulation in grafted cells. Consistently, it was shown in a PFF mouse model that neuroinflammatory response precede α-syn aggregation (Izco et al., 2021). Another study revealed that both astrocytes and microglia are highly activated upon striatal PFF injection in mouse before the acceleration of α-syn accumulation, possibly contributing to pα-syn aggregation (Lai et al., 2021). Taken together, these findings suggest that neuroinflammation might precede and contribute to pathological α-syn propagation, which contrasts with a previous notion of inflammation being (solely) a consequence of synucleinopathy. Interestingly, a recent study in PFF-injected mice reported that the activation of microglia, triggered by oligomeric α-syn, occurs even before the presence of pα-syn inclusions and neurodegeneration. Further, neurodegeneration and microgliosis is detected in regions with and absent of pα-syn inclusions. Their findings indicate that microgliosis, not α-syn aggregates, might be the major driver of degeneration of the midbrain (Garcia et al., 2022). All these findings show that further research has to be conducted to elucidate whether inflammation is cause or consequence of α-syn pathology, or both, which ultimately leads to neurodegeneration of midbrain neurons. To investigate neuroinflammation and the occurrence of reactive astrocytes and microglia, IHC and/or immunoblots against Iba1 (all microglia marker), MHC-II (antigen-presenting microglia marker) and GFAP (astrocyte marker) can be performed (Duffy et al., 2018b; Lai et al., 2019). Also, RNAscope in situ hybridization (against Iba-1, MHC-II) has been performed in past studies (Duffy et al., 2018b).

In this study we show that pα-syn aggregates behave like a prion, spreading from the injection site to other brain areas. We hypothesize that the routes of transmissibility follow interneuronal connectivity via fibrillary retrograde transport (Gómez-Benito et al., 2020). Some studies of PFF models did not detect pα-syn aggregates in glial cells like astrocytes, microglia or oligodendrocytes, proposing transneuronal transport of α-syn seeds (Rey et al., 2016; Paumier et al., 2015). However, several studies observed that pα-syn inclusions are not only found in neurons, but also glial cells such as microglia and/or astrocytes in several brain regions (Lai et al., 2021; Luk et al., 2012b; Sorrentino et al., 2017; Sorrentino et al., 2018). This observation is consistent with reports that α-

syn seeds can be transferred between neurons and astrocytes, potentially via exosomes or tunneling tubes (Rostami et al., 2017). Interestingly, it has been postulated that microglia are a key player in the transmission of α-syn via exosomal pathways (Xia et al., 2019) and microglial exosomes are implicated in the progression of α-syn pathology (Guo et al., 2020). Hence, Lai et al. (2021) hypothesized that activated microglia might take up pathological α-syn to clear it up, and then release fragmented α-syn via exosomes. These could be transferred to other cells/neurons and enable accelerated α-syn transmission. Together, these findings suggest that α-syn transfer might not only appear via the canonical interneuronal connections, but that glia-neuronal transmission could also be associated with α-syn spreading. Therefore, it would be interesting to determine if pα-syn inclusions are present not only in neurons, but also in other cell types such as astrocytes and microglia. IHC against phosphorylated α-syn, Iba1, GFAP can be conducted to assess if pα-syn deposits co-localize with markers of glial cell types.

In addition, it would be interesting to further investigate the conformational nature of the detected pathological α-syn using conformation-specific antibodies. Previously, it has been proposed that oligomeric species are the most toxic entity of α-syn (Winner et al., 2011; Karpinar et al., 2009). However, α-syn exists in numerous forms – monomers, tetramers, oligomers, fibrils – and during disease α-syn undergoes conformational changes that ultimately lead to the formation of abnormal aggregates and inclusion bodies. Since it is known that α-syn exists in many states which are differently implicated in disease progression, it would be interesting to study whether specific conformations of α-syn have an increased potential in spreading along the neuroaxis depending on their toxicity, transmissibility and seeding (see “Introduction – Parkinson’s disease – α-Synuclein – propagation and spreading”). Further supporting this objective is the fact that structurally distinct α-syn assemblies or strains have been discovered that target distinct brain areas/cell types, and cause different clinical-pathological responses, giving rise to different manifestations of synucleinopathies (PD, DLB, MSA) (see “Introduction – Parkinson’s disease – Aggregation and toxicity”). To study conformational species of α-syn, IHC using antibodies against O2 (anti-α-syn fibrils/oligomers) and F2 (anti-α-syn fibrils) can be performed and compared with immunoreactivity to pα-syn (Vaikath et al., 2015; Duffy et al., 2018b; Patterson et al., 2019).

Lastly, I want to mention that this PD mouse model is a good model system to study therapy strategies. It is well established that α-syn PFF models of PD are an inducible model which enables the spatio-temporal control of pathology induction. It provides a wide temporal window that allows monitoring and/or tracking of pathology onset and progression. Furthermore, this model is useful to study human PD progression since α-syn levels in PFF models are much closer to that of human condition, in contrast to viral vector-based or some transgenic models. Also, pathology is induced by disease-relevant changes of endogenous α-syn upon α-syn PFF injection (Polinski et al., 2018; Volpicelli-Daley et al., 2011; Luk et al., 2012a; Paumier et al., 2015). Since the PFF-based model of PD relatively robustly mimics the propagation of α-syn, it might be of use to study therapeutic intervention that aim to prevent the development of α-syn, halt its progression, or restrict α-syn transmission. It has been proposed that the exosomal transmission of α-syn might be an interesting therapeutic target (Xia et al., 2019; Guo et al., 2020). Moreover, the utility of antibodies against α-syn as a diagnostic tool and therapeutic target has been proposed. Disease-modifying therapies using antibodies

have focused on reducing α-syn expression, decreasing α-syn aggregation, increasing α-syn clearance via autophagy, preventing the seeding/spreading of α-syn and nanobodies targeting α-syn have been used as a therapeutic approach (reviewed in Vaikath et al., 2019). Recently, nanobodies have been tested in α-syn PFF models. One study has shown that the fibril-specific nanobody PFFNB2 prevented PFF induced α-syn phosphorylation and propagation from the injection site to the cortex (Butler et al., 2022), supporting that PFF models are a promising tool to study disease mechanisms as well as disease-modifying interventions.

Conclusions

From the results obtained in this study, we can draw the following conclusions:

1. The intrastriatal inoculation with human wild-type α-syn pre-formed fibrils (PFFs) into *SNCA*-OVX mice seeds the formation of pathological α-syn aggregates.
2. Pathological α-syn deposits propagate from the injection site to distant brain areas in both hemispheres, possibly along interneuronal connectivity via retrograde transmission.
3. Pathological α-syn inclusions display properties of human Lewy bodies and Lewy neurites.
4. PFF-seeded α-syn pathology is accompanied by disturbances of the nigrostriatal system, including unilateral loss of striatal terminals and dopaminergic neurons in the SNpc, along with dopaminergic denervation in the SNr.
5. No robust motor impairment is observed in the PFF-injected *SNCA*-OVX mouse model using the challenging beam transversal test, but additional tests should be performed.

It was the first time that PFFs were injected into *SNCA*-OVX transgenic mice. Given our obtained results and the characteristics of the used transgenic mouse line (Janezic et al., 2013), including the spatio-temporal expression pattern of human α-syn, the absence of endogenous murine α-syn, and α-syn expression levels similar to that observed in human PD patients, we conclude that this novel PD mouse model more closely reflects α-syn pathology and disease processes underlying human PD compared to previous PD model systems. Further, we established a model that is a useful tool to study therapeutic approaches aiming to prevent or halt α-syn pathology and its consequences.

Lastly, we did not observe clear sex-specific differences in our data, but the number of animals was very low per group. To further characterize this PD mouse model, additional experiments should be conducted. It would be interesting to investigate neuroinflammation, α-syn pathology in glial cells, and conformational species of α-syn. For a detailed summary of obtained results see **Table 6** in supplementary material.

References

Abbott, R. D., Petrovitch, H., White, L. R., Masaki, K. H., Tanner, C. M., Curb, J. D., Grandinetti, A., Blanchette, P. L., Popper, J. S., & Ross, G. W. (2001). Frequency of bowel movements and the future risk of Parkinson's disease. Neurology, 57(3), 456–462. https://doi.org/10.1212/wnl.57.3.456

Abeliovich, A., Schmitz, Y., Fariñas, I., Choi-Lundberg, D., Ho, W. H., Castillo, P. E., Shinsky, N., Verdugo, J. M., Armanini, M., Ryan, A., Hynes, M., Phillips, H., Sulzer, D., & Rosenthal, A. (2000). Mice lacking alpha-synuclein display functional deficits in the nigrostriatal dopamine system. Neuron, 25(1), 239–252. https://doi.org/10.1016/s0896-6273(00)80886-7

Abounit, S., Bousset, L., Loria, F., Zhu, S., de Chaumont, F., Pieri, L., Olivo-Marin, J. C., Melki, R., & Zurzolo, C. (2016). Tunneling nanotubes spread fibrillar α-synuclein by intercellular trafficking of lysosomes. The EMBO journal, 35(19), 2120–2138. https://doi.org/10.15252/embj.201593411

Akundi, R. S., Huang, Z., Eason, J., Pandya, J. D., Zhi, L., Cass, W. A., Sullivan, P. G., & Büeler, H. (2011). Increased mitochondrial calcium sensitivity and abnormal expression of innate immunity genes precede dopaminergic defects in Pink1-deficient mice. PloS one, 6(1), e16038. https://doi.org/10.1371/journal.pone.0016038

Ares-Santos, S., Granado, N., Oliva, I., O'Shea, E., Martin, E. D., Colado, M. I., & Moratalla, R. (2012). Dopamine D(1) receptor deletion strongly reduces neurotoxic effects of methamphetamine. Neurobiology of disease, 45(2), 810–820. https://doi.org/10.1016/j.nbd.2011.11.005

Ares-Santos, S., Granado, N., Espadas, I., Martinez-Murillo, R., & Moratalla, R. (2014). Methamphetamine causes degeneration of dopamine cell bodies and terminals of the nigrostriatal pathway evidenced by silver staining. Neuropsychopharmacology: official publication of the American College of Neuropsychopharmacology, 39(5), 1066–1080. https://doi.org/10.1038/npp.2013.307

Arganda-Carreras, I., Fernández-González, R., Muñoz-Barrutia, A., & Ortiz-De-Solorzano, C. (2010). 3D reconstruction of histological sections: Application to mammary gland tissue. Microscopy research and technique, 73(11), 1019–1029. https://doi.org/10.1002/jemt.20829

Arzt, M., Deschamps, J., Schmied, C., Pietzsch, T., Schmidt, D., Tomancak, P., Haase, R., & Jug, F. (2022). LABKIT: Labeling and Segmentation Toolkit for Big Image Data. Frontiers in Computer Science, 4. https://doi.org/10.3389/fcomp.2022.777728

Balestrino, R., & Schapira, A. H. V. (2020). Parkinson disease. European journal of neurology, 27(1), 27–42. https://doi.org/10.1111/ene.14108

Bartels, T., Choi, J. G., & Selkoe, D. J. (2011). α-Synuclein occurs physiologically as a helically folded tetramer that resists aggregation. Nature, 477(7362), 107–110. https://doi.org/10.1038/nature10324

Berardelli, A., Wenning, G. K., Antonini, A., Berg, D., Bloem, B. R., Bonifati, V., Brooks, D., Burn, D. J., Colosimo, C., Fanciulli, A., Ferreira, J., Gasser, T., Grandas, F., Kanovsky, P., Kostic, V., Kulisevsky, J., Oertel, W., Poewe, W., Reese, J. P., Relja, M., … Vidailhet, M. (2013). EFNS/MDS-ES/ENS [corrected] recommendations for the

diagnosis of Parkinson's disease. European journal of neurology, 20(1), 16–34. https://doi.org/10.1111/ene.12022

Blesa, J., & Przedborski, S. (2014). Parkinson's disease: animal models and dopaminergic cell vulnerability. Frontiers in neuroanatomy, 8, 155. https://doi.org/10.3389/fnana.2014.00155

Bloem, B. R., Okun, M. S., & Klein, C. (2021). Parkinson's disease. Lancet (London, England), 397(10291), 2284–2303. https://doi.org/10.1016/S0140-6736(21)00218-X

Boeve, B. F., Silber, M. H., Saper, C. B., Ferman, T. J., Dickson, D. W., Parisi, J. E., Benarroch, E. E., Ahlskog, J. E., Smith, G. E., Caselli, R. C., Tippman-Peikert, M., Olson, E. J., Lin, S. C., Young, T., Wszolek, Z., Schenck, C. H., Mahowald, M. W., Castillo, P. R., Del Tredici, K., & Braak, H. (2007). Pathophysiology of REM sleep behaviour disorder and relevance to neurodegenerative disease. Brain : a journal of neurology, 130(Pt 11), 2770–2788. https://doi.org/10.1093/brain/awm056

Bohnen, N. I., Studenski, S. A., Constantine, G. M., & Moore, R. Y. (2008). Diagnostic performance of clinical motor and non-motor tests of Parkinson disease: a matched case-control study. European journal of neurology, 15(7), 685–691. https://doi.org/10.1111/j.1468-1331.2008.02148.x

Braak, H., Del Tredici, K., Rüb, U., de Vos, R. A., Jansen Steur, E. N., & Braak, E. (2003). Staging of brain pathology related to sporadic Parkinson's disease. Neurobiology of aging, 24(2), 197–211. https://doi.org/10.1016/s0197-4580(02)00065-9

Braak, H., de Vos, R. A., Bohl, J., & Del Tredici, K. (2006). Gastric alpha-synuclein immunoreactive inclusions in Meissner's and Auerbach's plexuses in cases staged for Parkinson's disease-related brain pathology. Neuroscience letters, 396(1), 67–72. https://doi.org/10.1016/j.neulet.2005.11.012

Braak, H., Ghebremedhin, E., Rüb, U., Bratzke, H., & Del Tredici, K. (2004). Stages in the development of Parkinson's disease-related pathology. Cell and tissue research, 318(1), 121–134. https://doi.org/10.1007/s00441-004-0956-9

Brown, R. E., & Wong, A. A. (2007). The influence of visual ability on learning and memory performance in 13 strains of mice. Learning & memory (Cold Spring Harbor, N.Y.), 14(3), 134–144. https://doi.org/10.1101/lm.473907

Bryant, J., Yi, P., Miller, L., Peek, K., & Lee, D. (2018). Potential Sex Bias Exists in Orthopaedic Basic Science and Translational Research. The Journal of bone and joint surgery. American volume, 100(2), 124–130. https://doi.org/10.2106/JBJS.17.00458

Butler, Y. R., Liu, Y., Kumbhar, R., Zhao, P., Gadhave, K., Wang, N., Li, Y., Mao, X., & Wang, W. (2022). α-Synuclein fibril-specific nanobody reduces prion-like α-synuclein spreading in mice. Nature communications, 13(1), 4060. https://doi.org/10.1038/s41467-022-31787-2

Burré, J., Sharma, M., Tsetsenis, T., Buchman, V., Etherton, M. R., & Südhof, T. C. (2010). Alpha-synuclein promotes SNARE-complex assembly in vivo and in vitro. Science (New York, N.Y.), 329(5999), 1663–1667. https://doi.org/10.1126/science.1195227

Burré, J., Vivona, S., Diao, J., Sharma, M., Brunger, A. T., & Südhof, T. C. (2013). Properties of native brain α-synuclein. Nature, 498(7453), E4–E7. https://doi.org/10.1038/nature12125

Calabresi, P., Picconi, B., Tozzi, A., Ghiglieri, V., & Di Filippo, M. (2014). Direct and indirect pathways of basal ganglia: a critical reappraisal. Nature neuroscience, 17(8), 1022–1030. https://doi.org/10.1038/nn.3743

Cannon, J. R., Geghman, K. D., Tapias, V., Sew, T., Dail, M. K., Li, C., & Greenamyre, J. T. (2013). Expression of human E46K-mutated α-synuclein in BAC-transgenic rats replicates early-stage Parkinson's disease features and enhances vulnerability to mitochondrial impairment. Experimental neurology, 240, 44–56. https://doi.org/10.1016/j.expneurol.2012.11.007

Charcot J. M. (1872). De la paralysie agitante. Oeuvres Complètes (t 1) Leçons sur les maladies du système nerveux, 155–188.

Cerri, S., Mus, L., & Blandini, F. (2019). Parkinson's Disease in Women and Men: What's the Difference?. Journal of Parkinson's disease, 9(3), 501–515. https://doi.org/10.3233/JPD-191683

Chatterjee, D., Bhatt, M., Butler, D., De Genst, E., Dobson, C. M., Messer, A., & Kordower, J. H. (2018). Proteasome-targeted nanobodies alleviate pathology and functional decline in an α-synuclein-based Parkinson's disease model. NPJ Parkinson's disease, 4, 25. https://doi.org/10.1038/s41531-018-0062-4

Cheng, H. C., Ulane, C. M., & Burke, R. E. (2010). Clinical progression in Parkinson disease and the neurobiology of axons. Annals of neurology, 67(6), 715–725. https://doi.org/10.1002/ana.21995

Choi, W., Zibaee, S., Jakes, R., Serpell, L. C., Davletov, B., Crowther, R. A., & Goedert, M. (2004). Mutation E46K increases phospholipid binding and assembly into filaments of human alpha-synuclein. FEBS letters, 576(3), 363–368. https://doi.org/10.1016/j.febslet.2004.09.038

Chiu, W. H., Kovacheva, L., Musgrove, R. E., Arien-Zakay, H., Koprich, J. B., Brotchie, J. M., Yaka, R., Ben-Zvi, D., Hanani, M., Roeper, J., & Goldberg, J. A. (2021). α-Synuclein-induced Kv4 channelopathy in mouse vagal motoneurons drives nonmotor parkinsonian symptoms. Science advances, 7(11), eabd3994. https://doi.org/10.1126/sciadv.abd3994

Chung, H. K., Ho, H. A., Pérez-Acuña, D., & Lee, S. J. (2019). Modeling α-Synuclein Propagation with Preformed Fibril Injections. Journal of movement disorders, 12(3), 139–151. https://doi.org/10.14802/jmd.19046

Coiro, P., & Pollak, D. D. (2019). Sex and gender bias in the experimental neurosciences: the case of the maternal immune activation model. Translational psychiatry, 9(1), 90. https://doi.org/10.1038/s41398-019-0423-8

Coleman, C., & Martin, I. (2022). Unraveling Parkinson's Disease Neurodegeneration: Does Aging Hold the Clues?. Journal of Parkinson's disease, 12(8), 2321–2338. https://doi.org/10.3233/JPD-223363

Conway, K. A., Harper, J. D., & Lansbury, P. T. (1998). Accelerated in vitro fibril formation by a mutant alpha-synuclein linked to early-onset Parkinson disease. Nature medicine, 4(11), 1318–1320. https://doi.org/10.1038/3311

Conway, K. A., Lee, S. J., Rochet, J. C., Ding, T. T., Williamson, R. E., & Lansbury, P. T., Jr (2000). Acceleration of oligomerization, not fibrillization, is a shared property of both alpha-synuclein mutations linked to early-onset Parkinson's disease: implications

for pathogenesis and therapy. Proceedings of the National Academy of Sciences of the United States of America, 97(2), 571–576. https://doi.org/10.1073/pnas.97.2.571

Creed, R. B., Memon, A. A., Komaragiri, S. P., Barodia, S. K., & Goldberg, M. S. (2022). Analysis of hemisphere-dependent effects of unilateral intrastriatal injection of α-synuclein pre-formed fibrils on mitochondrial protein levels, dynamics, and function. Acta neuropathologica communications, 10(1), 78. https://doi.org/10.1186/s40478-022-01374-z

Dauer, W., & Przedborski, S. (2003). Parkinson's disease: mechanisms and models. Neuron, 39(6), 889–909. https://doi.org/10.1016/s0896-6273(03)00568-3

Dauvilliers, Y., Schenck, C. H., Postuma, R. B., Iranzo, A., Luppi, P. H., Plazzi, G., Montplaisir, J., & Boeve, B. (2018). REM sleep behaviour disorder. Nature reviews. Disease primers, 4(1), 19. https://doi.org/10.1038/s41572-018-0016-5

Decressac, M., Mattsson, B., Lundblad, M., Weikop, P., & Björklund, A. (2012). Progressive neurodegenerative and behavioural changes induced by AAV-mediated overexpression of α-synuclein in midbrain dopamine neurons. Neurobiology of disease, 45(3), 939–953. https://doi.org/10.1016/j.nbd.2011.12.013

Delamarre, A., & Meissner, W. G. (2017). Epidemiology, environmental risk factors and genetics of Parkinson's disease. Presse medicale (Paris, France : 1983), 46(2 Pt 1), 175–181. https://doi.org/10.1016/j.lpm.2017.01.001

Del Tredici, K., & Braak, H. (2016). Review: Sporadic Parkinson's disease: development and distribution of α-synuclein pathology. Neuropathology and applied neurobiology, 42(1), 33–50. https://doi.org/10.1111/nan.12298

Desplats, P., Lee, H. J., Bae, E. J., Patrick, C., Rockenstein, E., Crews, L., Spencer, B., Masliah, E., & Lee, S. J. (2009). Inclusion formation and neuronal cell death through neuron-to-neuron transmission of alpha-synuclein. Proceedings of the National Academy of Sciences of the United States of America, 106(31), 13010–13015. https://doi.org/10.1073/pnas.0903691106

Dickson D. W. (2018). Neuropathology of Parkinson disease. Parkinsonism & related disorders, 46 Suppl 1(Suppl 1), S30–S33. https://doi.org/10.1016/j.parkreldis.2017.07.033

Dickson, D. W., Braak, H., Duda, J. E., Duyckaerts, C., Gasser, T., Halliday, G. M., Hardy, J., Leverenz, J. B., Del Tredici, K., Wszolek, Z. K., & Litvan, I. (2009). Neuropathological assessment of Parkinson's disease: refining the diagnostic criteria. The Lancet. Neurology, 8(12), 1150–1157. https://doi.org/10.1016/S1474-4422(09)70238-8

Doherty, K. M., Silveira-Moriyama, L., Parkkinen, L., Healy, D. G., Farrell, M., Mencacci, N. E., Ahmed, Z., Brett, F. M., Hardy, J., Quinn, N., Counihan, T. J., Lynch, T., Fox, Z. V., Revesz, T., Lees, A. J., & Holton, J. L. (2013). Parkin disease: a clinicopathologic entity?. JAMA neurology, 70(5), 571–579. https://doi.org/10.1001/jamaneurol.2013.172

Dorsey, E. R., Sherer, T., Okun, M. S., & Bloem, B. R. (2018). The Emerging Evidence of the Parkinson Pandemic. Journal of Parkinson's disease, 8(s1), S3–S8. https://doi.org/10.3233/JPD-181474

Driver, J. A., Logroscino, G., Gaziano, J. M., & Kurth, T. (2009). Incidence and remaining lifetime risk of Parkinson disease in advanced age. Neurology, 72(5), 432–438. https://doi.org/10.1212/01.wnl.0000341769.50075.bb

Duffy, M. F., Collier, T. J., Patterson, J. R., Kemp, C. J., Fischer, D. L., Stoll, A. C., & Sortwell, C. E. (2018a). Quality Over Quantity: Advantages of Using Alpha-Synuclein Preformed Fibril Triggered Synucleinopathy to Model Idiopathic Parkinson's Disease. Frontiers in neuroscience, 12, 621. https://doi.org/10.3389/fnins.2018.00621

Duffy, M. F., Collier, T. J., Patterson, J. R., Kemp, C. J., Luk, K. C., Tansey, M. G., Paumier, K. L., Kanaan, N. M., Fischer, D. L., Polinski, N. K., Barth, O. L., Howe, J. W., Vaikath, N. N., Majbour, N. K., El-Agnaf, O. M. A., & Sortwell, C. E. (2018b). Lewy body-like alpha-synuclein inclusions trigger reactive microgliosis prior to nigral degeneration. Journal of neuroinflammation, 15(1), 129. https://doi.org/10.1186/s12974-018-1171-z

Earls, R. H., Menees, K. B., Chung, J., Gutekunst, C. A., Lee, H. J., Hazim, M. G., Rada, B., Wood, L. B., & Lee, J. K. (2020). NK cells clear α-synuclein and the depletion of NK cells exacerbates synuclein pathology in a mouse model of α-synucleinopathy. Proceedings of the National Academy of Sciences of the United States of America, 117(3), 1762–1771. https://doi.org/10.1073/pnas.1909110117

Estaun-Panzano, J., Arotcarena, M. L., & Bezard, E. (2023). Monitoring α-synuclein aggregation. Neurobiology of disease, 176, 105966. https://doi.org/10.1016/j.nbd.2022.105966

Eusebi, P., Giannandrea, D., Biscetti, L., Abraha, I., Chiasserini, D., Orso, M., Calabresi, P., & Parnetti, L. (2017). Diagnostic utility of cerebrospinal fluid α-synuclein in Parkinson's disease: A systematic review and meta-analysis. Movement disorders : official journal of the Movement Disorder Society, 32(10), 1389–1400. https://doi.org/10.1002/mds.27110

Fan, B., Jabeen, R., Bo, B., Guo, C., Han, M., Zhang, H., Cen, J., Ji, X., & Wei, J. (2020). What and How Can Physical Activity Prevention Function on Parkinson's Disease?. Oxidative medicine and cellular longevity, 2020, 4293071. https://doi.org/10.1155/2020/4293071

Fares, M. B., Ait-Bouziad, N., Dikiy, I., Mbefo, M. K., Jovičić, A., Kiely, A., Holton, J. L., Lee, S. J., Gitler, A. D., Eliezer, D., & Lashuel, H. A. (2014). The novel Parkinson's disease linked mutation G51D attenuates in vitro aggregation and membrane binding of α-synuclein, and enhances its secretion and nuclear localization in cells. Human molecular genetics, 23(17), 4491–4509. https://doi.org/10.1093/hmg/ddu165

Fares, M. B., Maco, B., Oueslati, A., Rockenstein, E., Ninkina, N., Buchman, V. L., Masliah, E., & Lashuel, H. A. (2016). Induction of de novo α-synuclein fibrillization in a neuronal model for Parkinson's disease. Proceedings of the National Academy of Sciences of the United States of America, 113(7), E912–E921. https://doi.org/10.1073/pnas.1512876113

Fayyad, M., Salim, S., Majbour, N., Erskine, D., Stoops, E., Mollenhauer, B., & El-Agnaf, O. M. A. (2019). Parkinson's disease biomarkers based on α-synuclein. Journal of neurochemistry, 150(5), 626–636. https://doi.org/10.1111/jnc.14809

Ferrer, I., Martinez, A., Blanco, R., Dalfó, E., & Carmona, M. (2011). Neuropathology of sporadic Parkinson disease before the appearance of parkinsonism: preclinical

Parkinson disease. Journal of neural transmission (Vienna, Austria : 1996), 118(5), 821–839. https://doi.org/10.1007/s00702-010-0482-8

Fernández-Pérez, A., Sanz-Magro, A., Moratalla, R., & Vallejo, M. (2022). Restricting feeding to dark phase fails to entrain circadian activity and energy expenditure oscillations in Pitx3-mutant Aphakia mice. Cell reports, 38(2), 110241. https://doi.org/10.1016/j.celrep.2021.110241

Fleming, S. M., Ekhator, O. R., & Ghisays, V. (2013). Assessment of sensorimotor function in mouse models of Parkinson's disease. Journal of visualized experiments : JoVE, (76), 50303. https://doi.org/10.3791/50303

Fleming, S. M., Salcedo, J., Fernagut, P. O., Rockenstein, E., Masliah, E., Levine, M. S., & Chesselet, M. F. (2004). Early and progressive sensorimotor anomalies in mice overexpressing wild-type human alpha-synuclein. The Journal of neuroscience : the official journal of the Society for Neuroscience, 24(42), 9434–9440. https://doi.org/10.1523/JNEUROSCI.3080-04.2004

Fujiwara, H., Hasegawa, M., Dohmae, N., Kawashima, A., Masliah, E., Goldberg, M. S., Shen, J., Takio, K., & Iwatsubo, T. (2002). alpha-Synuclein is phosphorylated in synucleinopathy lesions. Nature cell biology, 4(2), 160–164. https://doi.org/10.1038/ncb748

Gaig, C., Martí, M. J., Ezquerra, M., Cardozo, A., Rey, M. J., & Tolosa, E. (2009). G2019S LRRK2 mutation causing Parkinson's disease without Lewy bodies. BMJ case reports, 2009, bcr08.2008.0632. https://doi.org/10.1136/bcr.08.2008.0632

Garcia, P., Jürgens-Wemheuer, W., Uriarte Huarte, O., Michelucci, A., Masuch, A., Brioschi, S., Weihofen, A., Koncina, E., Coowar, D., Heurtaux, T., Glaab, E., Balling, R., Sousa, C., Kaoma, T., Nicot, N., Pfander, T., Schulz-Schaeffer, W., Allouche, A., Fischer, N., Biber, K., … Buttini, M. (2022). Neurodegeneration and neuroinflammation are linked, but independent of alpha-synuclein inclusions, in a seeding/spreading mouse model of Parkinson's disease. Glia, 70(5), 935–960. https://doi.org/10.1002/glia.24149

Garcia-Reitböck, P., Anichtchik, O., Bellucci, A., Iovino, M., Ballini, C., Fineberg, E., Ghetti, B., Della Corte, L., Spano, P., Tofaris, G. K., Goedert, M., & Spillantini, M. G. (2010). SNARE protein redistribution and synaptic failure in a transgenic mouse model of Parkinson's disease. Brain : a journal of neurology, 133(Pt 7), 2032–2044. https://doi.org/10.1093/brain/awq132

García-Sanz, P., M F G Aerts, J., & Moratalla, R. (2021). The Role of Cholesterol in α-Synuclein and Lewy Body Pathology in GBA1 Parkinson's Disease. Movement disorders : official journal of the Movement Disorder Society, 36(5), 1070–1085. https://doi.org/10.1002/mds.28396

García-Sanz, P., Orgaz, L., Bueno-Gil, G., Espadas, I., Rodríguez-Traver, E., Kulisevsky, J., Gutierrez, A., Dávila, J. C., González-Polo, R. A., Fuentes, J. M., Mir, P., Vicario, C., & Moratalla, R. (2017). N370S-GBA1 mutation causes lysosomal cholesterol accumulation in Parkinson's disease. Movement disorders : official journal of the Movement Disorder Society, 32(10), 1409–1422. https://doi.org/10.1002/mds.27119

GBD 2016 Neurology Collaborators (2019). Global, regional, and national burden of neurological disorders, 1990-2016: a systematic analysis for the Global Burden of

Disease Study 2016. The Lancet. Neurology, 18(5), 459–480. https://doi.org/10.1016/S1474-4422(18)30499-X

Ghanem, S. S., Majbour, N. K., Vaikath, N. N., Ardah, M. T., Erskine, D., Jensen, N. M., Fayyad, M., Sudhakaran, I. P., Vasili, E., Melachroinou, K., Abdi, I. Y., Poggiolini, I., Santos, P., Dorn, A., Carloni, P., Vekrellis, K., Attems, J., McKeith, I., Outeiro, T. F., Jensen, P. H., … El-Agnaf, O. M. A. (2022). α-Synuclein phosphorylation at serine 129 occurs after initial protein deposition and inhibits seeded fibril formation and toxicity. Proceedings of the National Academy of Sciences of the United States of America, 119(15), e2109617119. https://doi.org/10.1073/pnas.2109617119

Ghosh, D., Mehra, S., Sahay, S., Singh, P. K., & Maji, S. K. (2017). α-synuclein aggregation and its modulation. International journal of biological macromolecules, 100, 37–54. https://doi.org/10.1016/j.ijbiomac.2016.10.021

Ghosh, D., Mondal, M., Mohite, G. M., Singh, P. K., Ranjan, P., Anoop, A., Ghosh, S., Jha, N. N., Kumar, A., & Maji, S. K. (2013). The Parkinson's disease-associated H50Q mutation accelerates α-Synuclein aggregation in vitro. Biochemistry, 52(40), 6925–6927. https://doi.org/10.1021/bi400999d

Ghosh, D., Sahay, S., Ranjan, P., Salot, S., Mohite, G. M., Singh, P. K., Dwivedi, S., Carvalho, E., Banerjee, R., Kumar, A., & Maji, S. K. (2014). The newly discovered Parkinson's disease associated Finnish mutation (A53E) attenuates α-synuclein aggregation and membrane binding. Biochemistry, 53(41), 6419–6421. https://doi.org/10.1021/bi5010365

Giasson, B. I., Duda, J. E., Quinn, S. M., Zhang, B., Trojanowski, J. Q., & Lee, V. M. (2002). Neuronal alpha-synucleinopathy with severe movement disorder in mice expressing A53T human alpha-synuclein. Neuron, 34(4), 521–533. https://doi.org/10.1016/s0896-6273(02)00682-7

Giasson, B. I., Murray, I. V., Trojanowski, J. Q., & Lee, V. M. (2001). A hydrophobic stretch of 12 amino acid residues in the middle of alpha-synuclein is essential for filament assembly. The Journal of biological chemistry, 276(4), 2380–2386. https://doi.org/10.1074/jbc.M008919200

Goetz C. G. (2011). The history of Parkinson's disease: early clinical descriptions and neurological therapies. Cold Spring Harbor perspectives in medicine, 1(1), a008862. https://doi.org/10.1101/cshperspect.a008862

Goldberg, M. S., Fleming, S. M., Palacino, J. J., Cepeda, C., Lam, H. A., Bhatnagar, A., Meloni, E. G., Wu, N., Ackerson, L. C., Klapstein, G. J., Gajendiran, M., Roth, B. L., Chesselet, M. F., Maidment, N. T., Levine, M. S., & Shen, J. (2003). Parkin-deficient mice exhibit nigrostriatal deficits but not loss of dopaminergic neurons. The Journal of biological chemistry, 278(44), 43628–43635. https://doi.org/10.1074/jbc.M308947200

Goldberg, M. S., Pisani, A., Haburcak, M., Vortherms, T. A., Kitada, T., Costa, C., Tong, Y., Martella, G., Tscherter, A., Martins, A., Bernardi, G., Roth, B. L., Pothos, E. N., Calabresi, P., & Shen, J. (2005). Nigrostriatal dopaminergic deficits and hypokinesia caused by inactivation of the familial Parkinsonism-linked gene DJ-1. Neuron, 45(4), 489–496. https://doi.org/10.1016/j.neuron.2005.01.041

Gombash, S. E., Manfredsson, F. P., Kemp, C. J., Kuhn, N. C., Fleming, S. M., Egan, A. E., Grant, L. M., Ciucci, M. R., MacKeigan, J. P., & Sortwell, C. E. (2013). Morphological and behavioral impact of AAV2/5-mediated overexpression of human

wildtype alpha-synuclein in the rat nigrostriatal system. PloS one, 8(11), e81426. https://doi.org/10.1371/journal.pone.0081426

Gómez-Benito, M., Granado, N., García-Sanz, P., Michel, A., Dumoulin, M., & Moratalla, R. (2020). Modeling Parkinson's Disease With the Alpha-Synuclein Protein. Frontiers in pharmacology, 11, 356. https://doi.org/10.3389/fphar.2020.00356

Guo, M., Wang, J., Zhao, Y., Feng, Y., Han, S., Dong, Q., Cui, M., & Tieu, K. (2020). Microglial exosomes facilitate α-synuclein transmission in Parkinson's disease. Brain : a journal of neurology, 143(5), 1476–1497. https://doi.org/10.1093/brain/awaa090

Guzman, J. N., Sánchez-Padilla, J., Chan, C. S., & Surmeier, D. J. (2009). Robust pacemaking in substantia nigra dopaminergic neurons. The Journal of neuroscience : the official journal of the Society for Neuroscience, 29(35), 11011–11019. https://doi.org/10.1523/JNEUROSCI.2519-09.2009

Granado, N., O'Shea, E., Bove, J., Vila, M., Colado, M. I., & Moratalla, R. (2008). Persistent MDMA-induced dopaminergic neurotoxicity in the striatum and substantia nigra of mice. Journal of neurochemistry, 107(4), 1102–1112. https://doi.org/10.1111/j.1471-4159.2008.05705.x

Gründemann, J., Schlaudraff, F., Haeckel, O., & Liss, B. (2008). Elevated alpha-synuclein mRNA levels in individual UV-laser-microdissected dopaminergic substantia nigra neurons in idiopathic Parkinson's disease. Nucleic acids research, 36(7), e38. https://doi.org/10.1093/nar/gkn084

Hansson, O., Hall, S., Ohrfelt, A., Zetterberg, H., Blennow, K., Minthon, L., Nägga, K., Londos, E., Varghese, S., Majbour, N. K., Al-Hayani, A., & El-Agnaf, O. M. (2014). Levels of cerebrospinal fluid α-synuclein oligomers are increased in Parkinson's disease with dementia and dementia with Lewy bodies compared to Alzheimer's disease. Alzheimer's research & therapy, 6(3), 25. https://doi.org/10.1186/alzrt255

Herman, S., Djaldetti, R., Mollenhauer, B., & Offen, D. (2023). CSF-derived extracellular vesicles from patients with Parkinson's disease induce symptoms and pathology. Brain : a journal of neurology, 146(1), 209–224. https://doi.org/10.1093/brain/awac261

Hernandez, D. G., Reed, X., & Singleton, A. B. (2016). Genetics in Parkinson disease: Mendelian versus non-Mendelian inheritance. Journal of neurochemistry, 139 Suppl 1(Suppl 1), 59–74. https://doi.org/10.1111/jnc.13593

Hinkle, K. M., Yue, M., Behrouz, B., Dächsel, J. C., Lincoln, S. J., Bowles, E. E., Beevers, J. E., Dugger, B., Winner, B., Prots, I., Kent, C. B., Nishioka, K., Lin, W. L., Dickson, D. W., Janus, C. J., Farrer, M. J., & Melrose, H. L. (2012). LRRK2 knockout mice have an intact dopaminergic system but display alterations in exploratory and motor co-ordination behaviors. Molecular neurodegeneration, 7, 25. https://doi.org/10.1186/1750-1326-7-25

Holmqvist, S., Chutna, O., Bousset, L., Aldrin-Kirk, P., Li, W., Björklund, T., Wang, Z. Y., Roybon, L., Melki, R., & Li, J. Y. (2014). Direct evidence of Parkinson pathology spread from the gastrointestinal tract to the brain in rats. Acta neuropathologica, 128(6), 805–820. https://doi.org/10.1007/s00401-014-1343-6

Hoyer, W., Cherny, D., Subramaniam, V., & Jovin, T. M. (2004). Impact of the acidic C-terminal region comprising amino acids 109-140 on alpha-synuclein aggregation in vitro. Biochemistry, 43(51), 16233–16242. https://doi.org/10.1021/bi048453u

Huang, Z., Xu, Z., Wu, Y., & Zhou, Y. (2011). Determining nuclear localization of alpha-synuclein in mouse brains. Neuroscience, 199, 318–332. https://doi.org/10.1016/j.neuroscience.2011.10.016

Hwang, D. Y., Ardayfio, P., Kang, U. J., Semina, E. V., & Kim, K. S. (2003). Selective loss of dopaminergic neurons in the substantia nigra of Pitx3-deficient aphakia mice. Brain research. Molecular brain research, 114(2), 123–131. https://doi.org/10.1016/s0169-328x(03)00162-1

Hwang, D. Y., Fleming, S. M., Ardayfio, P., Moran-Gates, T., Kim, H., Tarazi, F. I., Chesselet, M. F., & Kim, K. S. (2005). 3,4-dihydroxyphenylalanine reverses the motor deficits in Pitx3-deficient aphakia mice: behavioral characterization of a novel genetic model of Parkinson's disease. The Journal of neuroscience : the official journal of the Society for Neuroscience, 25(8), 2132–2137. https://doi.org/10.1523/JNEUROSCI.3718-04.2005

Ip, C. W., Klaus, L. C., Karikari, A. A., Visanji, N. P., Brotchie, J. M., Lang, A. E., Volkmann, J., & Koprich, J. B. (2017). AAV1/2-induced overexpression of A53T-α-synuclein in the substantia nigra results in degeneration of the nigrostriatal system with Lewy-like pathology and motor impairment: a new mouse model for Parkinson's disease. Acta neuropathologica communications, 5(1), 11. https://doi.org/10.1186/s40478-017-0416-x

Iranzo, A., Tolosa, E., Gelpi, E., Molinuevo, J. L., Valldeoriola, F., Serradell, M., Sanchez-Valle, R., Vilaseca, I., Lomeña, F., Vilas, D., Lladó, A., Gaig, C., & Santamaria, J. (2013). Neurodegenerative disease status and post-mortem pathology in idiopathic rapid-eye-movement sleep behaviour disorder: an observational cohort study. The Lancet. Neurology, 12(5), 443–453. https://doi.org/10.1016/S1474-4422(13)70056-5

Izco, M., Blesa, J., Verona, G., Cooper, J. M., & Alvarez-Erviti, L. (2021). Glial activation precedes alpha-synuclein pathology in a mouse model of Parkinson's disease. Neuroscience research, 170, 330–340. https://doi.org/10.1016/j.neures.2020.11.004

Jan, A., Gonçalves, N. P., Vaegter, C. B., Jensen, P. H., & Ferreira, N. (2021). The Prion-Like Spreading of Alpha-Synuclein in Parkinson's Disease: Update on Models and Hypotheses. International journal of molecular sciences, 22(15), 8338. https://doi.org/10.3390/ijms22158338

Janezic, S., Threlfell, S., Dodson, P. D., Dowie, M. J., Taylor, T. N., Potgieter, D., Parkkinen, L., Senior, S. L., Anwar, S., Ryan, B., Deltheil, T., Kosillo, P., Cioroch, M., Wagner, K., Ansorge, O., Bannerman, D. M., Bolam, J. P., Magill, P. J., Cragg, S. J., & Wade-Martins, R. (2013). Deficits in dopaminergic transmission precede neuron loss and dysfunction in a new Parkinson model. Proceedings of the National Academy of Sciences of the United States of America, 110(42), E4016–E4025. https://doi.org/10.1073/pnas.1309143110

Jao, C. C., Der-Sarkissian, A., Chen, J., & Langen, R. (2004). Structure of membrane-bound alpha-synuclein studied by site-directed spin labeling. Proceedings of the

National Academy of Sciences of the United States of America, 101(22), 8331–8336. https://doi.org/10.1073/pnas.0400553101

Johansen, K. K., Torp, S. H., Farrer, M. J., Gustavsson, E. K., & Aasly, J. O. (2018). A Case of Parkinson's Disease with No Lewy Body Pathology due to a Homozygous Exon Deletion in Parkin. Case reports in neurological medicine, 2018, 6838965. https://doi.org/10.1155/2018/6838965

Kalia, L. V., & Lang, A. E. (2015). Parkinson's disease. Lancet (London, England), 386(9996), 896–912. https://doi.org/10.1016/S0140-6736(14)61393-3

Karpinar, D. P., Balija, M. B., Kügler, S., Opazo, F., Rezaei-Ghaleh, N., Wender, N., Kim, H. Y., Taschenberger, G., Falkenburger, B. H., Heise, H., Kumar, A., Riedel, D., Fichtner, L., Voigt, A., Braus, G. H., Giller, K., Becker, S., Herzig, A., Baldus, M., Jäckle, H., … Zweckstetter, M. (2009). Pre-fibrillar alpha-synuclein variants with impaired beta-structure increase neurotoxicity in Parkinson's disease models. The EMBO journal, 28(20), 3256–3268. https://doi.org/10.1038/emboj.2009.257

Kim, C., Ho, D. H., Suk, J. E., You, S., Michael, S., Kang, J., Joong Lee, S., Masliah, E., Hwang, D., Lee, H. J., & Lee, S. J. (2013). Neuron-released oligomeric α-synuclein is an endogenous agonist of TLR2 for paracrine activation of microglia. Nature communications, 4, 1562. https://doi.org/10.1038/ncomms2534

Kim, S., Kwon, S. H., Kam, T. I., Panicker, N., Karuppagounder, S. S., Lee, S., Lee, J. H., Kim, W. R., Kook, M., Foss, C. A., Shen, C., Lee, H., Kulkarni, S., Pasricha, P. J., Lee, G., Pomper, M. G., Dawson, V. L., Dawson, T. M., & Ko, H. S. (2019). Transneuronal Propagation of Pathologic α-Synuclein from the Gut to the Brain Models Parkinson's Disease. Neuron, 103(4), 627–641.e7. https://doi.org/10.1016/j.neuron.2019.05.035

Kim, Y. E., Lai, T. T., Kim, Y. J., & Jeon, B. (2020). Preferential microglial activation associated with pathological alpha synuclein transmission. Journal of clinical neuroscience : official journal of the Neurosurgical Society of Australasia, 81, 469–476. https://doi.org/10.1016/j.jocn.2020.09.027

Kim, R. H., Smith, P. D., Aleyasin, H., Hayley, S., Mount, M. P., Pownall, S., Wakeham, A., You-Ten, A. J., Kalia, S. K., Horne, P., Westaway, D., Lozano, A. M., Anisman, H., Park, D. S., & Mak, T. W. (2005). Hypersensitivity of DJ-1-deficient mice to 1-methyl-4-phenyl-1,2,3,6-tetrahydropyrindine (MPTP) and oxidative stress. Proceedings of the National Academy of Sciences of the United States of America, 102(14), 5215–5220. https://doi.org/10.1073/pnas.0501282102

Kin, K., Yasuhara, T., Kameda, M., & Date, I. (2019). Animal Models for Parkinson's Disease Research: Trends in the 2000s. International journal of molecular sciences, 20(21), 5402. https://doi.org/10.3390/ijms20215402

Kirik, D., Annett, L. E., Burger, C., Muzyczka, N., Mandel, R. J., & Björklund, A. (2003). Nigrostriatal alpha-synucleinopathy induced by viral vector-mediated overexpression of human alpha-synuclein: a new primate model of Parkinson's disease. Proceedings of the National Academy of Sciences of the United States of America, 100(5), 2884–2889. https://doi.org/10.1073/pnas.0536383100

Kirik, D., Rosenblad, C., Burger, C., Lundberg, C., Johansen, T. E., Muzyczka, N., Mandel, R. J., & Björklund, A. (2002). Parkinson-like neurodegeneration induced by targeted overexpression of alpha-synuclein in the nigrostriatal system. The Journal of

neuroscience : the official journal of the Society for Neuroscience, 22(7), 2780–2791. https://doi.org/10.1523/JNEUROSCI.22-07-02780.2002

Klein, C., & Westenberger, A. (2012). Genetics of Parkinson's disease. Cold Spring Harbor perspectives in medicine, 2(1), a008888. https://doi.org/10.1101/cshperspect.a008888

Kong, B. Y., Haugh, I. M., Schlosser, B. J., Getsios, S., & Paller, A. S. (2016). Mind the Gap: Sex Bias in Basic Skin Research. The Journal of investigative dermatology, 136(1), 12–14. https://doi.org/10.1038/JID.2015.298

Konnova, E. A., & Swanberg, M. (2018). Animal Models of Parkinson's Disease. In T. B. Stoker (Eds.) et. al., Parkinson's Disease: Pathogenesis and Clinical Aspects. Codon Publications.

Koprich, J. B., Johnston, T. H., Huot, P., Reyes, M. G., Espinosa, M., & Brotchie, J. M. (2011). Progressive neurodegeneration or endogenous compensation in an animal model of Parkinson's disease produced by decreasing doses of alpha-synuclein. PloS one, 6(3), e17698. https://doi.org/10.1371/journal.pone.0017698

Kordower, J. H., Chu, Y., Hauser, R. A., Freeman, T. B., & Olanow, C. W. (2008). Lewy body-like pathology in long-term embryonic nigral transplants in Parkinson's disease. Nature medicine, 14(5), 504–506. https://doi.org/10.1038/nm1747

Krüger, R., Kuhn, W., Müller, T., Woitalla, D., Graeber, M., Kösel, S., Przuntek, H., Epplen, J. T., Schöls, L., & Riess, O. (1998). Ala30Pro mutation in the gene encoding alpha-synuclein in Parkinson's disease. Nature genetics, 18(2), 106–108. https://doi.org/10.1038/ng0298-106

Kumar, K. R., Djarmati-Westenberger, A., & Grünewald, A. (2011). Genetics of Parkinson's disease. Seminars in neurology, 31(5), 433–440. https://doi.org/10.1055/s-0031-1299782

Kumar, K. R., Weissbach, A., Heldmann, M., Kasten, M., Tunc, S., Sue, C. M., Svetel, M., Kostić, V. S., Segura-Aguilar, J., Ramirez, A., Simon, D. K., Vieregge, P., Münte, T. F., Hagenah, J., Klein, C., & Lohmann, K. (2012). Frequency of the D620N mutation in VPS35 in Parkinson disease. Archives of neurology, 69(10), 1360–1364. https://doi.org/10.1001/archneurol.2011.3367

Kuusisto, E., Salminen, A., & Alafuzoff, I. (2001). Ubiquitin-binding protein p62 is present in neuronal and glial inclusions in human tauopathies and synucleinopathies. Neuroreport, 12(10), 2085–2090. https://doi.org/10.1097/00001756-200107200-00009

Kuzuhara, S., Mori, H., Izumiyama, N., Yoshimura, M., & Ihara, Y. (1988). Lewy bodies are ubiquitinated. A light and electron microscopic immunocytochemical study. Acta neuropathologica, 75(4), 345–353. https://doi.org/10.1007/BF00687787

Lai, T. T., Kim, Y. J., Nguyen, P. T., Koh, Y. H., Nguyen, T. T., Ma, H. I., & Kim, Y. E. (2021). Temporal Evolution of Inflammation and Neurodegeneration With Alpha-Synuclein Propagation in Parkinson's Disease Mouse Model. Frontiers in integrative neuroscience, 15, 715190. https://doi.org/10.3389/fnint.2021.715190

Lamontagne-Proulx, J., Coulombe, K., Morissette, M., Rieux, M., Calon, F., Di Paolo, T., & Soulet, D. (2023). Sex and Age Differences in a Progressive Synucleinopathy Mouse Model. Biomolecules, 13(6), 977. https://doi.org/10.3390/biom13060977

Lanciego, J. L., Luquin, N., & Obeso, J. A. (2012). Functional neuroanatomy of the basal ganglia. Cold Spring Harbor perspectives in medicine, 2(12), a009621. https://doi.org/10.1101/cshperspect.a009621

Lau, A., So, R. W. L., Lau, H. H. C., Sang, J. C., Ruiz-Riquelme, A., Fleck, S. C., Stuart, E., Menon, S., Visanji, N. P., Meisl, G., Faidi, R., Marano, M. M., Schmitt-Ulms, C., Wang, Z., Fraser, P. E., Tandon, A., Hyman, B. T., Wille, H., Ingelsson, M., Klenerman, D., … Watts, J. C. (2020). α-Synuclein strains target distinct brain regions and cell types. Nature neuroscience, 23(1), 21–31. https://doi.org/10.1038/s41593-019-0541-x

Lee, S. J., Jeon, H., & Kandror, K. V. (2008). Alpha-synuclein is localized in a subpopulation of rat brain synaptic vesicles. Acta neurobiologiae experimentalis, 68(4), 509–515.

Lee, T.C., Kashyap, R.L., & C.N. (1994). Building Skeleton Models via 3-D Medial Surface Axis Thinning Algorithms. CVGIP: Graphical Models and Image Processing, 56(6), 462-478. https://doi.org/10.1006/cgip.1994.1042

Lee, S. B., Park, S. M., Ahn, K. J., Chung, K. C., Paik, S. R., & Kim, J. (2009). Identification of the amino acid sequence motif of alpha-synuclein responsible for macrophage activation. Biochemical and biophysical research communications, 381(1), 39–43. https://doi.org/10.1016/j.bbrc.2009.02.002

Lesage, S., Anheim, M., Letournel, F., Bousset, L., Honoré, A., Rozas, N., Pieri, L., Madiona, K., Dürr, A., Melki, R., Verny, C., Brice, A., & French Parkinson's Disease Genetics Study Group (2013). G51D α-synuclein mutation causes a novel parkinsonian-pyramidal syndrome. Annals of neurology, 73(4), 459–471. https://doi.org/10.1002/ana.23894

Lesage, S., Condroyer, C., Lannuzel, A., Lohmann, E., Troiano, A., Tison, F., Damier, P., Thobois, S., Ouvrard-Hernandez, A. M., Rivaud-Péchoux, S., Brefel-Courbon, C., Destée, A., Tranchant, C., Romana, M., Leclere, L., Dürr, A., Brice, A., & French Parkinson's Disease Genetics Study Group (2009). Molecular analyses of the LRRK2 gene in European and North African autosomal dominant Parkinson's disease. Journal of medical genetics, 46(7), 458–464. https://doi.org/10.1136/jmg.2008.062612

Lesage, S., Dürr, A., & Brice, A. (2006). LRRK2, gène majeur de la maladie de Parkinson dans les pays du Maghreb [LRRK2 is a major gene in North African parkinsonism]. Medecine sciences : M/S, 22(5), 470–471. https://doi.org/10.1051/medsci/2006225470

Li, J. Y., Englund, E., Holton, J. L., Soulet, D., Hagell, P., Lees, A. J., Lashley, T., Quinn, N. P., Rehncrona, S., Björklund, A., Widner, H., Revesz, T., Lindvall, O., & Brundin, P. (2008). Lewy bodies in grafted neurons in subjects with Parkinson's disease suggest host-to-graft disease propagation. Nature medicine, 14(5), 501–503. https://doi.org/10.1038/nm1746

Lin, X., Parisiadou, L., Gu, X. L., Wang, L., Shim, H., Sun, L., Xie, C., Long, C. X., Yang, W. J., Ding, J., Chen, Z. Z., Gallant, P. E., Tao-Cheng, J. H., Rudow, G., Troncoso, J. C., Liu, Z., Li, Z., & Cai, H. (2009). Leucine-rich repeat kinase 2 regulates the progression of neuropathology induced by Parkinson's-disease-related mutant alpha-synuclein. Neuron, 64(6), 807–827. https://doi.org/10.1016/j.neuron.2009.11.006

Liu, H., Koros, C., Strohäker, T., Schulte, C., Bozi, M., Varvaresos, S., Ibáñez de Opakua, A., Simitsi, A. M., Bougea, A., Voumvourakis, K., Maniati, M., Papageorgiou, S. G., Hauser, A. K., Becker, S., Zweckstetter, M., Stefanis, L., & Gasser, T. (2021). A Novel SNCA A30G Mutation Causes Familial Parkinson's Disease. Movement disorders : official journal of the Movement Disorder Society, 36(7), 1624–1633. https://doi.org/10.1002/mds.28534

Ltic, S., Perovic, M., Mladenovic, A., Raicevic, N., Ruzdijic, S., Rakic, L., & Kanazir, S. (2004). Alpha-synuclein is expressed in different tissues during human fetal development. Journal of molecular neuroscience : MN, 22(3), 199–204. https://doi.org/10.1385/jmn:22:3:199

Luk, K. C., Covell, D. J., Kehm, V. M., Zhang, B., Song, I. Y., Byrne, M. D., Pitkin, R. M., Decker, S. C., Trojanowski, J. Q., & Lee, V. M. (2016). Molecular and Biological Compatibility with Host Alpha-Synuclein Influences Fibril Pathogenicity. Cell reports, 16(12), 3373–3387. https://doi.org/10.1016/j.celrep.2016.08.053

Luk, K. C., Kehm, V., Carroll, J., Zhang, B., O'Brien, P., Trojanowski, J. Q., & Lee, V. M. (2012a). Pathological α-synuclein transmission initiates Parkinson-like neurodegeneration in nontransgenic mice. Science (New York, N.Y.), 338(6109), 949–953. https://doi.org/10.1126/science.1227157

Luk, K. C., Kehm, V. M., Zhang, B., O'Brien, P., Trojanowski, J. Q., & Lee, V. M. (2012b). Intracerebral inoculation of pathological α-synuclein initiates a rapidly progressive neurodegenerative α-synucleinopathy in mice. The Journal of experimental medicine, 209(5), 975–986. https://doi.org/10.1084/jem.20112457

Luk, K. C., Song, C., O'Brien, P., Stieber, A., Branch, J. R., Brunden, K. R., Trojanowski, J. Q., & Lee, V. M. (2009). Exogenous alpha-synuclein fibrils seed the formation of Lewy body-like intracellular inclusions in cultured cells. Proceedings of the National Academy of Sciences of the United States of America, 106(47), 20051–20056. https://doi.org/10.1073/pnas.0908005106

Luong, T. N., Carlisle, H. J., Southwell, A., & Patterson, P. H. (2011). Assessment of motor balance and coordination in mice using the balance beam. Journal of visualized experiments : JoVE, (49), 2376. https://doi.org/10.3791/2376

Ma, L., Yang, C., Zhang, X., Li, Y., Wang, S., Zheng, L., & Huang, K. (2018). C-terminal truncation exacerbates the aggregation and cytotoxicity of α-Synuclein: A vicious cycle in Parkinson's disease. Biochimica et biophysica acta. Molecular basis of disease, 1864(12), 3714–3725. https://doi.org/10.1016/j.bbadis.2018.10.003

Mao, X., Ou, M. T., Karuppagounder, S. S., Kam, T. I., Yin, X., Xiong, Y., Ge, P., Umanah, G. E., Brahmachari, S., Shin, J. H., Kang, H. C., Zhang, J., Xu, J., Chen, R., Park, H., Andrabi, S. A., Kang, S. U., Gonçalves, R. A., Liang, Y., Zhang, S., … Dawson, T. M. (2016). Pathological α-synuclein transmission initiated by binding lymphocyte-activation gene 3. Science (New York, N.Y.), 353(6307), aah3374. https://doi.org/10.1126/science.aah3374

Masuda-Suzukake, M., Nonaka, T., Hosokawa, M., Oikawa, T., Arai, T., Akiyama, H., Mann, D. M., & Hasegawa, M. (2013). Prion-like spreading of pathological α-synuclein in brain. Brain : a journal of neurology, 136(Pt 4), 1128–1138. https://doi.org/10.1093/brain/awt037

Matsuda, W., Furuta, T., Nakamura, K. C., Hioki, H., Fujiyama, F., Arai, R., & Kaneko, T. (2009). Single nigrostriatal dopaminergic neurons form widely spread and highly dense axonal arborizations in the neostriatum. The Journal of neuroscience : the official journal of the Society for Neuroscience, 29(2), 444–453. https://doi.org/10.1523/JNEUROSCI.4029-08.2009

Maroteaux, L., Campanelli, J. T., & Scheller, R. H. (1988). Synuclein: a neuron-specific protein localized to the nucleus and presynaptic nerve terminal. The Journal of neuroscience : the official journal of the Society for Neuroscience, 8(8), 2804–2815. https://doi.org/10.1523/JNEUROSCI.08-08-02804.1988

Marsden C. D. (1983). Neuromelanin and Parkinson's disease. Journal of neural transmission. Supplementum, 19, 121–141.

Migdalska-Richards, A., & Schapira, A. H. (2016). The relationship between glucocerebrosidase mutations and Parkinson disease. Journal of neurochemistry, 139 Suppl 1(Suppl Suppl 1), 77–90. https://doi.org/10.1111/jnc.13385

Milanese, C., Cerri, S., Ulusoy, A., Gornati, S. V., Plat, A., Gabriels, S., Blandini, F., Di Monte, D. A., Hoeijmakers, J. H., & Mastroberardino, P. G. (2018). Activation of the DNA damage response in vivo in synucleinopathy models of Parkinson's disease. Cell death & disease, 9(8), 818. https://doi.org/10.1038/s41419-018-0848-7

Miličić Stanić, B., Maddox, S., de Souza, A. M. A., Wu, X., Mehranfard, D., Ji, H., Speth, R. C., & Sandberg, K. (2021). Male bias in ACE2 basic science research: missed opportunity for discovery in the time of COVID-19. American journal of physiology. Regulatory, integrative and comparative physiology, 320(6), R925–R937. https://doi.org/10.1152/ajpregu.00356.2020

Miller, I. N., & Cronin-Golomb, A. (2010). Gender differences in Parkinson's disease: clinical characteristics and cognition. Movement disorders : official journal of the Movement Disorder Society, 25(16), 2695–2703. https://doi.org/10.1002/mds.23388

Miller, D. W., Hague, S. M., Clarimon, J., Baptista, M., Gwinn-Hardy, K., Cookson, M. R., & Singleton, A. B. (2004). Alpha-synuclein in blood and brain from familial Parkinson disease with SNCA locus triplication. Neurology, 62(10), 1835–1838. https://doi.org/10.1212/01.wnl.0000127517.33208.f4

Mizutani, Y., Yokochi, M., & Oyanagi, S. (1991). Juvenile parkinsonism: a case with first clinical manifestation at the age of six years and with neuropathological findings suggesting a new pathogenesis. Clinical neuropathology, 10(2), 91–97.

Mollenhauer, B., Bowman, F. D., Drake, D., Duong, J., Blennow, K., El-Agnaf, O., Shaw, L. M., Masucci, J., Taylor, P., Umek, R. M., Dunty, J. M., Smith, C. L., Stoops, E., Vanderstichele, H., Schmid, A. W., Moniatte, M., Zhang, J., Kruse, N., Lashuel, H. A., Teunissen, C., … Zetterberg, H. (2019). Antibody-based methods for the measurement of α-synuclein concentration in human cerebrospinal fluid - method comparison and round robin study. Journal of neurochemistry, 149(1), 126–138. https://doi.org/10.1111/jnc.14569

Mori, H., Hattori, N., & Mizuno, Y. (2003). Genotype-phenotype correlation: familial Parkinson disease. Neuropathology : official journal of the Japanese Society of Neuropathology, 23(1), 90–94. https://doi.org/10.1046/j.1440-1789.2003.00476.x

Mysiris, D. S., Vavougios, G. D., Karamichali, E., Papoutsopoulou, S., Stavrou, V. T., Papayianni, E., Boutlas, S., Mavridis, T., Foka, P., Zarogiannis, S. G., Gourgoulianis, K., & Xiromerisiou, G. (2022). Post-COVID-19 Parkinsonism and Parkinson's Disease Pathogenesis: The Exosomal Cargo Hypothesis. International journal of molecular sciences, 23(17), 9739. https://doi.org/10.3390/ijms23179739

Nalls, M. A., Blauwendraat, C., Vallerga, C. L., Heilbron, K., Bandres-Ciga, S., Chang, D., Tan, M., Kia, D. A., Noyce, A. J., Xue, A., Bras, J., Young, E., von Coelln, R., Simón-Sánchez, J., Schulte, C., Sharma, M., Krohn, L., Pihlstrøm, L., Siitonen, A., Iwaki, H., … International Parkinson's Disease Genomics Consortium (2019). Identification of novel risk loci, causal insights, and heritable risk for Parkinson's disease: a meta-analysis of genome-wide association studies. The Lancet. Neurology, 18(12), 1091–1102. https://doi.org/10.1016/S1474-4422(19)30320-5

Nalls, M. A., Pankratz, N., Lill, C. M., Do, C. B., Hernandez, D. G., Saad, M., DeStefano, A. L., Kara, E., Bras, J., Sharma, M., Schulte, C., Keller, M. F., Arepalli, S., Letson, C., Edsall, C., Stefansson, H., Liu, X., Pliner, H., Lee, J. H., Cheng, R., … Singleton, A. B. (2014). Large-scale meta-analysis of genome-wide association data identifies six new risk loci for Parkinson's disease. Nature genetics, 46(9), 989–993. https://doi.org/10.1038/ng.3043

Ni, R. J., Huang, Z. H., Shu, Y. M., Wang, Y., Li, T., & Zhou, J. N. (2018). Atlas of the Striatum and Globus Pallidus in the Tree Shrew: Comparison with Rat and Mouse. Neuroscience bulletin, 34(3), 405–418. https://doi.org/10.1007/s12264-018-0212-z

Olanow, C. W., Savolainen, M., Chu, Y., Halliday, G. M., & Kordower, J. H. (2019). Temporal evolution of microglia and α-synuclein accumulation following foetal grafting in Parkinson's disease. Brain : a journal of neurology, 142(6), 1690–1700. https://doi.org/10.1093/brain/awz104

Oliveras-Salvá, M., Van der Perren, A., Casadei, N., Stroobants, S., Nuber, S., D'Hooge, R., Van den Haute, C., & Baekelandt, V. (2013). rAAV2/7 vector-mediated overexpression of alpha-synuclein in mouse substantia nigra induces protein aggregation and progressive dose-dependent neurodegeneration. Molecular neurodegeneration, 8, 44. https://doi.org/10.1186/1750-1326-8-44

Ortiz, O., Delgado-García, J. M., Espadas, I., Bahí, A., Trullas, R., Dreyer, J. L., Gruart, A., & Moratalla, R. (2010). Associative learning and CA3-CA1 synaptic plasticity are impaired in D1R null, Drd1a-/- mice and in hippocampal siRNA silenced Drd1a mice. The Journal of neuroscience : the official journal of the Society for Neuroscience, 30(37), 12288–12300. https://doi.org/10.1523/JNEUROSCI.2655-10.2010

Oueslati A. (2016). Implication of Alpha-Synuclein Phosphorylation at S129 in Synucleinopathies: What Have We Learned in the Last Decade?. Journal of Parkinson's disease, 6(1), 39–51. https://doi.org/10.3233/JPD-160779

Paleologou, K. E., Kragh, C. L., Mann, D. M., Salem, S. A., Al-Shami, R., Allsop, D., Hassan, A. H., Jensen, P. H., & El-Agnaf, O. M. (2009). Detection of elevated levels of soluble alpha-synuclein oligomers in post-mortem brain extracts from patients with dementia with Lewy bodies. Brain : a journal of neurology, 132(Pt 4), 1093–1101. https://doi.org/10.1093/brain/awn349

Pan, W. X., Mao, T., & Dudman, J. T. (2010). Inputs to the dorsal striatum of the mouse reflect the parallel circuit architecture of the forebrain. Frontiers in neuroanatomy, 4, 147. https://doi.org/10.3389/fnana.2010.00147

Parkkinen, L., Pirttilä, T., Tervahauta, M., & Alafuzoff, I. (2005). Widespread and abundant alpha-synuclein pathology in a neurologically unimpaired subject. Neuropathology : official journal of the Japanese Society of Neuropathology, 25(4), 304–314. https://doi.org/10.1111/j.1440-1789.2005.00644.x

Parkinson J. (2002). An essay on the shaking palsy. 1817. The Journal of neuropsychiatry and clinical neurosciences, 14(2), 223–222. https://doi.org/10.1176/jnp.14.2.223

Parnetti, L., Chiasserini, D., Persichetti, E., Eusebi, P., Varghese, S., Qureshi, M. M., Dardis, A., Deganuto, M., De Carlo, C., Castrioto, A., Balducci, C., Paciotti, S., Tambasco, N., Bembi, B., Bonanni, L., Onofrj, M., Rossi, A., Beccari, T., El-Agnaf, O., & Calabresi, P. (2014). Cerebrospinal fluid lysosomal enzymes and alpha-synuclein in Parkinson's disease. Movement disorders : official journal of the Movement Disorder Society, 29(8), 1019–1027. https://doi.org/10.1002/mds.25772

Pasanen, P., Myllykangas, L., Siitonen, M., Raunio, A., Kaakkola, S., Lyytinen, J., Tienari, P. J., Pöyhönen, M., & Paetau, A. (2014). Novel α-synuclein mutation A53E associated with atypical multiple system atrophy and Parkinson's disease-type pathology. Neurobiology of aging, 35(9), 2180.e1–2180.e21805. https://doi.org/10.1016/j.neurobiolaging.2014.03.024

Pasquier, D. A., Kemper, T. L., Forbes, W. B., & Morgane, P. J. (1977). Dorsal raphe, substantia nigra and locus coeruleus: interconnections with each other and the neostriatum. Brain research bulletin, 2(5), 323–339. https://doi.org/10.1016/0361-9230(77)90066-1

Patterson, J. R., Duffy, M. F., Kemp, C. J., Howe, J. W., Collier, T. J., Stoll, A. C., Miller, K. M., Patel, P., Levine, N., Moore, D. J., Luk, K. C., Fleming, S. M., Kanaan, N. M., Paumier, K. L., El-Agnaf, O. M. A., & Sortwell, C. E. (2019). Time course and magnitude of alpha-synuclein inclusion formation and nigrostriatal degeneration in the rat model of synucleinopathy triggered by intrastriatal α-synuclein preformed fibrils. Neurobiology of disease, 130, 104525. https://doi.org/10.1016/j.nbd.2019.104525

Paumier, K. L., Luk, K. C., Manfredsson, F. P., Kanaan, N. M., Lipton, J. W., Collier, T. J., Steece-Collier, K., Kemp, C. J., Celano, S., Schulz, E., Sandoval, I. M., Fleming, S., Dirr, E., Polinski, N. K., Trojanowski, J. Q., Lee, V. M., & Sortwell, C. E. (2015). Intrastriatal injection of pre-formed mouse α-synuclein fibrils into rats triggers α-synuclein pathology and bilateral nigrostriatal degeneration. Neurobiology of disease, 82, 185–199. https://doi.org/10.1016/j.nbd.2015.06.003

Peng, X., Tehranian, R., Dietrich, P., Stefanis, L., & Perez, R. G. (2005). Alpha-synuclein activation of protein phosphatase 2A reduces tyrosine hydroxylase phosphorylation in dopaminergic cells. Journal of cell science, 118(Pt 15), 3523–3530. https://doi.org/10.1242/jcs.02481

Peng, C., Trojanowski, J. Q., & Lee, V. M. (2020). Protein transmission in neurodegenerative disease. Nature reviews. Neurology, 16(4), 199–212. https://doi.org/10.1038/s41582-020-0333-7

Pérez-Acuña, D., Rhee, K. H., Shin, S. J., Ahn, J., Lee, J. Y., & Lee, S. J. (2023). Retina-to-brain spreading of α-synuclein after intravitreal injection of preformed fibrils. Acta neuropathologica communications, 11(1), 83. https://doi.org/10.1186/s40478-023-01575-0

Polinski N. K. (2021). A Summary of Phenotypes Observed in the In Vivo Rodent Alpha-Synuclein Preformed Fibril Model. Journal of Parkinson's disease, 11(4), 1555–1567. https://doi.org/10.3233/JPD-212847

Polinski, N. K., Volpicelli-Daley, L. A., Sortwell, C. E., Luk, K. C., Cremades, N., Gottler, L. M., Froula, J., Duffy, M. F., Lee, V. M. Y., Martinez, T. N., & Dave, K. D. (2018). Best Practices for Generating and Using Alpha-Synuclein Pre-Formed Fibrils to Model Parkinson's Disease in Rodents. Journal of Parkinson's disease, 8(2), 303–322. https://doi.org/10.3233/JPD-171248

Polymeropoulos, M. H., Lavedan, C., Leroy, E., Ide, S. E., Dehejia, A., Dutra, A., Pike, B., Root, H., Rubenstein, J., Boyer, R., Stenroos, E. S., Chandrasekharappa, S., Athanassiadou, A., Papapetropoulos, T., Johnson, W. G., Lazzarini, A. M., Duvoisin, R. C., Di Iorio, G., Golbe, L. I., & Nussbaum, R. L. (1997). Mutation in the alpha-synuclein gene identified in families with Parkinson's disease. Science (New York, N.Y.), 276(5321), 2045–2047. https://doi.org/10.1126/science.276.5321.2045

Postuma, R. B., Aarsland, D., Barone, P., Burn, D. J., Hawkes, C. H., Oertel, W., & Ziemssen, T. (2012). Identifying prodromal Parkinson's disease: pre-motor disorders in Parkinson's disease. Movement disorders : official journal of the Movement Disorder Society, 27(5), 617–626. https://doi.org/10.1002/mds.24996

Postuma, R. B., Gagnon, J. F., Bertrand, J. A., Génier Marchand, D., & Montplaisir, J. Y. (2015). Parkinson risk in idiopathic REM sleep behavior disorder: preparing for neuroprotective trials. Neurology, 84(11), 1104–1113. https://doi.org/10.1212/WNL.0000000000001364

Pringsheim, T., Jette, N., Frolkis, A., & Steeves, T. D. (2014). The prevalence of Parkinson's disease: a systematic review and meta-analysis. Movement disorders : official journal of the Movement Disorder Society, 29(13), 1583–1590. https://doi.org/10.1002/mds.25945

Proukakis, C., Dudzik, C. G., Brier, T., MacKay, D. S., Cooper, J. M., Millhauser, G. L., Houlden, H., & Schapira, A. H. (2013). A novel α-synuclein missense mutation in Parkinson disease. Neurology, 80(11), 1062–1064. https://doi.org/10.1212/WNL.0b013e31828727ba

Qamar, M. A., Sauerbier, A., Politis, M., Carr, H., Loehrer, P., & Chaudhuri, K. R. (2017). Presynaptic dopaminergic terminal imaging and non-motor symptoms assessment of Parkinson's disease: evidence for dopaminergic basis?. NPJ Parkinson's disease, 3, 5. https://doi.org/10.1038/s41531-016-0006-9

Raudino F. (2012). The Parkinson disease before James Parkinson. Neurological sciences : official journal of the Italian Neurological Society and of the Italian Society of Clinical Neurophysiology, 33(4), 945–948. https://doi.org/10.1007/s10072-011-0816-9

Recasens, A., Dehay, B., Bové, J., Carballo-Carbajal, I., Dovero, S., Pérez-Villalba, A., Fernagut, P. O., Blesa, J., Parent, A., Perier, C., Fariñas, I., Obeso, J. A., Bezard, E., & Vila, M. (2014). Lewy body extracts from Parkinson disease brains trigger α-synuclein

pathology and neurodegeneration in mice and monkeys. Annals of neurology, 75(3), 351–362. https://doi.org/10.1002/ana.24066

Reeve, A., Simcox, E., & Turnbull, D. (2014). Ageing and Parkinson's disease: why is advancing age the biggest risk factor?. Ageing research reviews, 14(100), 19–30. https://doi.org/10.1016/j.arr.2014.01.004

Reijnders, J. S., Ehrt, U., Weber, W. E., Aarsland, D., & Leentjens, A. F. (2008). A systematic review of prevalence studies of depression in Parkinson's disease. Movement disorders : official journal of the Movement Disorder Society, 23(2), 183–313. https://doi.org/10.1002/mds.21803

Rey, N. L., George, S., Steiner, J. A., Madaj, Z., Luk, K. C., Trojanowski, J. Q., Lee, V. M., & Brundin, P. (2018). Spread of aggregates after olfactory bulb injection of α-synuclein fibrils is associated with early neuronal loss and is reduced long term. Acta neuropathologica, 135(1), 65–83. https://doi.org/10.1007/s00401-017-1792-9

Rey, N. L., Steiner, J. A., Maroof, N., Luk, K. C., Madaj, Z., Trojanowski, J. Q., Lee, V. M., & Brundin, P. (2016). Widespread transneuronal propagation of α-synucleinopathy triggered in olfactory bulb mimics prodromal Parkinson's disease. The Journal of experimental medicine, 213(9), 1759–1778. https://doi.org/10.1084/jem.20160368

Reyes, J. F., Olsson, T. T., Lamberts, J. T., Devine, M. J., Kunath, T., & Brundin, P. (2015). A cell culture model for monitoring α-synuclein cell-to-cell transfer. Neurobiology of disease, 77, 266–275. https://doi.org/10.1016/j.nbd.2014.07.003

Rinne J. O. (1993). Nigral degeneration in Parkinson's disease. Movement disorders : official journal of the Movement Disorder Society, 8 Suppl 1, S31–S35. https://doi.org/10.1002/mds.870080507

Rizek, P., Kumar, N., & Jog, M. S. (2016). An update on the diagnosis and treatment of Parkinson disease. CMAJ : Canadian Medical Association journal = journal de l'Association medicale canadienne, 188(16), 1157–1165. https://doi.org/10.1503/cmaj.151179

Rockenstein, E., Mallory, M., Hashimoto, M., Song, D., Shults, C. W., Lang, I., & Masliah, E. (2002). Differential neuropathological alterations in transgenic mice expressing alpha-synuclein from the platelet-derived growth factor and Thy-1 promoters. Journal of neuroscience research, 68(5), 568–578. https://doi.org/10.1002/jnr.10231

Ross, G. W., Abbott, R. D., Petrovitch, H., Tanner, C. M., & White, L. R. (2012). Pre-motor features of Parkinson's disease: the Honolulu-Asia Aging Study experience. Parkinsonism & related disorders, 18 Suppl 1, S199–S202. https://doi.org/10.1016/S1353-8020(11)70062-1

Rostami, J., Holmqvist, S., Lindström, V., Sigvardson, J., Westermark, G. T., Ingelsson, M., Bergström, J., Roybon, L., & Erlandsson, A. (2017). Human Astrocytes Transfer Aggregated Alpha-Synuclein via Tunneling Nanotubes. The Journal of neuroscience : the official journal of the Society for Neuroscience, 37(49), 11835–11853. https://doi.org/10.1523/JNEUROSCI.0983-17.2017

Sacino, A. N., Brooks, M., Thomas, M. A., McKinney, A. B., Lee, S., Regenhardt, R. W., McGarvey, N. H., Ayers, J. I., Notterpek, L., Borchelt, D. R., Golde, T. E., & Giasson, B. I. (2014). Intramuscular injection of α-synuclein induces CNS α-synuclein

pathology and a rapid-onset motor phenotype in transgenic mice. Proceedings of the National Academy of Sciences of the United States of America, 111(29), 10732–10737. https://doi.org/10.1073/pnas.1321785111

Sacino, A. N., Brooks, M., McKinney, A. B., Thomas, M. A., Shaw, G., Golde, T. E., & Giasson, B. I. (2014). Brain injection of α-synuclein induces multiple proteinopathies, gliosis, and a neuronal injury marker. The Journal of neuroscience : the official journal of the Society for Neuroscience, 34(37), 12368–12378. https://doi.org/10.1523/JNEUROSCI.2102-14.2014

Santos García, D., de Deus Fonticoba, T., Suárez Castro, E., Borrué, C., Mata, M., Solano Vila, B., Cots Foraster, A., Álvarez Sauco, M., Rodríguez Pérez, A. B., Vela, L., Macías, Y., Escalante, S., Esteve, P., Reverté Villarroya, S., Cubo, E., Casas, E., Arnaiz, S., Carrillo Padilla, F., Pueyo Morlans, M., Mir, P., … Coppadis Study Group (2019). Non-motor symptoms burden, mood, and gait problems are the most significant factors contributing to a poor quality of life in non-demented Parkinson's disease patients: Results from the COPPADIS Study Cohort. Parkinsonism & related disorders, 66, 151–157. https://doi.org/10.1016/j.parkreldis.2019.07.031

Santos-García, D., & de la Fuente-Fernández, R. (2013). Impact of non-motor symptoms on health-related and perceived quality of life in Parkinson's disease. Journal of the neurological sciences, 332(1-2), 136–140. https://doi.org/10.1016/j.jns.2013.07.005

Schapira A. H. (2015). Glucocerebrosidase and Parkinson disease: Recent advances. Molecular and cellular neurosciences, 66(Pt A), 37–42. https://doi.org/10.1016/j.mcn.2015.03.013

Schapira, A. H. V., Chaudhuri, K. R., & Jenner, P. (2017). Non-motor features of Parkinson disease. Nature reviews. Neuroscience, 18(7), 435–450. https://doi.org/10.1038/nrn.2017.62

Shahmoradian, S. H., Lewis, A. J., Genoud, C., Hench, J., Moors, T. E., Navarro, P. P., Castaño-Díez, D., Schweighauser, G., Graff-Meyer, A., Goldie, K. N., Sütterlin, R., Huisman, E., Ingrassia, A., Gier, Y., Rozemuller, A. J. M., Wang, J., Paepe, A., Erny, J., Staempfli, A., Hoernschemeyer, J., … Lauer, M. E. (2019). Lewy pathology in Parkinson's disease consists of crowded organelles and lipid membranes. Nature neuroscience, 22(7), 1099–1109. https://doi.org/10.1038/s41593-019-0423-2

Shi, M., Liu, C., Cook, T. J., Bullock, K. M., Zhao, Y., Ginghina, C., Li, Y., Aro, P., Dator, R., He, C., Hipp, M. J., Zabetian, C. P., Peskind, E. R., Hu, S. C., Quinn, J. F., Galasko, D. R., Banks, W. A., & Zhang, J. (2014). Plasma exosomal α-synuclein is likely CNS-derived and increased in Parkinson's disease. Acta neuropathologica, 128(5), 639–650. https://doi.org/10.1007/s00401-014-1314-y

Shiba, M., Bower, J. H., Maraganore, D. M., McDonnell, S. K., Peterson, B. J., Ahlskog, J. E., Schaid, D. J., & Rocca, W. A. (2000). Anxiety disorders and depressive disorders preceding Parkinson's disease: a case-control study. Movement disorders : official journal of the Movement Disorder Society, 15(4), 669–677. https://doi.org/10.1002/1531-8257(200007)15:4<669::aid-mds1011>3.0.co;2-5

Shibasaki, Y., Baillie, D. A., St Clair, D., & Brookes, A. J. (1995). High-resolution mapping of SNCA encoding alpha-synuclein, the non-A beta component of Alzheimer's disease amyloid precursor, to human chromosome 4q21.3-->q22 by fluorescence in

situ hybridization. Cytogenetics and cell genetics, 71(1), 54–55. https://doi.org/10.1159/000134061

Shimozawa, A., Ono, M., Takahara, D., Tarutani, A., Imura, S., Masuda-Suzukake, M., Higuchi, M., Yanai, K., Hisanaga, S. I., & Hasegawa, M. (2017). Propagation of pathological α-synuclein in marmoset brain. Acta neuropathologica communications, 5(1), 12. https://doi.org/10.1186/s40478-017-0413-0

Song, Y. J., Halliday, G. M., Holton, J. L., Lashley, T., O'Sullivan, S. S., McCann, H., Lees, A. J., Ozawa, T., Williams, D. R., Lockhart, P. J., & Revesz, T. R. (2009). Degeneration in different parkinsonian syndromes relates to astrocyte type and astrocyte protein expression. Journal of neuropathology and experimental neurology, 68(10), 1073–1083. https://doi.org/10.1097/NEN.0b013e3181b66f1b

Sorrentino, Z. A., Brooks, M. M. T., Hudson, V., 3rd, Rutherford, N. J., Golde, T. E., Giasson, B. I., & Chakrabarty, P. (2017). Intrastriatal injection of α-synuclein can lead to widespread synucleinopathy independent of neuroanatomic connectivity. Molecular neurodegeneration, 12(1), 40. https://doi.org/10.1186/s13024-017-0182-z

Sorrentino, Z. A., Xia, Y., Funk, C., Riffe, C. J., Rutherford, N. J., Ceballos Diaz, C., Sacino, A. N., Price, N. D., Golde, T. E., Giasson, B. I., & Chakrabarty, P. (2018). Motor neuron loss and neuroinflammation in a model of α-synuclein-induced neurodegeneration. Neurobiology of disease, 120, 98–106. https://doi.org/10.1016/j.nbd.2018.09.005

Souza, J. M., Giasson, B. I., Lee, V. M., & Ischiropoulos, H. (2000). Chaperone-like activity of synucleins. FEBS letters, 474(1), 116–119. https://doi.org/10.1016/s0014-5793(00)01563-5

Specht, C. G., & Schoepfer, R. (2001). Deletion of the alpha-synuclein locus in a subpopulation of C57BL/6J inbred mice. BMC neuroscience, 2, 11. https://doi.org/10.1186/1471-2202-2-11

Spillantini, M. G., Crowther, R. A., Jakes, R., Cairns, N. J., Lantos, P. L., & Goedert, M. (1998a). Filamentous alpha-synuclein inclusions link multiple system atrophy with Parkinson's disease and dementia with Lewy bodies. Neuroscience letters, 251(3), 205–208. https://doi.org/10.1016/s0304-3940(98)00504-7

Spillantini, M. G., Crowther, R. A., Jakes, R., Hasegawa, M., & Goedert, M. (1998b). alpha-Synuclein in filamentous inclusions of Lewy bodies from Parkinson's disease and dementia with lewy bodies. Proceedings of the National Academy of Sciences of the United States of America, 95(11), 6469–6473. https://doi.org/10.1073/pnas.95.11.6469

Spillantini, M. G., Schmidt, M. L., Lee, V. M., Trojanowski, J. Q., Jakes, R., & Goedert, M. (1997). Alpha-synuclein in Lewy bodies. Nature, 388(6645), 839–840. https://doi.org/10.1038/42166

Stokholm, M. G., Danielsen, E. H., Hamilton-Dutoit, S. J., & Borghammer, P. (2016). Pathological α-synuclein in gastrointestinal tissues from prodromal Parkinson disease patients. Annals of neurology, 79(6), 940–949. https://doi.org/10.1002/ana.24648

Stoyka, L. E., Mahoney, C. L., Thrasher, D. R., Russell, D. L., Cook, A. K., Harris, A. T., Narayanan, A., Janado, T. P., Standaert, D. G., Roberson, E. D., & Volpicelli-Daley, L. A. (2021). Templated α-Synuclein Inclusion Formation Is Independent of

Endogenous Tau. eNeuro, 8(3), ENEURO.0458-20.2021. https://doi.org/10.1523/ENEURO.0458-20.2021

Stuendl, A., Kunadt, M., Kruse, N., Bartels, C., Moebius, W., Danzer, K. M., Mollenhauer, B., & Schneider, A. (2016). Induction of α-synuclein aggregate formation by CSF exosomes from patients with Parkinson's disease and dementia with Lewy bodies. Brain : a journal of neurology, 139(Pt 2), 481–494. https://doi.org/10.1093/brain/awv346

Surmeier, D. J., Obeso, J. A., & Halliday, G. M. (2017). Selective neuronal vulnerability in Parkinson disease. Nature reviews. Neuroscience, 18(2), 101–113. https://doi.org/10.1038/nrn.2016.178

Taguchi, T., Ikuno, M., Yamakado, H., & Takahashi, R. (2020). Animal Model for Prodromal Parkinson's Disease. International journal of molecular sciences, 21(6), 1961. https://doi.org/10.3390/ijms21061961

Takeda, A., Hashimoto, M., Mallory, M., Sundsumo, M., Hansen, L., Sisk, A., & Masliah, E. (1998). Abnormal distribution of the non-Abeta component of Alzheimer's disease amyloid precursor/alpha-synuclein in Lewy body disease as revealed by proteinase K and formic acid pretreatment. Laboratory investigation; a journal of technical methods and pathology, 78(9), 1169–1177.

Tanaka, M., Kim, Y. M., Lee, G., Junn, E., Iwatsubo, T., & Mouradian, M. M. (2004). Aggresomes formed by alpha-synuclein and synphilin-1 are cytoprotective. The Journal of biological chemistry, 279(6), 4625–4631. https://doi.org/10.1074/jbc.M310994200

Thacker, E. L., & Ascherio, A. (2008). Familial aggregation of Parkinson's disease: a meta-analysis. Movement disorders : official journal of the Movement Disorder Society, 23(8), 1174–1183. https://doi.org/10.1002/mds.22067

Thierry, A. M., Gioanni, Y., Dégénétais, E., & Glowinski, J. (2000). Hippocampo-prefrontal cortex pathway: anatomical and electrophysiological characteristics. Hippocampus, 10(4), 411–419. https://doi.org/10.1002/1098-1063(2000)10:4<411::AID-HIPO7>3.0.CO;2-A

Tofaris, G. K., Garcia Reitböck, P., Humby, T., Lambourne, S. L., O'Connell, M., Ghetti, B., Gossage, H., Emson, P. C., Wilkinson, L. S., Goedert, M., & Spillantini, M. G. (2006). Pathological changes in dopaminergic nerve cells of the substantia nigra and olfactory bulb in mice transgenic for truncated human alpha-synuclein(1-120): implications for Lewy body disorders. The Journal of neuroscience : the official journal of the Society for Neuroscience, 26(15), 3942–3950. https://doi.org/10.1523/JNEUROSCI.4965-05.2006

Tolosa, E., Garrido, A., Scholz, S. W., & Poewe, W. (2021). Challenges in the diagnosis of Parkinson's disease. The Lancet. Neurology, 20(5), 385–397. https://doi.org/10.1016/S1474-4422(21)00030-2

Uemura, N., Yagi, H., Uemura, M. T., Hatanaka, Y., Yamakado, H., & Takahashi, R. (2018). Inoculation of α-synuclein preformed fibrils into the mouse gastrointestinal tract induces Lewy body-like aggregates in the brainstem via the vagus nerve. Molecular neurodegeneration, 13(1), 21. https://doi.org/10.1186/s13024-018-0257-5

Ulmer, T. S., Bax, A., Cole, N. B., & Nussbaum, R. L. (2005). Structure and dynamics of micelle-bound human alpha-synuclein. The Journal of biological chemistry, 280(10), 9595–9603. https://doi.org/10.1074/jbc.M411805200

Vaidya, B., Dhamija, K., Guru, P., & Sharma, S. S. (2021). Parkinson's disease in women: Mechanisms underlying sex differences. European journal of pharmacology, 895, 173862. https://doi.org/10.1016/j.ejphar.2021.173862

Vaikath, N. N., Hmila, I., Gupta, V., Erskine, D., Ingelsson, M., & El-Agnaf, O. M. A. (2019). Antibodies against alpha-synuclein: tools and therapies. Journal of neurochemistry, 150(5), 612–625. https://doi.org/10.1111/jnc.14713

Vaikath, N. N., Majbour, N. K., Paleologou, K. E., Ardah, M. T., van Dam, E., van de Berg, W. D., Forrest, S. L., Parkkinen, L., Gai, W. P., Hattori, N., Takanashi, M., Lee, S. J., Mann, D. M., Imai, Y., Halliday, G. M., Li, J. Y., & El-Agnaf, O. M. (2015). Generation and characterization of novel conformation-specific monoclonal antibodies for α-synuclein pathology. Neurobiology of disease, 79, 81–99. https://doi.org/10.1016/j.nbd.2015.04.009

Van der Perren, A., Van den Haute, C., & Baekelandt, V. (2015). Viral vector-based models of Parkinson's disease. Current topics in behavioral neurosciences, 22, 271–301. https://doi.org/10.1007/7854_2014_310

Venda, L. L., Cragg, S. J., Buchman, V. L., & Wade-Martins, R. (2010). α-Synuclein and dopamine at the crossroads of Parkinson's disease. Trends in neurosciences, 33(12), 559–568. https://doi.org/10.1016/j.tins.2010.09.004

Verstraeten, A., Theuns, J., & Van Broeckhoven, C. (2015). Progress in unraveling the genetic etiology of Parkinson disease in a genomic era. Trends in genetics : TIG, 31(3), 140–149. https://doi.org/10.1016/j.tig.2015.01.004

Vijiaratnam, N., Simuni, T., Bandmann, O., Morris, H. R., & Foltynie, T. (2021). Progress towards therapies for disease modification in Parkinson's disease. The Lancet. Neurology, 20(7), 559–572. https://doi.org/10.1016/S1474-4422(21)00061-2

Villar-Piqué, A., Lopes da Fonseca, T., & Outeiro, T. F. (2016). Structure, function and toxicity of alpha-synuclein: the Bermuda triangle in synucleinopathies. Journal of neurochemistry, 139 Suppl 1, 240–255. https://doi.org/10.1111/jnc.13249

Volpicelli-Daley, L. A., Luk, K. C., Patel, T. P., Tanik, S. A., Riddle, D. M., Stieber, A., Meaney, D. F., Trojanowski, J. Q., & Lee, V. M. (2011). Exogenous α-synuclein fibrils induce Lewy body pathology leading to synaptic dysfunction and neuron death. Neuron, 72(1), 57–71. https://doi.org/10.1016/j.neuron.2011.08.033

Wagner, J. M., Sichler, M. E., Schleicher, E. M., Franke, T. N., Irwin, C., Löw, M. J., Beindorff, N., Bouter, C., Bayer, T. A., & Bouter, Y. (2019). Analysis of Motor Function in the Tg4-42 Mouse Model of Alzheimer's Disease. Frontiers in behavioral neuroscience, 13, 107. https://doi.org/10.3389/fnbeh.2019.00107

Wakabayashi, K., Takahashi, H., Obata, K., & Ikuta, F. (1992). Immunocytochemical localization of synaptic vesicle-specific protein in Lewy body-containing neurons in Parkinson's disease. Neuroscience letters, 138(2), 237–240. https://doi.org/10.1016/0304-3940(92)90923-u

Wakabayashi, K., Tanji, K., Mori, F., & Takahashi, H. (2007). The Lewy body in Parkinson's disease: molecules implicated in the formation and degradation of alpha-

synuclein aggregates. Neuropathology : official journal of the Japanese Society of Neuropathology, 27(5), 494–506. https://doi.org/10.1111/j.1440-1789.2007.00803.x

Wakabayashi, K., Tanji, K., Odagiri, S., Miki, Y., Mori, F., & Takahashi, H. (2013). The Lewy body in Parkinson's disease and related neurodegenerative disorders. Molecular neurobiology, 47(2), 495–508. https://doi.org/10.1007/s12035-012-8280-y

Walf, A. A., & Frye, C. A. (2007). The use of the elevated plus maze as an assay of anxiety-related behavior in rodents. Nature protocols, 2(2), 322–328. https://doi.org/10.1038/nprot.2007.44

Wall, N. R., De La Parra, M., Callaway, E. M., & Kreitzer, A. C. (2013). Differential innervation of direct- and indirect-pathway striatal projection neurons. Neuron, 79(2), 347–360. https://doi.org/10.1016/j.neuron.2013.05.014

Watanabe, Y., Tatebe, H., Taguchi, K., Endo, Y., Tokuda, T., Mizuno, T., Nakagawa, M., & Tanaka, M. (2012). p62/SQSTM1-dependent autophagy of Lewy body-like α-synuclein inclusions. PloS one, 7(12), e52868. https://doi.org/10.1371/journal.pone.0052868

Webb, J. L., Ravikumar, B., Atkins, J., Skepper, J. N., & Rubinsztein, D. C. (2003). Alpha-Synuclein is degraded by both autophagy and the proteasome. The Journal of biological chemistry, 278(27), 25009–25013. https://doi.org/10.1074/jbc.M300227200

Winner, B., Jappelli, R., Maji, S. K., Desplats, P. A., Boyer, L., Aigner, S., Hetzer, C., Loher, T., Vilar, M., Campioni, S., Tzitzilonis, C., Soragni, A., Jessberger, S., Mira, H., Consiglio, A., Pham, E., Masliah, E., Gage, F. H., & Riek, R. (2011). In vivo demonstration that alpha-synuclein oligomers are toxic. Proceedings of the National Academy of Sciences of the United States of America, 108(10), 4194–4199. https://doi.org/10.1073/pnas.1100976108

Wong, Y. C., Luk, K., Purtell, K., Burke Nanni, S., Stoessl, A. J., Trudeau, L. E., Yue, Z., Krainc, D., Oertel, W., Obeso, J. A., & Volpicelli-Daley, L. A. (2019). Neuronal vulnerability in Parkinson disease: Should the focus be on axons and synaptic terminals?. Movement disorders : official journal of the Movement Disorder Society, 34(10), 1406–1422. https://doi.org/10.1002/mds.27823

Wooten, G. F., Currie, L. J., Bovbjerg, V. E., Lee, J. K., & Patrie, J. (2004). Are men at greater risk for Parkinson's disease than women?. Journal of neurology, neurosurgery, and psychiatry, 75(4), 637–639. https://doi.org/10.1136/jnnp.2003.020982

Xia, Y., Zhang, G., Han, C., Ma, K., Guo, X., Wan, F., Kou, L., Yin, S., Liu, L., Huang, J., Xiong, N., & Wang, T. (2019). Microglia as modulators of exosomal alpha-synuclein transmission. Cell death & disease, 10(3), 174. https://doi.org/10.1038/s41419-019-1404-9

Yoon, D. Y., Mansukhani, N. A., Stubbs, V. C., Helenowski, I. B., Woodruff, T. K., & Kibbe, M. R. (2014). Sex bias exists in basic science and translational surgical research. Surgery, 156(3), 508–516. https://doi.org/10.1016/j.surg.2014.07.001

Young, C. B., Reddy, V., & Sonne, J. (2023). Neuroanatomy, Basal Ganglia. In StatPearls. StatPearls Publishing.

Zarranz, J. J., Alegre, J., Gómez-Esteban, J. C., Lezcano, E., Ros, R., Ampuero, I., Vidal, L., Hoenicka, J., Rodriguez, O., Atarés, B., Llorens, V., Gomez Tortosa, E., del Ser, T., Muñoz, D. G., & de Yebenes, J. G. (2004). The new mutation, E46K, of alpha-

synuclein causes Parkinson and Lewy body dementia. Annals of neurology, 55(2), 164–173. https://doi.org/10.1002/ana.10795

Zhang, B., Kehm, V., Gathagan, R., Leight, S. N., Trojanowski, J. Q., Lee, V. M., & Luk, K. C. (2019). Stereotaxic Targeting of Alpha-Synuclein Pathology in Mouse Brain Using Preformed Fibrils. Methods in molecular biology (Clifton, N.J.), 1948, 45–57. https://doi.org/10.1007/978-1-4939-9124-2_5

Zhang, W., Wang, T., Pei, Z., Miller, D. S., Wu, X., Block, M. L., Wilson, B., Zhang, W., Zhou, Y., Hong, J. S., & Zhang, J. (2005). Aggregated alpha-synuclein activates microglia: a process leading to disease progression in Parkinson's disease. FASEB journal : official publication of the Federation of American Societies for Experimental Biology, 19(6), 533–542. https://doi.org/10.1096/fj.04-2751com

Zhang, L., Zhang, C., Zhu, Y., Cai, Q., Chan, P., Uéda, K., Yu, S., & Yang, H. (2008). Semi-quantitative analysis of alpha-synuclein in subcellular pools of rat brain neurons: an immunogold electron microscopic study using a C-terminal specific monoclonal antibody. Brain research, 1244, 40–52. https://doi.org/10.1016/j.brainres.2008.08.067

Zimprich, A., Benet-Pagès, A., Struhal, W., Graf, E., Eck, S. H., Offman, M. N., Haubenberger, D., Spielberger, S., Schulte, E. C., Lichtner, P., Rossle, S. C., Klopp, N., Wolf, E., Seppi, K., Pirker, W., Presslauer, S., Mollenhauer, B., Katzenschlager, R., Foki, T., Hotzy, C., … Strom, T. M. (2011). A mutation in VPS35, encoding a subunit of the retromer complex, causes late-onset Parkinson disease. American journal of human genetics, 89(1), 168–175. https://doi.org/10.1016/j.ajhg.2011.06.008

List of Figures

Fig. 1: Neuropathological hallmarks of Parkinson's disease (PD). 11
Fig. 2: Schematic overview of the classical direct/indirect motor pathway of the basal ganglia. 12
Fig. 3: Braak staging of Lewy body deposition.....15
Fig. 4: Key biological processes that are affected in aging and PD. 19
Fig. 5: Schematic representation of α-syn aggregation, nucleation processes and the physiological functions of α-syn that are impaired in pathological α-syn state.....23
Fig. 6: Experimental design of the study.....32
Fig. 7: Schematic diagram of stereotaxic PFF injection into the right dorsal striatum...34
Fig. 8: Induction and transmission of pα-syn pathology after intrastriatal inoculation with human α-syn PFFs.....40
Fig. 9: Pathological characterization of α-syn aggregates. 42
Fig. 10: PFF seeded pα-syn pathology in the striatum. 43
Fig. 11: Pathological pα-syn aggregates in the SNpc induced by α-syn PFFs. 44
Fig. 12: Loss of dopaminergic innervation after inoculation with α-syn PFFs. 45
Fig. 13: Integrity of dopaminergic neurons in the SNpc after inoculation with α-syn PFFs. 46
Fig. 14: Loss of dopaminergic innervation density of the SNr after inoculation with human wild-type α-syn PFFs. 47
Fig. 15: Motor performance and fine motor control of control and PFF-inoculated mice. 48
Fig. 16: Correlation studies of obtained results.....49
Fig. 17: Pathological α-syn inclusions in the Striatum and SNpc comparing sexes.....50
Fig. 18: Nigrostriatal pathway comparing sexes. 51
Fig. 19: Motor performance and fine motor control comparing sexes.....52

Fig. S1: Scoring of pα-syn propagation per selected brain region. 93
Fig. S2: Automatic quantification of pα-syn aggregates in the Striatum using ImageJ. 94
Fig. S3: Manual quantification of pα-syn in the SNpc. 95
Fig. S4: Quantification of innervation density in the SNr.....95
Fig. S5: Morphology of pα-syn aggregates induced by human wild-type α-syn PFF inoculation.....96
Fig. S6: Weight increase of WT, Ctrl and OVX mice over time.....97

List of Tables

Table 1: Motor and non-motor symptoms of PD. 13
Table 2: Genetics of PD. Genes implicated in mendelian and non-mendelian transmission of PD.....17
Table 3: Familial mutations that have been used in genetic animal models of PD. 27
Table 4: Primary and secondary antibodies used in this study.....35
Table 5: Number of animals used for “Fig. S6: Weight increase of WT, Ctrl and OVX mice over time”.....98
Table 6: The murine PFF-based PD model established in this study. 98

List of Abbreviations

6-OHDA	6-Hydroxydopamine
AAV	Adeno-associated virus
Ab1	Primary antibody
Ab2	Secondary antibody
Ac	Anterior commissure
ACo	Anterior cortical amygdala nucleus
ANOVA	Analysis of variance
AuV	Secondary auditory cortex, ventral
BAC	bacterial artificial chromosome
BBB	Blood-brain-barrier
BFB	Basal forebrain
BLA	Basolateral amygdala nucleus, anterior
BLP	Basolateral amygdala nucleus, posterior
BMA	Basomedial amygdala nucleus, anterior
BMP	Basomedial amygdala nucleus, posterior
Cc	Corpus callosum
CeA	Central amygdala nucleus, anterior
Cg1	Cingulate cortex 1
Cg2	Cingulate cortex 2
CI	Capsula interna
CNS	Central nervous system
Ctx	Cortex
Cx Amyg	Cortex amygdala
CxA	Cortex-amygdala transition zone
D1R	Dopamine receptor subtype 1
D2R	Dopamine receptor subtype 2
DA	Dopamine
DAB	3,3'-Diaminobenzidine
DLB	dementia with Lewy bodies
DMX	Dorsal motor nucleus of the vagus nerve
Dpi	Days post injection
DR	Dorsal raphe nucleus
Ect	Ectorhinal cortex
ENS	enteric nervous system
GABA	Gamma aminobutyric acid
GIT	gastrointestinal tract
GPe	External segment of globus pallidus
GPi	Internal segment of globus pallidus
GWAS	genome-wide association studies
HRP	Horseradish peroxidase
Hyp	Hypothalamus
IF	Immunofluorescence
IHC	Immunohistochemistry
LB	Lewy body
LGP	Lateral globus pallidus
LN	Lewy neurite
M1	Primary motor cortex
M2	Secondary motor cortex
MPTP	1-methyl-4-phenyl-1,2,3,6-tetrahydropyridine
MSA	multiple systems atrophy
MSNs	medium-sized spiny neurons
MTC	Medial temporal cortex
NGS	Normal goat serum
NHP	Non-human primates
OB	Olfactory bulb
OVX	Overexpression
PD	Parkinson’s disease
PFFs	Pre-formed fibrils
Pir	Piriform cortex
PLCo	Postlateral cortex amygdala nucleus
PMCo	Postmedial cortex amygdala nucleus
PrP	prion protein
pα-syn	Phosphorylated alpha-synuclein
RBD	rapid eye movement (REM) sleep behaviour disorder
RT	Room temperature
S1	Primary somatosensory cortex
S2	Secondary somatosensory cortex
SEM	Standard error of the mean
SNCA	Synuclein Alpha
SNpc	Substantia nigra pars compacta
SNr	Substantia nigra pars reticulata
STN	Subthalamic nucleus
STR	Striatum
TH	Tyrosine Hydroxylase
Thal	Thalamus
V2	Secondary visual cortex
α-syn	Alpha-synuclein

Supplementary Material

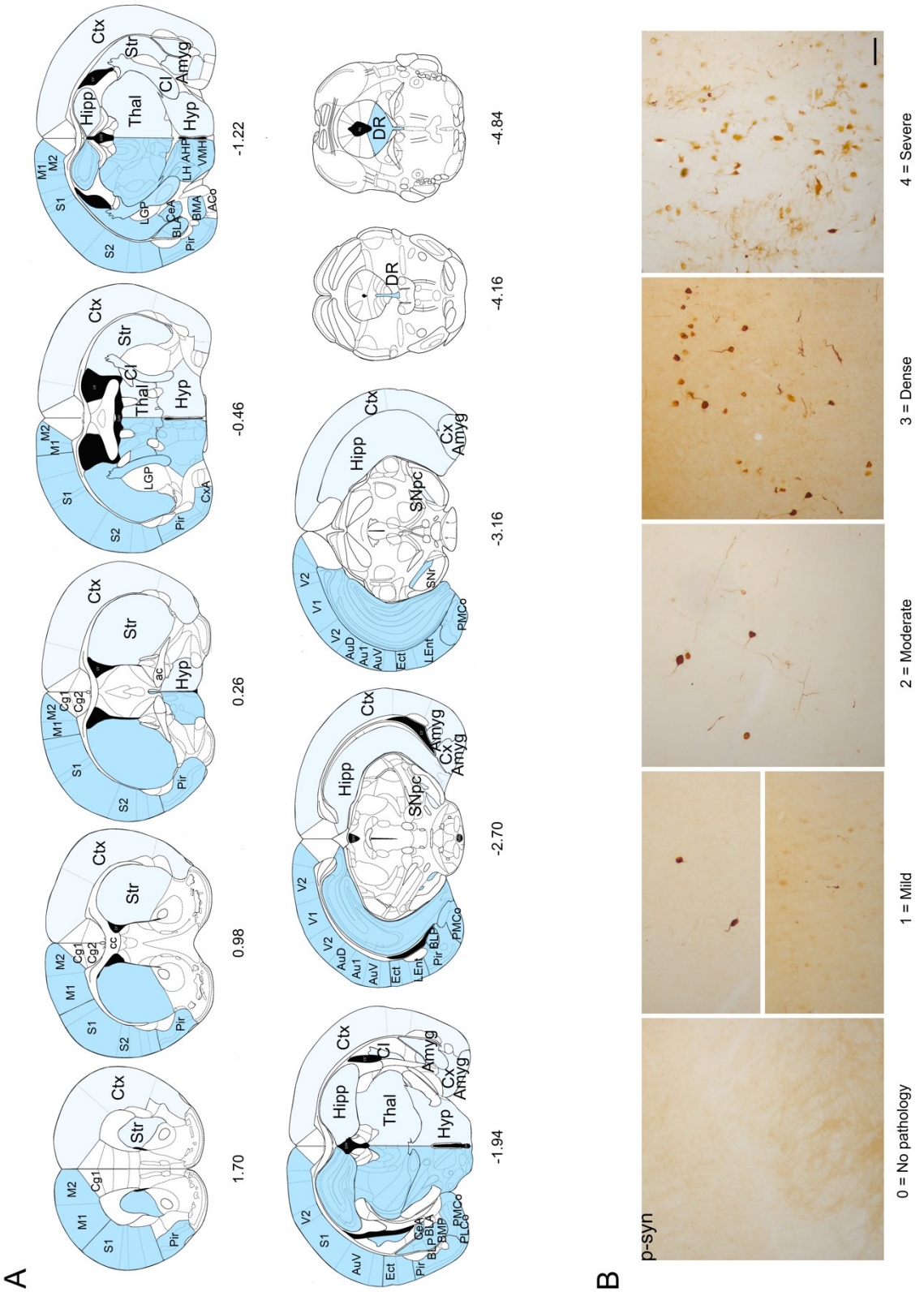

Fig. S1: Scoring of pα-syn propagation per selected brain region. (**A**) Brain regions that were considered for scoring map are indicated in blue. Caudo-rostral levels of brain sections are indicated from Bregma. Complete terminology for brain regions can be found in the List of Abbreviations. (**B**) The template scale was used to assign scores to each region for each animal, ranging from no pathology (0) to severe pathology (4). Scale bar: 50 µm (20x)

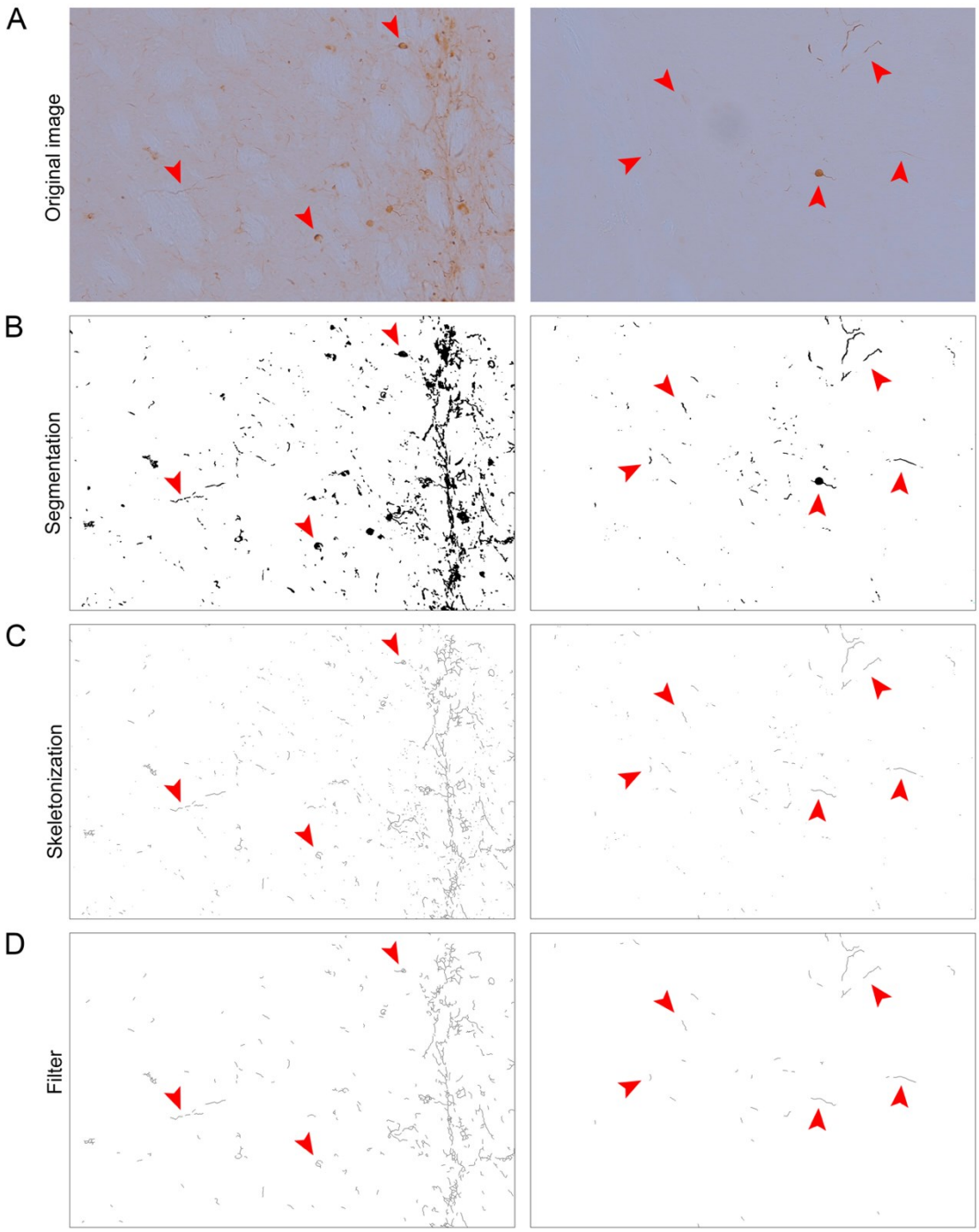

Fig. S2: Automatic quantification of pα-syn aggregates in the Striatum using ImageJ. (**A**) Representative images of pα-syn immunostained tissue in the ipsilateral striatum of PFF-injected animals with many (left) and few (right) pα-syn aggregates. Red arrows mark some pα-syn aggregates/fibers (possibly located within cell bodies or processes), exemplary for processing steps. The original image was taken with a Thunder microscope using a 20x objective. (**B**) Image segmentation was performed using the plugin Labkit. The classifier creates a binary image to distinguish background (here white) from pixels of interest, the pα-syn aggregates (here black). (**C**) Skeletonization of objects of interest was performed using Skeletonize 2D/3D plugin. (**D**) As a last step, a size-dependent filter was applied to exclude artifacts and unspecific segmented objects. Remaining objects are counted to obtain the number of pα-syn aggregates per individual image of the section per animal.

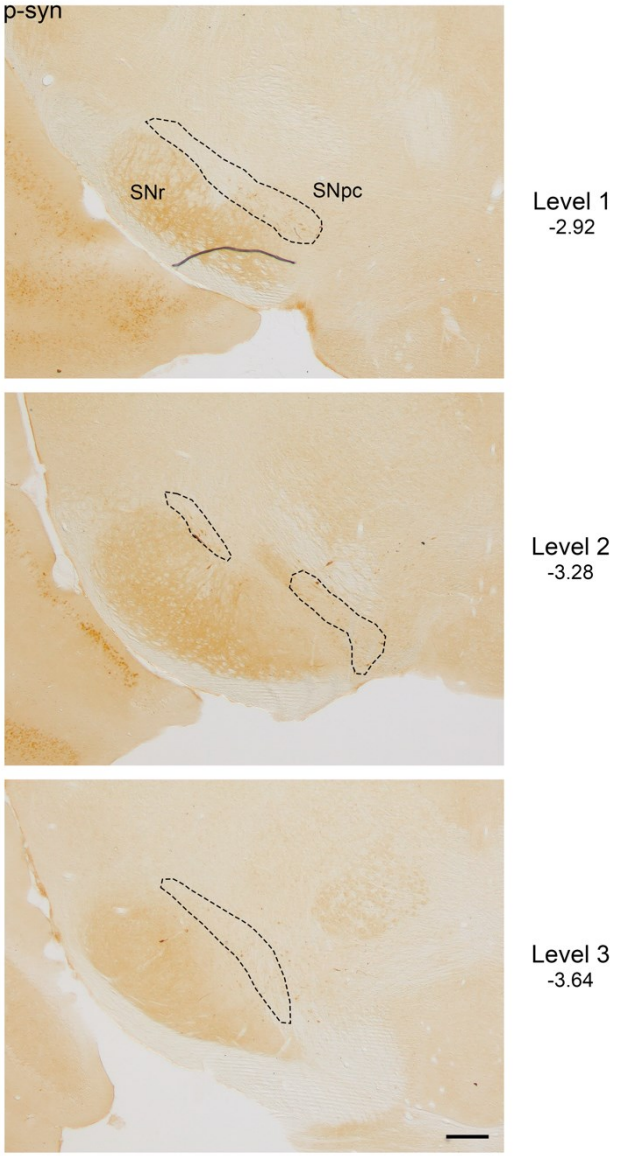

Fig. S3: Manual quantification of pα-syn in the SNpc. Approximate caudo-rostral levels used for the counting of pα-syn aggregates are presented. Coordinates are indicated from Bregma. Scale bar: 200 µm (5x)

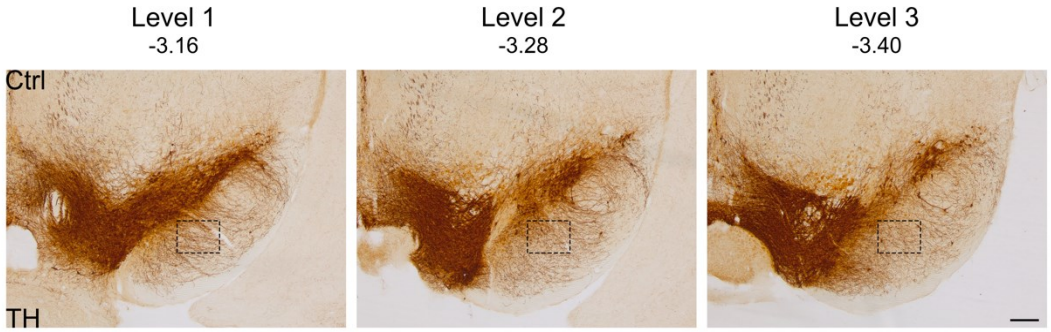

Fig. S4: Quantification of innervation density in the SNr. Per animal images of 3 different caudo-rostral levels were quantified and captured approximately within the same region of the SNr (indicated as a square) using a 40x objective. Caudo-rostral coordinates are indicated from Bregma. Scale bar: 200 µm (5x)

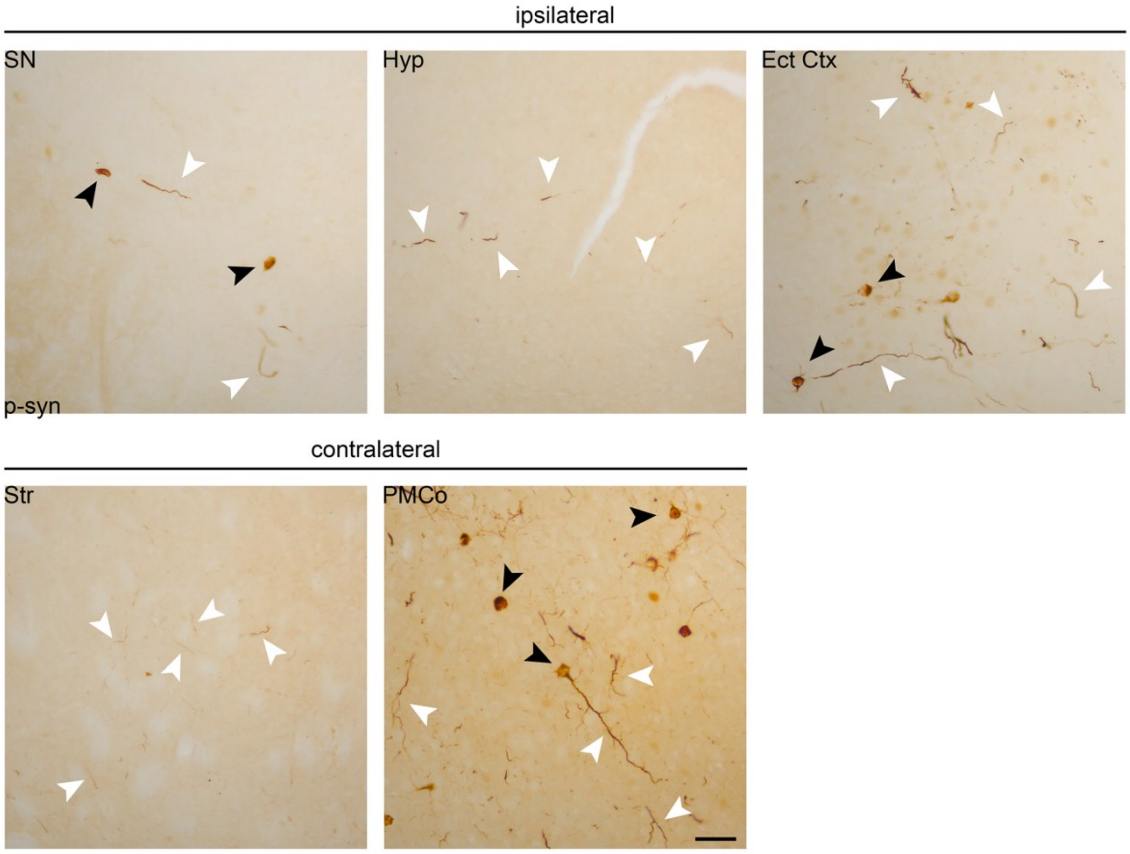

Fig. S5: Morphology of pα-syn aggregates induced by human wild-type α-syn PFF inoculation. Representative images of pα-syn aggregates in the SN, hypothalamus, entorhinal cortex (ipsilateral) and striatum, PMCo (contralateral) are presented. Dense inclusions in cell bodies are indicated with black arrows, while aggregates in fibers are highlighted in white. Scale bar: 50 µm (20x)

Weight increase of WT, Ctrl and OVX animals

The weight growth of WT, Ctrl and OVX animals was monitored at 3, 6 and 12 months (**Fig. S6 A**). It can be noted that all groups display the same weight at 3 months of age (WT: 20.8 g, Ctrl: 22.47 g, OVX: 23.5 g). At 6 months, WT and Ctrl animals display similar body weight (WT: 33.37 g, Ctrl: 32.17 g), whereas OVX gain significantly less compared to control animals (26.375 g). The disparity is even greater at 12 months (WT: 39.11 g, Ctrl: 37.31 g, OVX: 28.06 g). The observed differences are significant, and p-values are indicated in the figure legend.

When presenting data separated by sex (**Fig. S6 B**, **C**) the same trend can be observed. OVX mice gain significantly less mass compared to WT and Ctrl, although the weight difference at 6 and 12 months, respectively, is more prominent in male animals (**Fig.** S6 **C**). Further, it can be seen that Ctrl animals show significant sex-specific differences in weight. Male Ctrl mice weigh around 40 g at 6 months, whereas female display below 30 g (**Fig. S6 B, C**). See figure legends for p-values of statistically significant differences.

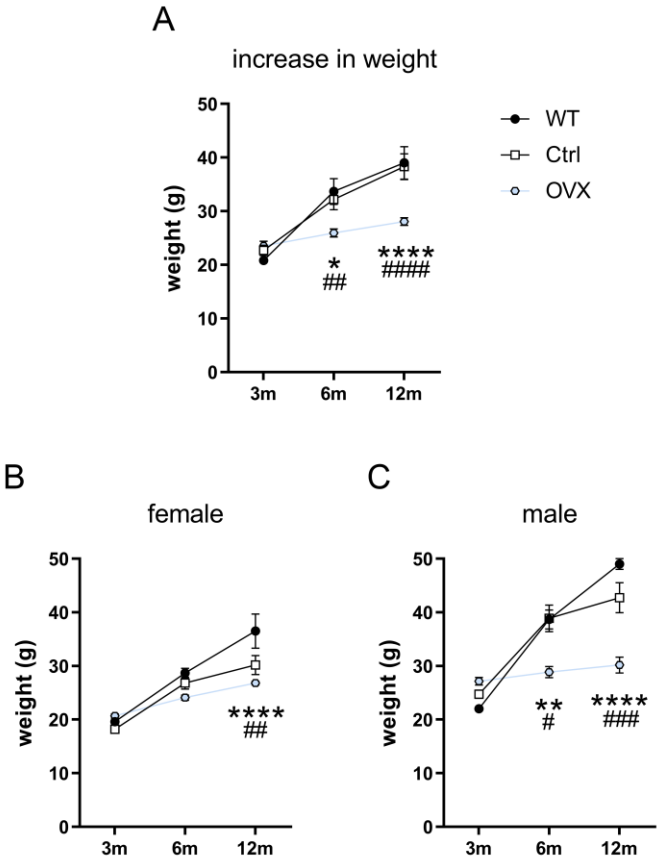

Fig. S6: Weight increase of WT, Ctrl and OVX mice over time. (**A**) Increase in weight of WT, Ctrl and OVX animals at 3, 6 and 12 months of age is presented. * p<0.05 comparing WT and OVX (p=0,022), ## p<0.01 comparing Ctrl and OVX (p=0,0075), **** p<0.0001 comparing WT and OVX, #### p<0.0001 comparing Ctrl and OVX. (**B**) Weight gain of female animals only. **** p<0.0001 comparing WT and OVX, ## p<0.01 comparing WT and Ctrl (p=0,0084). (**C**) Weight gain of male animals only. ** p<0.001 comparing Ctrl and OVX (p=0,0016), # p<0.05 comparing WT and OVX (p=0,0248), **** p<0,0001 comparing Ctrl and OVX, ### p<0.001 comparing WT and OVX (p=0,0002). 2-way ANOVA with Tukey's multiple comparisons test. N numbers are indicated in **Table 5**.

Numbers of animals used in **Fig. S6**

		WT	Ctrl	OVX
all animals	3m	n=10	n=16	n=16
Fig. S6 A	6m	n=6	n=18	n=18
	12m	n=10	n=17	n=16
female	3m	n=5	n=5	n=9
Fig. S6 B	6m	n=3	n=10	n=11
	12m	n=8	n=6	n=10
male	3m	n=5	n=11	n=7
Fig. S6 C	6m	n=3	n=8	n=7
	12m	n=2	n=11	n=6

Table 5: Number of animals used for "Fig. S6: Weight increase of WT, Ctrl and OVX mice over time".

Summary of obtained results in this study

Novel murine PD model based on α-syn inoculation	
Rodent strain	*SNCA*-OVX (C57BL/6OlaHsd)
Age	2-3 months
Injectate	Human wild-type α-syn pre-formed fibrils (PFFs)
Injection site	Right dorsal striatum (unilateral)
Total dose	2,5 µl (5 µg)
Sacrifice dpi	150
Ser129 pα-syn pathology	Striatum (ipsilateral: high, contralateral: low)
	SN (ipsilateral: low, contralateral: no)
	Cortex (ipsilateral: medium, contralateral: medium)
	Amygdala (ipsilateral: high, contralateral medium)
	Thalamus (ipsilateral: low, contralateral: no)
	Hypothalamus (ipsilateral: low, contralateral: no)
	Hippocampus (ipsilateral: low, contralateral: low)
	DR (low)
	Internal capsule, corpus callosum, anterior commissure (medium/high)
Striatal TH-loss	Ipsilateral
SNpc TH-positive cell loss	Ipsilateral
SNr TH-loss	Ipsilateral
Behavioural deficits	No robust motor deficits observed using the challenging beam transversal test
Future outlook	Neuroinflammation, implication of glial cell types, include additional motor assays, distinct conformational α-syn species, sex-specific phenotype

Table 6: The murine PFF-based PD model established in this study. Information about the generation of the model as well as observations and characterization of the PD-like pathology, and ideas for future experiments. (Idea for this table from Polinski et al., 2021)